國 立 交 通 大 學
電信工程學系
博 士 論 文

從網路觀點對天線技術於多用戶排程及
分時雙工/分碼多工無線系統之研究

A Network Perspective Investigation of MIMO
Antenna Techniques in Multiuser Scheduling and
TDD/CDMA Systems

研 究 生： 陳 瓊 璋

指導教授： 王 蒞 君 博士

中 華 民 國 九 十 四 年 一 月

從網路觀點對天線技術於多用戶排程及
分時雙工/分碼多工無線系統之研究
A Network Perspective Investigation of MIMO
Antenna Techniques in Multiuser Scheduling and
TDD/CDMA Systems

研 究 生: 陳瓊璋　　　　　　Student: Chiung-Jang Chen

指導教授: 王蒞君 博士　　　　Advisor: Dr. Li-Chun Wang

國 立 交 通 大 學
電 信 工 程 學 系
博 士 論 文

A Dissertation
Submitted to Institute of Communication Engineering
College of Electrical Engineering and Computer Science
National Chiao Tung University
in Partial Fulfillment of the Requirements
for the Degree of Doctor of Philosophy
in
Communication Engineering
Hsinchu, Taiwan

中 華 民 國 九 十 四 年 一 月

從網路觀點對天線技術於多用戶排程及
分時雙工/分碼多工無線系統之研究

研 究 生: 陳 瓊 璋 　　　指導教授: 王 蒞 君 博士

國 立 交 通 大 學
電 信 工 程 學 系

摘 要

　　應用天線技術所帶來的高容量增益，雖然可以讓使用者在不增加頻寬的環境下，提高無線通道的傳輸速率，但在實際應用該技術的同時，卻也可能面臨兩項主要的議題─硬體實現複雜度，以及可能的鏈路可靠度降低。針對上述兩項議題，傳統研究多採用實體層技術的解決方案，然而在本論文中，則嘗試從網路觀點來提供另一種解決問題的方法─開發並利用網路中已經存在的資源(例如用戶分集)，幾乎不需要額外增加成本，就可以提供更多解決問題的維度。在本論文中，除了印證利用網路觀點所得到的用戶分集，可以解決應用天線技術過程可能面臨的兩項議題外，更重要的是，若應用這整個網路觀點的設計概念，於其他通信系統的設計上，將有機會增加該系統的運作效能。

　　首先，我們考慮以分集為基礎(diversity-based)的天線技術在多用戶排程系統的應用，在這裡我們推導出一個可以同時整合用戶維度、天線維度、以及通道特性維度的公式，利用這個系統容量公式，可以說明多用戶排程技術的特性，以及解釋排程技術與天線分集之間的交互作用。分析結果顯示用戶分集是類似天線系統中的選擇分集，因此如果在一個多用戶通信系統中已經存在了很大的用戶分集增益，這時若使用以分集為基礎的天線技術，該技術所帶來的額外好處將會受限。另外，我們也說明了在多用戶排程系統中，若使用時空塊狀編碼(space time block code)天線技術，甚

至可能導致系統容量損失。

　　其次，我們考慮以多工為基礎(multiplexing-based)的天線技術在多用戶排程系統的應用。近來的研究顯示，使用以多工為基礎的天線技術，可能會犧牲使用以分集為基礎的天線技術所帶來的好處—鏈路穩定度，因此，我們提出了一個「最弱子通道優先」(strongest-weakest-normalized-subchannel-first, SWNSF)排程演算法，淬取出多用戶系統中的用戶分集來補償天線分集的不足，也就可以解決上述鏈路穩定度不足的缺點。接著，我們嘗試在一個使用 SWNSF 排程演算法的多用戶排程系統中，使用一個簡單的零強制(zero-forcing)接收器，當用戶數趨近無窮大時，我們證明零強制接收器可以是一個最佳接收器，換句話說，應用以多工為基礎的天線技術於多用戶排程系統時，可以用低成本的方式，同時增加系統容量與鏈路穩定度。

　　最後，我們考慮波束合成天線技術在分時雙工/分碼多工系統的應用，我們建議，使用波束合成天線技術，來解決基地站與基地站之間的強干擾問題，利用鄰近不同基地台之間的合作，我們介紹一個同時上鏈路接收與下鏈路發射的波束合成機制，來降低在分時雙工/分碼多工系統中出現的基地站對基地站之間的強干擾，分析結果顯示，利用我們建議的波束合成機制，可以在低成本的狀態下，有效消除基地站對基地站之間的強干擾問題。

A Network Perspective Investigation of MIMO Antenna Techniques in Multiuser Scheduling and TDD/CDMA Systems

Student: Chiung-Jang Chen   Advisor: Dr. Li-Chun Wang

Department of Communication Engineering,
National Chiao Tung University, Taiwan

Abstract

The huge capacity gain offered by the multiple-input multiple-output (MIMO) antenna technique can achieve higher data rates on wireless channels without sacrificing bandwidth efficiency. The primary challenge to apply the MIMO technique lies in the implementation complexity and the possible side effect of reliability performance degradation. Traditional efforts to resolve these issues associated with the MIMO technique are mostly based on the physical layer treatment. Differently, this dissertation presents a network perspective approach to revisit the MIMO technique with an aim to provide an alternative settlement. The main advantage of the network perspective approach is a full exploitation of existing dimensions in the network, e.g. the inherent multiuser diversity, with a negligible cost. More important than the results presented in this dissertation, however, is the hope that the network perspective methodology here will provide an innovative and flexible design paradigm for wireless systems.

First, the category of fading mitigation based (or diversity-based) MIMO antenna schemes is investigated for the multiuser scheduling system. A unified capacity formula connecting multiple domains of users, antennas and fading characteristics is derived. The analytical capacity formula is powerful in extracting the essence of multiuser scheduling and interpreting the interplay of antenna diversity and multiuser scheduling. Our analysis indicates that the scheduling technique intrinsically delivers multiuser diversity with an analogy of selection diversity in the multiple antenna system. As a result, we show that the additional capacity gain with the use of fading mitigation based antenna techniques is somewhat

limited because user population has contributed a large order of selection diversity in the multiuser scheduling system. It is also demonstrated that employing the space time block code (STBC) methods for the multiuser scheduling system may even cause a capacity loss due to the reduced amount of fading gain but without the supplement of array gain.

Second, the category of throughput enhancement based (or multiplexing-based) MIMO antenna schemes is studied for the multiuser scheduling system. Motivated by a recent result of diversity-multiplexing tradeoff in the MIMO system, we propose using the multiuser diversity to replenish the diversity-deficient spatial multiplexing MIMO system. Particularly, we develop a novel strongest-weakest-normalized-subchannel-first (SWNSF) scheduling algorithm, requiring only scalar feedback, to enhance the degraded reliability performance of the MIMO system. Our analysis and results indicate that the SWNSF scheduling can significantly increase the coverage of the multiuser MIMO system while improving the system capacity. Furthermore, we consider a simple spatial multiplexing MIMO system with the zero-forcing receiver. Somewhat surprisingly, from a multiuser scheduling network perspective, we prove that the zero-forcing receiver can be asymptotically optimal in the multiuser scheduling system as the number of users increases to infinity. In other words, the marriage of multiplexing-based MIMO antenna schemes and multiuser scheduling techniques can achieve an elegant cross-layer synergy of providing further capacity and reliability performance improvements in a cost-effective manner.

Finally, the type of interference suppression based antenna schemes (or antenna beamforming) is investigated for the time division duplex/code division multiple access (TDD/CDMA) system. We propose using antenna beamforming techniques to resolve the opposite direction interference problem in the TDD/CDMA system. Through exploiting the multiple antennas of adjacent base stations from the network point of view, we introduce a simultaneous downlink transmit beamforming and uplink receive beamforming scheme to alleviate the impact of the opposite direction interference. Our analysis and results demonstrate that the proposed antenna beamforming scheme can effectively suppress the opposite direction interference with an economical implementation cost.

Acknowledgement

Foremost, I would like to express my sincere gratitude to my advisor, Dr. Li-Chun Wang, for providing me insights into important research problems, encouragement and support throughout my Ph.D. studies. This work could not have been done without his advice, guidance and comments.

Special thanks go to my mates at Wireless Network Lab. in NCTU and my colleagues at Chunghwa Telecommunication Labs. in Chung-Li for their kind help in many aspects.

Finally, I am deeply indebted to my family whose love and understanding have accompanied me through this long journey.

Contents

List of Figures

xiii

List of Tables

Notations

- $|a|$: magnitude of the scalar a

- $\mathbf{I}_n$: $n \times n$ identity matrix

- $\mathbf{A}^H$: complex conjugate transpose of the matrix $\mathbf{A}$

- $\mathbf{A}^{-1}$: inverse of $\mathbf{A}$

- $\mathbf{A}^T$: transpose of $\mathbf{A}$

- $[\mathbf{A}]_{ij}$: (i, j)-th entry of $\mathbf{A}$

- $\mathbf{A}^\dagger$: pseudoinverse of $\mathbf{A}$

- $\|\mathbf{A}\|_F$: Frobenius norm of $\mathbf{A}$

- $\mathrm{tr}(\mathbf{A})$: trace of $\mathbf{A}$

- $\det(\mathbf{A})$: determinant of $\mathbf{A}$

- $\mathrm{E}[\,\cdot\,]$: expectation operation

- $\mathcal{CN}(0, 1)$: complex circular symmetric Gaussian random variable

- $E_r(x)$: exponential integer function of order r, defined as $E_r(x) = \int_1^\infty e^{-xt} t^{-r} dt$

- $\Gamma(x)$: gamma function, defined as $\Gamma(x) = \int_0^\infty t^{x-1} e^{-t} dt$

- $\Gamma(a, x)$: incomplete gamma function, defined as $\Gamma(a, x) = \int_x^\infty t^{a-1} e^{-t} dt$

- $\tilde{\Gamma}(a, x)$: normalized incomplete gamma function, defined as $\widetilde{\Gamma}(a, x) = \frac{1}{\Gamma(a)} \int_0^x t^{a-1} e^{-t} dt$

- $\Gamma_a(x)$: complex multivariate gamma function, defined as $\Gamma_a(x) = \pi^{a(a-1)/2} \prod_{i=1}^a \Gamma(x - i + 1)$

- $\psi(x)$: psi function, defined as $\psi(x) = -\beta + \sum_{k=1}^{x-1} k^{-1}$ for integer x
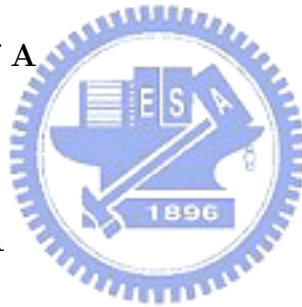
- $X_{1:L} \leq \cdots \leq X_{L:L}$: ordered statistics of a sample of size L from the random variable X

- $\phi_X(\omega)$: Laplace transform of the random variable X

- $f_X(x)$: PDF of the random variable X

- $f_{X_1,\cdots,X_N}(x_1,\cdots,x_N)$: joint PDF of the random variables $X_1 \cdots, X_N$

- $F_X(x)$: CDF of the random variable X

- $F_{X_1,\cdots,X_N}(x_1,\cdots,x_N)$: joint CDF of the random variables $X_1 \cdots, X_N$

- $\lceil x \rceil$: the smallest integer greater or equal to x

- $\min(x_1, x_2)$: minimum of x_1 and x_2

- β : Euler's constant $\simeq 0.5772$

Abbreviations

- AF : amount of fading

- CDF : cumulative distribution function

- CDMA : code division multiple access

- CSI : channel side information

- DCA : dynamic channel assignment

- DOA : direction of arrival

- EGC : equal gain combining

- EGT : equal gain transmission

- FDD : frequency division duplex

- IID : independent and identically distributed

- LCMV : linearly constrained minimum variance

- MAC : media access control

- MIMO : multiple input multiple output

- MISO : multiple input single output

- MMSE : minimum mean square error

- MVDR : minimum variance distortionless response

- MRC : maximum ratio combining

- MRT : maximum ratio transmission

- SC : selective combining
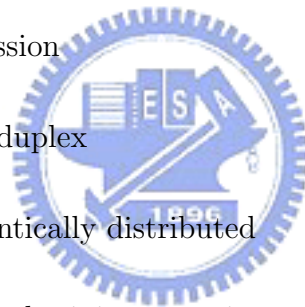
- ST : selective transmission

- STBC : space time block code

- SIMO : single input multiple output

- SISO : single input single output

- SNR : signal-to-noise ratio

- SWNSF : strongest-weakest-normalized-subchannel-first

- PDF : probability density function

- RR : round-robin

- SIC : successive interference canceller

- SVD : singular value decomposition

- TDD : time division duplex

- TDMA : time division multiple access

- UCA : uniform circular array

- ZF : zero-forcing
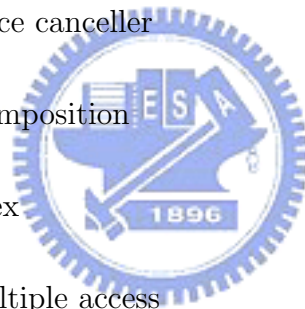
Symbols

- N_t : number of transmit antennas

- N_r : number of receive antennas

- K : number of users

- $C_{\text{link}}^{k^*}$: link capacity between the base station and the selected target user k^*

- $\langle C \rangle$: system capacity

- ρ : mean SNR

- p_{k^*} : probability of user k^* receiving services from the base station

- m : Nakagami fading parameter

- h_{ij} : channel gain from the jth transmit antenna to the ith receive antenna

- σ_n^2 : thermal noise power

- γ_k : effective output SNR at user k

- $\mathbf{H}_k$: normalized channel matrix between the base station and user k

- $\lambda_{\max}$: the maximum eigenvalue of $\mathbf{H}_k \mathbf{H}_k^H$

- f : amount of fading gain

- a : array gain

- S : selection order

- $\mathbf{x}_k$: transmit signal vectors for user k

- $\mathbf{y}_k$: receive signal vectors for user k

- $\mathbf{n}_k$: spatially white noise vectors for user k
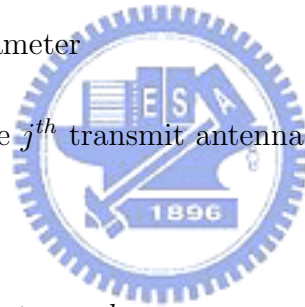
- $\mathbf{G}_k$: channel matrix between the base station and user k

- P_t : total transmit power of the base station

- μ : path loss exponent

- g_k : path loss for user k

- r_k : distance away from the base station

- $\{\lambda_{k,i}\}_{i=1}^N$: ordered eigenvalues of $\mathbf{H}_k \mathbf{H}_k^H$ with $\lambda_{k,N} \geq \lambda_{k,N-1} \geq \cdots \geq \lambda_{k,1} \geq 0$

- $S_{k,i}$: spacing random variable between $\lambda_{k,i}$ and the smallest eigenvalue $\lambda_{k,1}$

- γ_{th} : a predetermined SNR value

- P_{out} : outage probability

- $\tilde{\mathbf{H}}_k$: channel matrix selected by SWNSF scheduling

- $\{\tilde{\lambda}_{k,i}\}_{i=1}^N$: ordered eigenvalues of $\tilde{\mathbf{H}}_k \tilde{\mathbf{H}}_k^H$ with $\tilde{\lambda}_{k,N} \geq \tilde{\lambda}_{k,N-1} \geq \cdots \geq \tilde{\lambda}_{k,1} \geq 0$

- $\{\gamma_{k,i}\}_{i=1}^N$: ordered effective SNR at the subchannel output of the spatial multiplexing MIMO system with $\gamma_{k,N} \geq \gamma_{k,N-1} \geq \cdots \geq \gamma_{k,1} \geq 0$ for user k

- $\{\tilde{\gamma}_{k,i}\}_{i=1}^N$: ordered effective SNR at the subchannel output of the spatial multiplexing MIMO system with $\tilde{\gamma}_{k,N} \geq \tilde{\gamma}_{k,N-1} \geq \cdots \geq \tilde{\gamma}_{k,1} \geq 0$ for user k subject to SWNSF scheduling

- N : number of antennas at both ends of the spatial multiplexing MIMO system

- r : cell coverage subject to RR scheduling

- $\tilde{r}$: cell coverage subject to SWNSF scheduling

- C_k : link capacity for user k subject to RR scheduling

- $\tilde{C}_k$: link capacity for user k subject to SWNSF scheduling

- β : Euler's constant $\simeq 0.5772$

- C_{zf} : achievable link throughput for the zero-forcing receiver

- C_{opt} : achievable link throughput for the optimal receiver

- $\tilde{C}_{\mathrm{zf}}^{\mathrm{ma}}$, $\tilde{C}_{\mathrm{zf}}^{\mathrm{mi}}$, $\tilde{C}_{\mathrm{zf}}^{\mathrm{si}}$ and $\tilde{C}_{\mathrm{zf}}^{\mathrm{sg}}$: achievable link throughput for the zero-forcing receiver operating in the multiuser MIMO system with the max-max, max-min, spatially-independent and spatially-greedy scheduling policies, respectively

- $\tilde{P}_{\mathrm{out}}^{\mathrm{ma}}$, $\tilde{P}_{\mathrm{out}}^{\mathrm{mi}}$, $\tilde{P}_{\mathrm{out}}^{\mathrm{si}}$ and $\tilde{P}_{\mathrm{out}}^{\mathrm{sg}}$: outage probability for the zero-forcing receiver operating in the multiuser MIMO system with the max-max, max-min, spatially-independent and spatially-greedy scheduling policies, respectively

- $\{\tilde{\gamma}_{n:N}^{\mathrm{ma}}\}_{n=1}^{N}$, $\{\tilde{\gamma}_{n:N}^{\mathrm{mi}}\}_{n=1}^{N}$, $\{\tilde{\gamma}_{n:N}^{\mathrm{si}}\}_{n=1}^{N}$ and $\{\tilde{\gamma}_{n:N}^{\mathrm{sg}}\}_{n=1}^{N}$: ordered effective SNR at the subchannel output of the zero-forcing receiver operating in the multiuser MIMO system with the max-max, max-min, spatially-independent and spatially-greedy scheduling policies, respectively

- $\mathcal{B}_{sd}$ and $\mathcal{B}_{od}$: the set of the neighboring cells generating the same direction interference and the opposite direction interference, respectively

- K_j : number of active users in cell $j \in \mathcal{B}_{sd}$

- I_{od}, I_{sd} and I_{ic} : opposite direction interference, same direction interference and intra-cell interference, respectively

- P_r : the power-controlled level at the base station

- L : processing gain

- r_0 and r_{k_j} : the distance from mobile k_j $(j \in \mathcal{B}_{sd})$ to cell 0 and to cell j, respectively

- $\mathbf{a}_k$: array manifold vector for the signal arriving from the target user k

- $\mathbf{b}_j$: array manifold vector for the signal arriving from the base station of cell $j \in \mathcal{B}_{od}$

- $\tilde{\mathbf{a}}_k$: array manifold vector for the signal transmitting to the target user k

- $\tilde{\mathbf{b}}_j$: array manifold vector for the signal transmitting from cell $j \in \mathcal{B}_{od}$

- $\mathbf{x}_k$, $\mathbf{x}_{od}$, $\mathbf{x}_{sd}$ and $\mathbf{x}_{ic}$: received signal vectors with contributions from the desired user k, opposite direction interference, same direction interference and intracell interference, respectively

- $\mathbf{\Phi}_x$: covariance matrix of the received signal vector

- $\mathbf{\Phi}_{od}$, $\mathbf{\Phi}_{sd}$ and $\mathbf{\Phi}_{ic}$: covariance matrix of the received opposite direction interference, same direction interference and intracell interference, respectively

- $\mathbf{\Phi}_k$: normalized covariance matrix of the received interference plus noise

- $\tilde{\mathbf{\Phi}}_{od}$: covariance matrix of the received opposite direction interference when the beamforming Scheme IV is used

- $\tilde{\mathbf{\Phi}}_k$: normalized covariance matrix of the received interference plus noise when the beamforming Scheme IV is used

- $\mathbf{w}_{bs}$ and $\mathbf{w}_{mv}$: combining weight for the beam-steering and MVDR beamformers, respectively

- $\tilde{\mathbf{w}}_{bs}$: beamforming weight for the transmit beam-steering beamformer

- $\tilde{K}_j$: number of active users in cell $j \in \mathcal{B}_{od}$

- B : number of cells generating the opposite direction interference

- N : number of antenna elements at the base station for beamforming

- $c_k(\cdot)$: spreading code of user k

- T : bit duration

- $u_k(\cdot)$: bit waveform of user k

- τ_k : propagation delay of user k

- γ_{bs}, γ_{mv}, $\tilde{\gamma}_{bs}$ and $\tilde{\gamma}_{mv}$: the resulting bit energy-to-interference density ratio subject to the beamforming Schemes I, II, III and IV, respectively

Chapter 1

Introduction

As a famous quote in the movie Jurassic Park says, "Life will find a way," so will an innovation of thinking find a way, too. An ancient wisdom has also taught us how to escape from a deadlock of our lives: step back, take another broader view and we will find a whole different world. This philosophy turns out to be useful for designing practical wireless systems to meet the challenge of achieving higher bandwidth efficiency for the ever-increasing data rate requirement in the future. In response to this philosophy, this dissertation is going to present a story about a beautiful encounter of the multiple-input multiple-out (MIMO) antenna technique with its underlying wireless systems that may provide a different look to view the MIMO technique.

One of key techniques that promise significant capacity improvements for a wireless system is the MIMO antenna technique. This magic basically derives from an exciting theoretical prediction that the capacity of a MIMO system can be scalable with the number of antennas employed at both ends of the transmitter and receiver [1]. However, the advance of MIMO techniques does not only bring enthusiasm but also skepticism. The main concerns lie in receiver complexity [2] and the accompanying side effect of reliability performance degradation for the MIMO system [3]. Traditionally, many efforts made in resolving these concerns associated with the MIMO technique are mostly based on the physical layer treatment. This dissertation, however, adopts a network perspective approach to revisit the MIMO technique with an aim to provide an alternative settlement. Specifically, we will

consider the multiuser scheduling and time division duplex/code division multiple access (TDD/CDMA) systems with MIMO techniques.

Multiuser scheduling systems provide an opportunity for the multiple antennas among different users to cooperate with each other. A consequence of such a cooperation, from a network point of view, is an expansion of available dimensions since the number of exploitable antennas is virtually increased to the sum of the multiple antennas from all users. The additional dimension can be utilized to improve the system performance as well as reduce the implementation complexity of the MIMO receiver. Interestingly, what makes this happen is just a shift of a point of view: from the point-to-point perspective to the point-to-multipoint network perspective. The use of scheduling techniques for a wireless system, suggested in great part by the latest development of information theory, can take advantage of the delay-tolerant data characteristics to deliver a multiuser diversity gain. This system-wide benefit resulting from the scheduling strategy can be illustrated by an analogy of the water-filling principle: pouring the resource to the user with best channel quality. Wireless standards IS-856 [4] and 3GPP R5 [5] (the upgraded systems of cdma2000 and WCDMA) have changed the downlink design into a multiuser scheduling system for supporting efficient and high speed packet data access.

Another example that is used to demonstrate the strength of the network perspective approach is the cooperation of multiple antennas among different adjacent cells in the TDD/CDMA system. The story, however, is somewhat different from the multiuser scheduling system. In TDD/CDMA systems, the downlink capacity can be greatly enhanced to support asymmetric traffic by simply allocating different numbers of time slots for uplink and downlink transmissions. Nevertheless, this merit can invoke a severe opposite direction interference problem among adjacent cells of the TDD/CDMA system [6]. The issue of opposite direction interference, if not properly tackled, may hinder the TDD/CDMA system from being deployed in a large-scale network with multiple cells. From the network perspective to invite a cooperation between multiple antennas from adjacent cells, this dissertation will

show that a search for effective and economical antenna techniques to resolve the opposite direction interference issue thus becomes possible.

In summary, this dissertation is an attempt to exploit the possible interaction and cooperation between the MIMO technique and its underlying wireless system to simultaneously enhance the system performance and reduce implementation cost. The key idea behind the network perspective methodology is to encourage a full exploitation of all the available dimensions within the whole wireless network. While the dissertation focuses on the multiuser scheduling and TDD/CDMA systems, it is our hope that the network perspective design methodology can be also applied to the other wireless systems in the future.

1.1 Problem and Solution

The main question addressed here is: how to effectively and efficiently use the multiple antenna technique on top of the multiuser scheduling and TDD/CDMA systems? The research of multiple antenna techniques has been a fertile area in the history. Nevertheless, most of the studies are based on a point-to-point view without contemplating the interplay between the multiple antenna technique with its underlying communication system. In this dissertation, from a network point of view, we explore the interaction between the multiple antenna technique and the communication system to develop effective strategies for utilizing the MIMO technique on top of the multiuser scheduling and TDD/CDMA systems. Towards this end, the following methodology is adopted:

1. Examine the degrees of freedom that the various multiple antenna techniques can provide.

2. Distill the essences of the multiuser scheduling and TDD/CDMA communication systems.

3. Develop analytical frameworks to evaluate the marriage of different types of multiple antenna techniques and the considered communication system.

4. Suggest strategies to leverage the synergy of combining the multiple antenna techniques with the multiuser scheduling and TDD/CDMA systems.

As will be seen in the rest of the dissertation, there exist interesting and profound connections between the multiple antenna technique and its underlying communication system. Examples and results for illustrating the strength of the network perspective approach will be demonstrated later in the dissertation.

The following addresses the issues of combining the multiple antenna technique with the multiuser scheduling and TDD/CDMA systems.

1.1.1 Fading Mitigation Based Antenna Techniques for Multiuser Scheduling Systems

In point-to-multipoint communication systems, a special type of diversity, called the multiuser diversity, can be exploited to improve spectral efficiency [7, 8]. This kind of diversity can be explained as an analogy of the water-filling principle across multiple users: higher system spectral efficiency can be attained by pouring more resources to the user with better channel quality. A proper scheduling algorithm is the key to extract the multiuser diversity inherent in the multiuser system [9, 10, 11]. Some current industrial standards, such as the IS-856 [4] and the 3GPP R5 [5], have adopted scheduling techniques to enhance spectral efficiency for delay-insensitive data services.

Generally speaking, scheduling is a media access control (MAC) layer technique to deliver multiuser diversity gain by taking advantage of independent channel variations among user population. By contrast, antenna diversity is a physical layer approach to offer reliable transmissions with the major goal of mitigating channel fading. In a multiuser system where a channel-aware scheduling algorithm arranges transmissions based on the link quality of multiple users, various antenna diversity schemes may provide different effective link statistics and ultimately may lead to distinct capacity results with the effect of scheduling. Thus, the cross-layer interaction between antenna diversity and multiuser scheduling is not

straightforward and requires careful investigations. An analytical framework will be established to reveal insights into the interlay of antenna diversity and multiuser scheduling in Chapter 3.

1.1.2 Throughput Enhancement Based Antenna Techniques for Multiuser Scheduling Systems

Using the spatial multiplexing technique to transmit signals over a MIMO channel has attracted great attentions because of its capability to deliver remarkable capacity gain [1, 12, 13]. However, recent studies have revealed that the large capacity benefit resulting from the spatial multiplexing MIMO system may come at the price of link reliability degradation when the prior channel information is not available at the transmitter [3, 14]. In [3], the authors derived an optimal tradeoff curve for the maximum achievable diversity gain of an open-loop MIMO system given any realized multiplexing gain. In [14], the authors quantitatively evaluated some practical diversity-based and multiplexing-based MIMO schemes. Their numerical results indicated that it is difficult to simultaneously accomplish both diversity gain and multiplexing gain in an open-loop MIMO system. Due to the tradeoff of antenna multiplexing gain against antenna diversity gain, applying the spatial multiplexing scheme to transmit data over the MIMO channel may lead to smaller coverage areas subject to the same total transmit power and link reliability requirement. How to pursue high throughput with the spatial multiplexing MIMO scheme while maintaining satisfactory link reliability remains an open research issue. In Chapter 4, we will propose a scheduling scheme, called the strongest-weakest-normalized-subchannel-first (SWNSF) scheduling, to replenish the diversity-deficient MIMO multiplexing system with multiuser diversity.

1.1.3 Throughput Enhancement Based Antenna Techniques for Multiuser Scheduling Systems with Zero-Forcing Receivers

One popular approach to achieve the promised remarkable capacity gain of the MIMO system is the spatial-multiplexing method by sending parallel data streams across N_t multiple transmit antennas [2]. In order to decode the spatially multiplexed signals over the MIMO

system, various receiver architectures such as the zero-forcing receiver, the MMSE receiver and the successive interference canceller (SIC) have been introduced in the literature [13, 15]. Generally speaking, the performance enhancement from one type of MIMO receivers to another usually comes at the price of higher implementation cost. For example, the zero-forcing receiver is known to suffer from the effect of noise enhancement despite its simplicity. The SIC-based receiver, on the other hand, can possibly achieve the full capacity gain of the MIMO system with much higher complexity [16]. In contrast with those pure physical layer approaches, in Chapter 5 we will leverage the cross-layer cooperation between the simple zero-forcing receiver and scheduling technique to realize the full theoretical capacity of the MIMO channel.

1.1.4 Interference Suppression Based Antenna Techniques for TDD/CDMA Systems

One of the key advantages for the TDD system is the capability to deliver asymmetric traffic services by allocating different numbers of uplink and downlink time slots. However, in a TDD/CDMA system, asymmetric traffic may result in severe opposite direction interference because downlink transmitted signals from neighboring base stations may interfere with the uplink received signals of the home cell. In the literature, there are two research directions to avoid the opposite direction interference. The first research direction is from the perspective of channel assignment techniques, such as [17, 18]. Another research direction to alleviate the impact of the opposite direction interference in TDD/CDMA systems is to apply advanced antenna techniques [19, 20, 21]. Compared with other categories of smart antenna technology, beamforming is known for its capability of suppressing strong interference [22, 23]. In addition, beamforming can easily exploit the reciprocity of TDD channels to leverage the benefit of joint downlink and uplink beamforming. In Chapter 6, we will investigate the effect of beamforming technique to resolve the opposite direction interference in TDD/CDMA systems.

1.2 Dissertation Outline

This dissertation deals with the topics of combining the multiple antenna technique with the multiuser scheduling and TDD/CDMA systems. To be explicit, the multiple antenna techniques are categorized according to their design purposes into three families:

- Fading mitigation based antenna techniques.

- Throughput enhancement based antenna techniques.

- Interference suppression based antenna techniques.

Chapter 2 provides an overview of multiple antenna techniques that fall into the three categories and a brief introduction of the multiuser scheduling and TDD/CDMA communication systems. Fig. 1.1. illustrates the organization of the remaining chapters of the dissertation.

Chapter 3 investigates the interplay between the fading mitigation based antenna technique and the multiuser scheduling system. A unified capacity formula that connects the ingredients of fading characteristics, multiuser scheduling gain and antenna diversity gain is derived here. Through the unified capacity analysis, the interaction between multiuser scheduling techniques and various diversity-based antenna schemes will be unveiled.

Chapter 4 discusses the marriage of the throughput enhancement based antenna technique and the multiuser scheduling system. From the diversity-multiplexing compensation point of view, it is shown that the scheduling technique can significantly improve the degraded reliability performance of the multiplexing-based MIMO system while further enhancing the throughput performance. The outcome of cell coverage extension and system capacity improvement is shown in this chapter to substantiate this benefit.

Chapter 5 revisits the topic of combining the throughput enhancement based antenna technique with the multiuser scheduling system. In contrast with Chapter 4 where the optimal receiver is assumed, this chapter considers the zero-forcing receiver. By showing that the efficiency of the zero-forcing can approach that of the optimal receiver in the multiuser
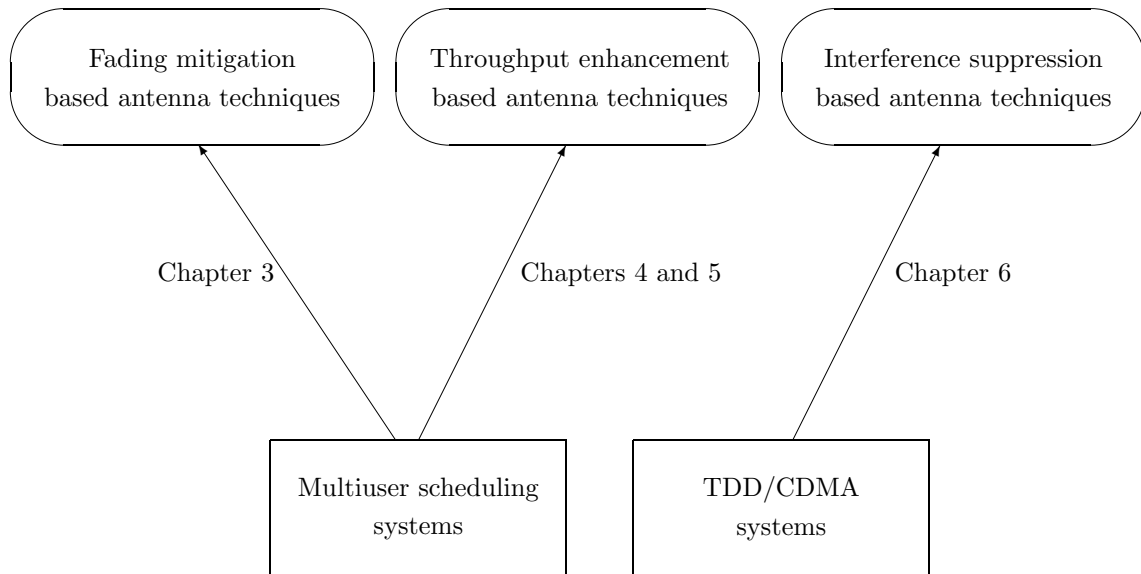
Figure 1.1: Chapter organization of the dissertation.

MIMO system with many users, this chapter endorses the elegant marriage of the throughput enhancement based antenna technique with the multiuser scheduling system.

Chapter 6 shifts the focus to the TDD/CDMA system. The interference suppression based antenna technique is investigated to resolve the opposite direction interference for the TDD/CDMA system. By exploiting the cooperation among multiple antennas of adjacent base stations, a low-cost and feasible scheme is introduced in this chapter.

Finally, Chapter 7 provides some concluding remarks and suggests topics for future research.

Chapter 2

Background and Literature Survey

2.1 Overview of Multiple Antenna Techniques

Consider a point-to-point link with N_t transmit antennas and N_r receive antennas or an (N_t, N_r) multiple-input multiple-output (MIMO) system. When only multiple antennas are employed at one end, multiple-input single-output (MISO) and single-input multiple-output (SIMO) are used to denote the $(N_t, 1)$ and $(1, N_r)$ MIMO systems, respectively. Likewise, for $N_t = N_r = 1$ the MIMO reduces to the single-input single-output (SISO) system. In the literature, dozens of antenna techniques have been developed to exploit the additional spatial (antenna) domain. Based on the design purpose, the multiple antenna technique can be classified into three categories: fading mitigation based antenna techniques, throughput enhancement based antenna techniques and interference suppression based antenna techniques.

2.1.1 Fading Mitigation Based Antenna Techniques

This family of fading mitigation based antenna techniques are basically designed for compensating again channel fading so as to provide stable channel variations. The central principle behind this category of antenna schemes is to produce independent replicas of the desired signal over the MIMO channel so that the receiver can utilize the multiple faded copies to restore the original signal with higher reliability. In order to guarantee high degrees of independence, the fading mitigation based antenna technique generally requires the multiple
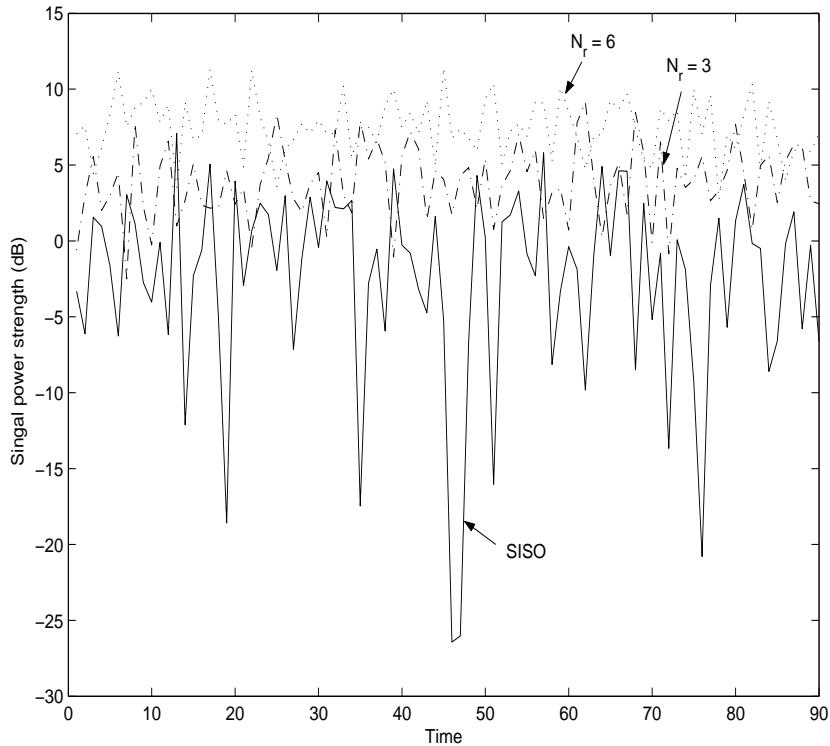
Figure 2.1: The link variation induced by the SISO system and the SIMO system with the fading mitigation based antenna technique under Rayleigh fading.

antennas be widely spaced.

What mostly characterizes the fading mitigation based antenna technique is its capability of delivering *antenna diversity gain* to mitigate channel fading. For simplicity, we shall also call the fading mitigation based antenna technique as the diversity-based antenna technique in this dissertation. Fig. 2.1 illustrates the induced link variation by using the fading mitigation based antenna technique under Rayleigh fading. Compared with the SISO system, one can see that the link fluctuation is more damped for the SIMO system with the diversity-based antenna scheme.

An operational definition for the antenna diversity gain can be made as follows. Assuming that an uncoded data signal is sent through the MIMO system and P_e is the resulting error probability at the receiver, the antenna diversity gain D can be measured by [3]

$$D = - \lim_{\rho \to \infty} \frac{\log \left(P_e(\rho) \right)}{\log \rho} \ , \tag{2.1}$$

where ρ is the operating signal-to-noise ratio (SNR). The definition of (2.1) states that the
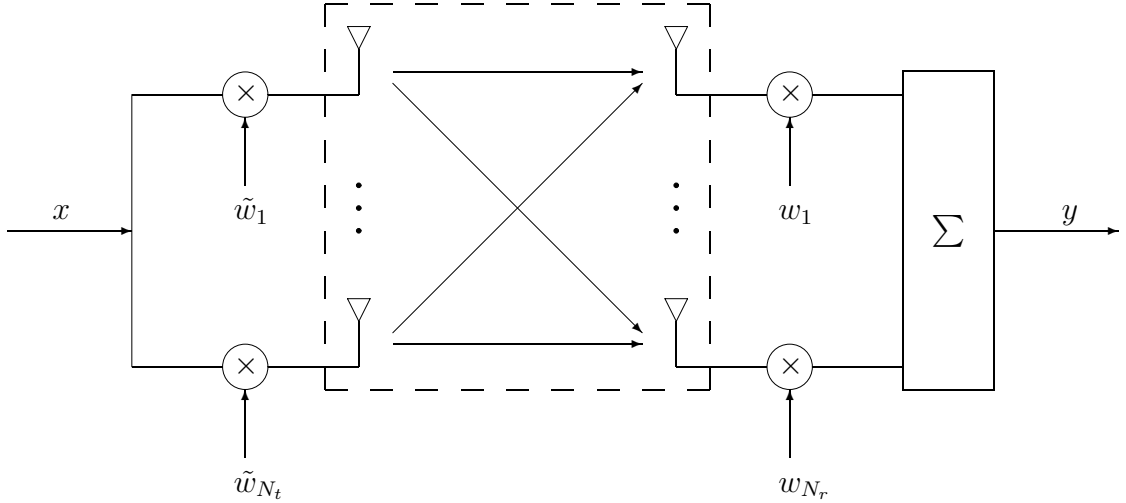
Figure 2.2: A generic fading mitigation based antenna scheme over the (N_t, N_r) MIMO system, where $\mathbf{w}_t = [\tilde{w}_1, \cdots, \tilde{w}_{N_t}]^T$ and $\mathbf{w}_r = [w_1, \cdots, w_{N_r}]^T$ are the transmit and receive antenna weights designed for delivering diversity.

antenna diversity gain corresponds to the slope of the error probability versus SNR curve on a log-log scale at the high SNR regime. When each antenna pair between the transmitter and receiver encounters independent fading, the maximum diversity gain that can be extracted from an (N_t, N_r) MIMO system is $D_{\max} = N_t N_r$.

Figure 2.2 illustrates a generic fading mitigation based antenna scheme for the MIMO system. With the properly designed antenna weights at the transmitter and/or receiver, some representative antenna schemes capable of delivering full antenna diversity gain are introduced as follows.

- For the SIMO system, receive methods such as selective combining (SC), equal gain combining (EGC) and maximum ratio combining (MRC) are commonly used to provide diversity gain [24, 25, 26].

- For the MISO system, transmit methods like selective transmission (ST), equal gain transmission (EGT) and maximum ratio transmission (MRT) can be also utilized to yield diversity gain [13, 27]. Compared with the receive methods, the implementation of transmit methods generally requires the prior channel knowledge at the transmitter. To overcome this weakness, the space time block code (STBC) method was introduced by [28, 29]. By putting different levels of correlation across the multiple transmit

11
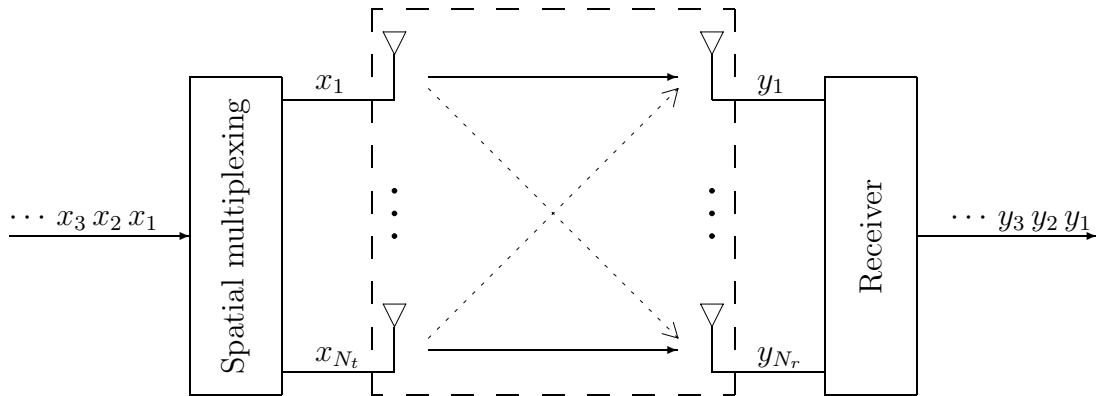
Figure 2.3: A generic spatial multiplexing MIMO system, where the dotted lines represent inter-subchannel interference.

antennas as well as several time slots, the STBC method can achieve full antenna diversity gain without the requirement of prior channel side information (CSI).

- For the MIMO system, both transmit and receive diversity can be obtained by using the hybrid schemes such as ST/MRC [30], EGT/EGC [31] and MRT/MRC [32, 33]. The STBC method can be also applied to the MIMO system with proper generalizations [34, 35].

2.1.2 Throughput Enhancement Based Antenna Techniques

A different line of thinking to design antenna schemes focuses on exploiting the spatial dimensions to enhance the transmission throughput. The development of this category of antenna schemes is mostly inspired by the pioneering works [1, 12, 36] where a theoretically remarkable capacity benefit from the MIMO system was predicted under the Rayleigh fading channel. Since that, a lot of efforts have been made to realize the promised capacity benefit by devising practical antenna techniques.

One popular approach to fulfill the promised capacity gain of the MIMO system is the spatial multiplexing method [2]. As shown in Fig. 2.3, the spatial multiplexing MIMO system sends parallel data streams across N_t transmit antennas. In case the channel exhibits

rich scattering and the receiver has N_r multiple antennas satisfying $N_r \geq N_t$, the spatially multiplexed signals can be successfully restored at the receiver, thereby providing an capacity gain or *multiplexing gain* approximately N_t times the SISO system [37]. However, the successful recovery of the spatially multiplexed signals calls for effective inter-subcahnnel interference cancellation mechanisms.

Various receiver architectures such as the zero-forcing (ZF) receiver, the minimum-mean-square-error (MMSE) receiver and the successive interference canceller (SIC) have been introduced to recover the spatially multiplexed signals in the literature [13, 15]. Generally speaking, the performance improvement from one type of the spatial multiplexing MIMO receiver to another usually comes at the price of higher implementation cost. For example, the zero-forcing receiver is known to suffer from the effect of noise enhancement despite its simplicity. By comparison, the SIC-based receiver can possibly achieve the full capacity gain of the MIMO system with much higher complexity [16]. Other receiver designs that try to reduce complexity while maintaining high performance can be also found, for example, in [38].

The multiplexing gain of an (N_t, N_r) MIMO system can be defined as [3]

$$R = \lim_{\rho \to \infty} \frac{\log (C(\rho))}{\log \rho} \ , \tag{2.2}$$

where $C(\rho)$ is the ergodic capacity of the MIMO system operating at the SNR condition of ρ. Accordingly, it is followed from [1] that the maximum multiplexing gain that can be achieved from an (N_t, N_r) MIMO system is $R_{\max} = \min(N_t, N_r)$. Since this category of antenna techniques feature the desirable linear growth of multiplexing gain, we will also call the throughput enhancement based antenna technique as the multiplexing-based antenna technique in the dissertation. Using the definition of (2.1) and (2.2), [3] theoretically demonstrated a fundamental tradeoff between the achievable diversity gain and multiplexing gain in an open-loop MIMO system. Similarly, [14] quantitatively evaluated several existing MIMO antenna schemes and concluded that it is difficult to simultaneously accomplish both diversity gain and multiplexing gain. Based on this understanding, some recent works such
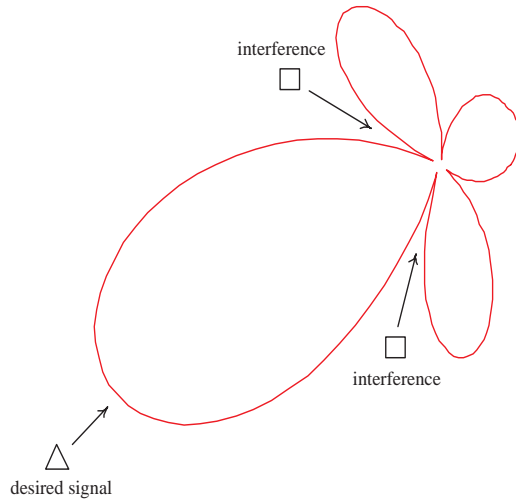
Figure 2.4: A beamforming pattern that receives a signal from a specific location and attenuate signals from other locations.

as [39] began to seek new coding schemes that provides flexible adjustment between the maximum achievable diversity gain and the maximum achievable multiplexing gain over the MIMO system.

2.1.3 Interference Suppression Based Antenna Techniques

Another aspect of using multiple antennas is to lay stress on its capability of rejecting strong interference. By exploiting the angular resolution provided by the antenna arrays, the interference suppression based technique can effectively cancel interference radiating from certain directions [40, 41, 22]. In order to ensure good resolvability in the angular domain, this category of antenna schemes generally requires the antenna arrays to be densely spaced [42]. In addition, antenna topology is relevant for the antenna arrays to create different spatial signatures that can result in different angular selectivity.

While other antenna techniques such as [43] can have the good capability of cancelling interference, we restrict to the antenna beamforming technique (also known as adaptive antenna array technique) as the interference suppression based technique is referred in this dissertation. The term "beamforming" derives from the fact that early spatial filters were

designed to form pencil beams to receive a signal from a specific location and attenuate signals from other locations [40]. As shown in Fig. 2.4, the beamforming pattern is commonly used to describe the angular resolvability of an antenna array. Some antenna beamforming schemes designed for reception or transmission are introduced as follows.

- For the SIMO system, receive beamforming techniques such as the beam-steering beam-former, minimum variance distortionless response (MVDR) beamformer and linearly constrained minimum variance (LCMV) beamformer can be used to perform spatial filtering [23, 44]. Generally speaking, in the $(1, N_r)$ SIMO system the degrees of freedom that can be used to cancel the undesired interference signals is $(N_r - L)$, where L is the number of constrains imposed on the optimization criterion in deriving the receive beamforming weight [40].

- For the MISO system, transmit beamforming schemes such as the transmit beam-steering beamformer can be used to concentrate the transmission energy towards the desired direction [42, 45]. Transmit beamforming differs from receive beamforming in that the desired signals from multiple users are only coupled by the transmission power, but also by the shape of the radiation pattern [46]. This poses a more difficult challenge for optimal transmit beamforming designs since the transmit power and beamforming weight for all users have to be jointly considered. Various optimal beamforming algorithms based on different optimization criteria can be found in [46, 47].

2.2 Introduction of Multiuser Scheduling Systems

Industrial standards such as IS-856 [4] and 3GPP R5 [5] are multiuser scheduling systems supporting high speed downlink packet data access. In this dissertation, we adopt IS-856 as a reference model to investigate the characteristics of the multiuser scheduling system.
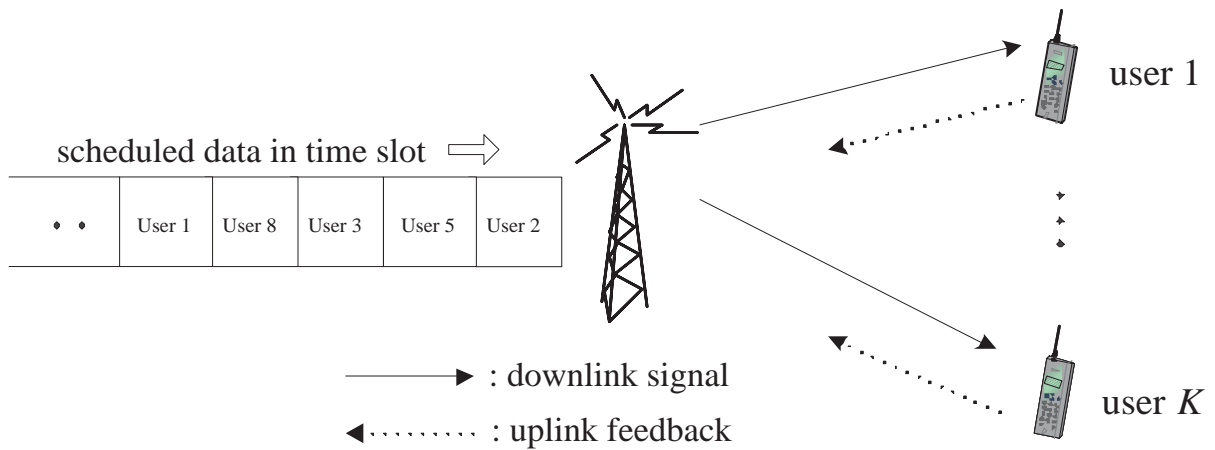
Figure 2.5: A downlink multiuser scheduling system with TDMA protocol.

2.2.1 Scheduling Technique and Multiuser Diversity

Consider a multiuser scheduling system with the base station serving K downlink users as shown in Fig. 2.5. The basic operations of the multiuser scheduling system supporting high speed downlink packet data access are described as follows [48].

- The time-division-multiple-access (TDMA) protocol is adopted for the base station to service one user at a time slot.

- Each user measures and tracks its channel condition via the downlink common pilot signal and reports back to the base station through the uplink feedback channel.

- With the channel information from the feedback of all users, the base station determines to service one target user according to certain scheduling policies.

- Once the target user is selected, the base station uses the rate control adaptive modulation to transmit as many information bits as possible to the target user with its full transmit power.

By taking advantage of delay-tolerant data characteristics, the scheduling technique can extract the *multiuser diversity* from such the multiuser system to improve spectral efficiency [7]. The multiuser diversity gain can be explained as an analogy of the water-filling principle

16

across multiple users: pouring more resources to the user with better channel quality [8]. While allocating more resources to the user with better channel quality, the system may immediately face another key issue – how to schedule the transmissions for other users whose channel qualities are poor. Therefore, one of the major challenges in designing wireless scheduling algorithms is to achieve higher total system throughput but without sacrificing fairness to individual users too much.

A literature survey regarding the wireless scheduling technique is discussed as follows. [49, 50] modified the fair scheduling policies used in traditional wireline systems to the wireless. However, their scheduling algorithms assume a simple two-state on-off channel model, which may not be able to fully capture all the wireless channel characteristics. In [9, 10, 51], several wireless scheduling algorithms were evaluated by Monte Carlo simulations for practical radio channels. In [52] and [53], it was shown that one-by-one time division scheduling scheme is better than the code division scheme from the standpoints of higher energy efficiency and better received signal quality, respectively.

2.2.2 Scheduling for Multiuser MIMO Systems

The multiuser scheduling system in Fig. 2.5 can be extended to the multiuser MIMO system. A multiuser MIMO system consists of the base station employed with N_t transmit antennas and K multiple users employed with N_r receive antennas each. Accordingly, each link between the base station and individual user constitutes an (N_t, N_r) MIMO system.

Generally speaking, scheduling is a media access control (MAC) layer technique to deliver multiuser diversity by exploiting independent channel variations among user population. By contrast, the multiple antenna technique is a physical layer approach to improve the performance of wireless links. A probe into the cross-layer interaction between the multiple antenna technique and multiuser scheduling has recently attracted attentions in the research community. In particular, a literature survey associated with the topic of scheduling for multiuser MIMO systems is discussed as follows.

- A number of works that used the fading mitigation based antenna techniques for the multiuser scheduling system can be found, for example, in [11, 51] and [54]-[58]. In [11], Viswanath and Tse proposed an opportunistic transmission scheme to increase the capacity of the multiuser scheduling system requiring only limited feedback. In [51], the authors conducted computer simulations to evaluate the capacity of the multiuser MIMO system with the ST and STBC antenna schemes. In [54], a semi-analytical result of spectral efficiency with the MRC antenna scheme and K-order multiuser diversity was derived. In [55], the impact of multiuser scheduling on the STBC methods was discussed in terms of the receive SNR distribution. Also, information theoretical treatments for the multiuser MIMO system with antenna diversity were provided in [56, 57, 58].

- Relatively, fewer works have taken advantage of scheduling techniques to improve the performance of the multiuser MIMO system with multiplexing-based antenna schemes, such as [59, 60]. Through simulation, the authors in [59] showed that multiuser diversity can provide additional capacity gain for the multiplexing-based MIMO system with linear receivers. In [60], the authors harnessed multiuser diversity to enhance the capacity of the multiplexing-based MIMO systems using a random beamforming technique.

- When the base station is allowed to simultaneously transmit multiple beams to different users (that is, not restricted to the TDMA protocol), both the temporal and spatial (antenna) domains can be exploited by scheduling to provide higher selection diversity order [61]-[64]. Because the signals to be transmitted for the multiple users are interfered with each other, the spatial-temporal domain scheduling is usually combined with additional pre-transmit signal processing techniques such as dirty-paper coding to achieve better performance [65]-[67].

In Chapter 3, we will introduce a unified analytical framework to investigate the capacity of the multiuser MIMO system with various diversity-based antenna schemes. In Chapters

4 and 5, we will discuss the topic of combining the multiplexing-based antenna scheme with the multiuser scheduling system.

2.3 Introduction of TDD/CDMA Systems

Time division duplex (TDD) is a duplex scheme where both uplink and downlink traffic takes place in the same unpaired frequency band. By allocating different numbers of slots for uplink and downlink, the TDD system can support asymmetric traffic services with great flexibility [68, 69]. Another merit of the TDD system over the frequency division duplex (FDD) system is the channel reciprocity that can be exploited to implement, for example, efficient open-loop power control [68, 70], pre-equalization [71, 72] and pre-rake diversity technique [73, 74]. With these advantages, modern cellular standards such as [75] have incorporated the TDD mode into their system designs.

2.3.1 Opposite Direction Interference

Despite the advantage of flexibly supporting traffic asymmetry in the TDD system, the TDD/CDMA system may pose a severe *opposite direction interference* problem across cells due to the universal frequency reuse of CDMA [6]. Figure 2.6 illustrates the typical interference scenario in the TDD/CDMA system. Assume that cells A and B in the figure have different rates of traffic asymmetry and allocate time slots independently according to their own traffic requirements. During a particular time slot t_o, one can find that the uplink received signals at cell A may suffer strong interference from the downlink transmitted signals of the neighboring cell B. In this dissertation, we call this kind of base stations to base stations interference the *opposite direction interference* because the desired signal is in the *uplink* direction, while the interference is from the *downlink* direction.

On the other hand, in time slot t_s of Fig. 2.6, the uplink transmissions from the users in cell B will interfere with the uplink signals of cell A. We call this kind of mobile stations to base stations interference the *same direction interference*. The same direction interference also occurs in FDD/CDMA systems. Many previous works, such as [76, 77], have analyzed

19
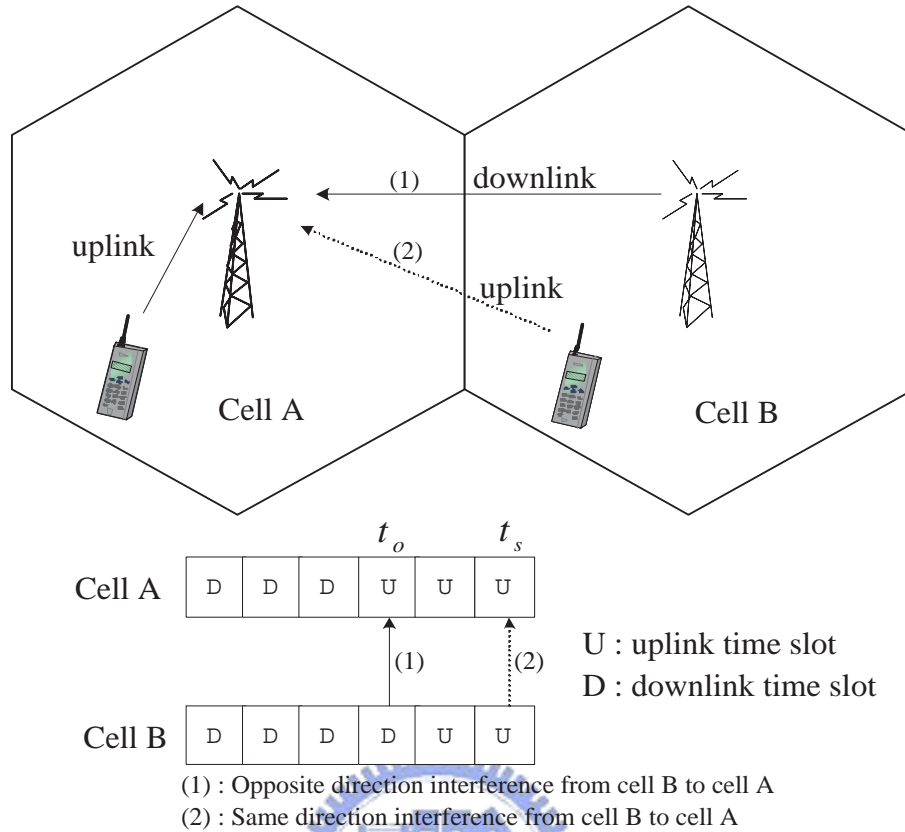
Figure 2.6: Opposite direction interference in the TDD/CDMA system.

the impact of the same direction interference. Thanks to power control mechanisms and other techniques, the impact of the same direction interference can be effectively managed in FDD/CDMA systems. However, the opposite direction interference, which is unique in TDD/CDMA systems, is substantially different from the same direction interference. First, it is difficult to coordinate many base stations throughout the entire service area to perform downlink power control simultaneously. Moreover, since the transmitter power of a base station is much higher than that of a mobile station, the opposite direction interference introduced by the neighboring base stations will severely degrade the quality of uplink signals transmitted from a mobile station [6, 78].

Usually, to avoid the opposite direction interference in TDD/CDMA systems, one can use different frequency carriers among adjacent cells. Obviously, this approach sacrifices frequency reuse efficiency. To use the same frequency carriers in every TDD/CDMA cell, one possible solution to avoid the opposite direction interference is to restrict all the neighboring

cells to adopting the same slot allocation pattern [79], i.e., all the assignments for either uplink or downlink transmissions in every time slot are the same. However, this approach implies that all cells will be forced to adopt the same rate of traffic asymmetry in the entire system, which is obviously not a very practical restriction. The key to relax this restriction is to overcome the opposite direction interference in the TDD/CDMA system. In the literature, there are two research directions to avoid the opposite direction interference:

- The first research direction is from the perspective of channel assignment techniques, such as [17, 18]. In [17], Haas and McLaughlin proposed a dynamic channel assignment algorithm to reduce the occurrence of the opposite direction interference due to asymmetric traffic. However, the authors in [18] concluded that it may be difficult to achieve the optimal time slot allocation in an environment with multiple TDD/CDMA cells.

- Another research direction to alleviate the impact of the opposite direction interference in TDD/CDMA systems is to apply the multiple antenna technique [19, 20, 21]. The authors in [19] and those in [20] proposed to adopt sector antennas combined with time slot allocation methods to suppress the opposite direction interference for the TDD/CDMA system and for the TDD/TDMA system, respectively. Furthermore, it was shown in [21] that the diversity-based SC and MRC antenna schemes are not feasible to resolve the opposite direction interference issue for the TDD/CDMA system.

In Chapter 6, we will investigate the effect of using the antenna beamforming technique to resolve the opposite direction interference in the TDD/CDMA system.

Chapter 3

Fading Mitigation Based Antenna Techniques for Multiuser Scheduling Systems

In this chapter, we develop an analytical framework to study the interaction between the fading mitigation based (or diversity-based) antenna technique and the multiuser scheduling system. We consider a multiuser scheduling system as described in Section 2.2. Under the generalized Nakagami fading channel model, we will derive a unified capacity formula applicable for the multiuser scheduling system with a number of fading mitigation based antenna schemes, including

- Selective transmission/selective combining (ST/SC), standing for that the selective transmission and selective combining schemes are utilized at the transmitter and the receiver, respectively.

- Maximum ratio transmission/maximum ratio combining (MRT/MRC).

- Selective transmission/maximum ratio combining (ST/MRC).

- Space-time block codes (STBC).

With a further change of parameters, the derived capacity formula can be versatile to interpret the interplay of antenna diversity and multiuser scheduling within the multiuser MIMO network.

3.1 Channel Model

To investigate the impact of channel fading on the multiuser scheduling system, this chapter considers the generalized Nakagami fading channel model. Consider a multiuser scheduling system with a base station serving K downlink users as shown in Fig. 2.5. To begin with, we assume that the base station and each user have only one single antenna. Let h_k be the channel gain between the base station and user k, and let σ_n^2 be the thermal noise power. Accordingly, $\gamma_k = |h_k|^2/\sigma_n^2$ denotes the received instantaneous SNR of user k. We assume that each link between the base station and any user is subject to independent Nakagami fading with a common Nakagami fading parameter m. Then, the probability density function (PDF) of the received SNR for user k is [24]

$$f_{\gamma_k}(\gamma) = \left(\frac{m}{\rho_k}\right)^m \frac{\gamma^{m-1}}{\Gamma(m)} \exp\left(-\frac{m\gamma}{\rho_k}\right), \quad \gamma > 0 \tag{3.1}$$

where ρ_k is the average received SNR, and $\Gamma(\cdot)$ is the gamma function defined by

$$\Gamma(m) = \int_0^\infty t^{m-1}e^{-t}dt \ . \tag{3.2}$$

When $m = 1$, the Nakagami fading channel is identical to the Rayleigh fading channel. For $m > 1$, a line-of-sight or a specular component exists. As $m \to \infty$, the Nakagami channel approaches to the AWGN channel.

To ease notation, we denote $X \sim \mathcal{G}(p, q)$ as a gamma distributed random variable with parameters p and q. Then, the PDF of X is given as [80]

$$f_X(x) = \frac{q^p}{\Gamma(p)}x^{p-1}e^{-qx}, \quad x > 0 \ . \tag{3.3}$$

Furthermore, the cumulative distribution function (CDF) of X can be expressed by

$$F_X(x) = \widetilde{\Gamma}(p, qx) \ , \tag{3.4}$$

where $\widetilde{\Gamma}(\cdot, \cdot)$ is the normalized incomplete gamma function defined by [82]

$$\widetilde{\Gamma}(a, x) = \frac{1}{\Gamma(a)} \int_0^x t^{a-1}e^{-t}dt \ . \tag{3.5}$$

23

Based on the above notation, the distribution of γ_k in the Nakagami fading channel model can be represented by $\gamma_k \sim \mathcal{G}\left(m, \frac{m}{\rho_k}\right)$. Next, we introduce two lemmas regarding the properties of gamma random variables, which will be used in Section 3.3.

Lemma 3.1 Let $X_1, X_2, \cdots, X_K$ be independent gamma random variables with parameters p_k and q, respectively. Let Y be the random variable given by $Y = X_1 + \cdots + X_K$. Then we have

$$Y \sim \mathcal{G}\left(\sum_{k=1}^{K} p_k, q\right) \quad . \tag{3.6}$$

Proof: Please refer to [80]. $\square$

Lemma 3.2 Let X be a gamma random variable with parameters p and q. Let Y be the random variable given by $Y = cX$, $c > 0$. Then we have

$$Y \sim \mathcal{G}\left(p, \frac{q}{c}\right) \quad . \tag{3.7}$$

Proof: The proof is completed by using a simple variable transformation $f_Y(y) = f_X(y/c)/c \sim \mathcal{G}\left(p, \frac{q}{c}\right)$. $\square$

3.2 System Capacity with Multiuser Scheduling

In this section, we derive the capacity expression for the multiuser scheduling system with only single antenna employed at the base station and all users. The basic operation of the multiuser scheduling system was described in Section 2.2. The base station is assumed to have the knowledge of $\{\gamma_k\}_{k=1}^{K}$ by means of the correct and instantaneous feedback from all users. We also assume that the channel variation remains constant over one time slot, but independently varies between different time slots. Accordingly, the base station shall determine to service one target user in every time slot according to certain scheduling policies.

3.2.1 Scheduling Policy and Conditional Link Capacity

The scheduling policy considered in this chapter is to select a target user k^* according to the following rule[1]

$$k^* = \arg\max_k \frac{\gamma_k}{\rho_k} \ , \tag{3.8}$$

where ρ_k is introduced in the denominator to resolve the fairness issue due to the near-far effect. In this chapter, we assume $\rho_k = \rho$ for all k to focus on the impact of the small-scale channel fading. The case of different ρ_k with large-scale path loss effect will be studied in the next chapter. Thus, the scheduling rule in (3.8) is reduced to

$$k^* = \arg\max_k \gamma_k \ . \tag{3.9}$$

Let $f_{\gamma_{\max}}(\gamma; p, q, K)$ be the PDF of $\max(\gamma_1, \cdots, \gamma_K)$, where $\{\gamma_k\}_{k=1}^K$ denotes a set of K independent and identically distributed (i.i.d.) gamma variates with parameters p and q. From [87], we can write

$$f_{\gamma_{\max}}(\gamma; p, q, K) = K f_\gamma(\gamma) \left[F_\gamma(\gamma)\right]^{K-1} \ , \tag{3.10}$$

where $f_\gamma(\gamma)$ and $F_\gamma(\gamma)$ are defined in (3.3) and (3.4). Let $f_{\text{link}}^{k^*}(\gamma)$ be the conditional PDF of the received SNR given that the connection between the base station and user k^* is established. Clearly, according to (3.9), we have

$$f_{\text{link}}^{k^*}(\gamma) = f_{\gamma_{\max}}(\gamma; p, q, K) \ . \tag{3.11}$$

Once the target user is determined, adaptive modulation is applied to transmit as many information bits as possible. From [81], the link capacity between the base station and the selected target user k^* then can be written as

$$C_{\text{link}}^{k^*} = \int_0^\infty \log(1 + \gamma) f_{\text{link}}^{k^*}(\gamma) d\gamma \ . \tag{3.12}$$

Note that the capacity expression in (3.12) is normalized to the bandwidth, thereby having the unit of nats/sec/Hz.

---

[1]The rule is slightly different from the proportional fair scheduling introduced in [9, 11]. If the data rate supported by the channel is proportional to SNR, both criteria are the same.

3.2.2 System Capacity Analysis

With link capacity, now we proceed to derive the system capacity. We define the system capacity as the sum of the link capacity delivered to each user on average. Let p_{k^*} denote the average probability of user k^* receiving services from the base station. Then the system capacity can be expressed by

$$\langle C \rangle = \sum_{k^*=1}^{K} C_{\text{link}}^{k^*} p_{k^*} \ . \tag{3.13}$$

We assume that the channel variations among multiple users are mutually independent so that $\{\gamma_k\}_{k=1}^{K}$ are i.i.d. across k. Thus, each user has the same probability to receive services from the base station or $p_{k^*} = 1/K$. Furthermore, the system capacity in (3.13) can be written as

$$\langle C \rangle = \frac{1}{K} \sum_{k^*=1}^{K} C_{\text{link}}^{k^*} = C_{\text{link}}^{k^*} \ . \tag{3.14}$$

Equation (3.14) implies that system capacity is equal to the conditional link capacity when a specific user is chosen from K users. In other words, the capacity gain is achieved by providing the system with multiuser diversity, i.e., more selections of independent channel variations experienced by multiple users. Finally, substituting (3.10) and (3.12) to (3.14) yields

$$\langle C \rangle = \frac{Kq^p}{\Gamma(p)} \int_0^\infty \log(1+\gamma) \left[\widetilde{\Gamma}(p, q\gamma) \right]^{K-1} \gamma^{p-1} e^{-q\gamma} d\gamma \ . \tag{3.15}$$

When the parameter p is an integer value, (3.15) can be derived as (see Appendix A)

$$
\begin{aligned}
\langle C \rangle &= \frac{K}{(p-1)!} \sum_{k=0}^{K-1} (-1)^k \binom{K-1}{k} e^{(k+1)q} \sum_{i=0}^{k(p-1)} a_i^k q^{p+i} \\
&\quad \cdot (p+i-1)! \sum_{j=1}^{p+i} \frac{(-1)^{p+i-j}}{(p+i-j)!} \left[\frac{1}{(k+1)q} \right]^j \left\{ E_1 \left((k+1)q \right) \right. \\
&\quad \left. - e^{-(k+1)q} \sum_{l=0}^{p+i-j-1} (-1)^l \, l! \left[\frac{1}{(k+1)q} \right]^{l+1} \right\} \\
&\triangleq \Lambda_1(p, q, K) \ , \tag{3.16}
\end{aligned}
$$

where a_i^k for $0 \le i \le k(p-1)$ can be recursively calculated by

$$
\begin{aligned}
a_0^k &= 1, \quad a_1^k = k, \\
a_i^k &= \frac{1}{i} \sum_{n=1}^{\min(i,\,p-1)} \frac{n(k+1)-i}{n!} a_{i-n}^k, \quad \text{for } 2 \le i < k(p-1), \\
a_i^k &= 1/[(p-1)!]^k, \quad \text{for } i = k(p-1) \;,
\end{aligned}
\tag{3.17}
$$

and $E_1(\cdot)$ is the exponential integral function of the first kind defined by [82]

$$
E_1(x) = \int_x^\infty \frac{e^{-t}}{t} dt \;.
\tag{3.18}
$$

As a result, for integer values of Nakagami fading parameter m, we have

$$
\langle C \rangle = \Lambda_1 \left(m, \frac{m}{\rho}, K \right) \;.
\tag{3.19}
$$

Some special cases of (3.19) can be further derived as follows:

- For the Rayleigh fading case ($m = 1$) with K-fold multiuser diversity, (3.19) is simplified to

$$
\langle C \rangle = K \sum_{k=0}^{K-1} (-1)^k \binom{K-1}{k} \frac{e^{(k+1)/\rho}}{k+1} E_1 \left(\frac{k+1}{\rho} \right) \;.
\tag{3.20}
$$

- For the single user case $K = 1$, multiuser diversity gain vanishes and (3.19) reduces to

$$
\langle C \rangle = \sum_{j=1}^m \frac{(-1)^{m-j}}{(m-j)!} \left(\frac{m}{\rho} \right)^{m-j} \left[e^{m/\rho} E_1 \left(\frac{m}{\rho} \right) - \sum_{l=0}^{m-j-1} (-1)^l l! \left(\frac{\rho}{m} \right)^{l+1} \right], \tag{3.21}
$$

which is identical to the link capacity of the Nakagami fading channel with optimal rate control [83, 84].

- For $m = 1$ and $K = 1$, (3.19) is simply reduced to the link capacity of the Rayleigh fading channel as shown in [85, 86]

$$
\langle C \rangle = e^{1/\rho} E_1 \left(\frac{1}{\rho} \right) \;.
\tag{3.22}
$$

When m is not restricted to an integer, (3.15) can be also efficiently computed with the help of the orthogonal Laguerre polynomial as follows:

$$
\begin{aligned}
\langle C \rangle &\simeq \frac{K}{\Gamma(p)} \sum_{i=1}^{N_L} w_i \log \left(1 + \frac{z_i}{q} \right) \left[\widetilde{\Gamma}(p, z_i) \right]^{K-1} z_i^{p-1} \\
&\triangleq \Lambda_2(p, q, K) \;,
\end{aligned}
\tag{3.23}
$$

27

where w_i and z_i are the weights and zeros of the Laguerre polynomial [82], and N_L is the order of polynomial chosen to make the approximation error negligibly small. Consequently, for the general Nakagami-m fading environments, the capacity of the multiuser scheduling system with K-fold multiuser diversity can be expressed by

$$\langle C \rangle = \Lambda_2 \left(m, \frac{m}{\rho}, K \right) \ . \tag{3.24}$$

With the expression (3.19) or (3.24), we have established a closed-form capacity formula that includes the contribution of K-fold multiuser diversity and the impact of Nakagami-m channel fading. Next, we give a numerical example using (3.19).

3.2.3 Impact of Channel Fading

Figure 3.1 shows the impact of Nakagami fading on the capacity of the multiuser scheduling system. The mean SNR is set to one, i.e. $\rho = 0$ dB, in this example. The information capacity of the AWGN channel with the same mean SNR is also plotted for comparison. From this figure, one can see that the capacity for $K = 1$ is always lower than that of the AWGN channel. Moreover, a more scattering environment with a smaller value of m yields lower capacity when $K = 1$. However, the story becomes totally different when more than one user reside in the system. One can find that, in the presence of multiuser diversity ($K \geq 2$), the capacity of the multiuser scheduling system is the highest for the Rayleigh fading channel ($m = 1$) and decreases as m increases. When $m \to \infty$, the channel becomes the AWGN channel and no scheduling gain can be exploited any more.

As shown in Fig. 3.1, a more scattering fading environment is beneficial for the considered multiuser scheduling system since the larger channel variations enable the scheduler to arrange transmissions at higher peaks of channel fading more likely. On the other hand, considering the possibly contradictory goal of stabilizing the fading link for most antenna diversity techniques, one should be careful in employing the fading mitigation based antenna schemes on top of the multiuser scheduling system. In the next section, we will examine the capacity achieved in the multiuser scheduling system with some typical fading mitigation

28
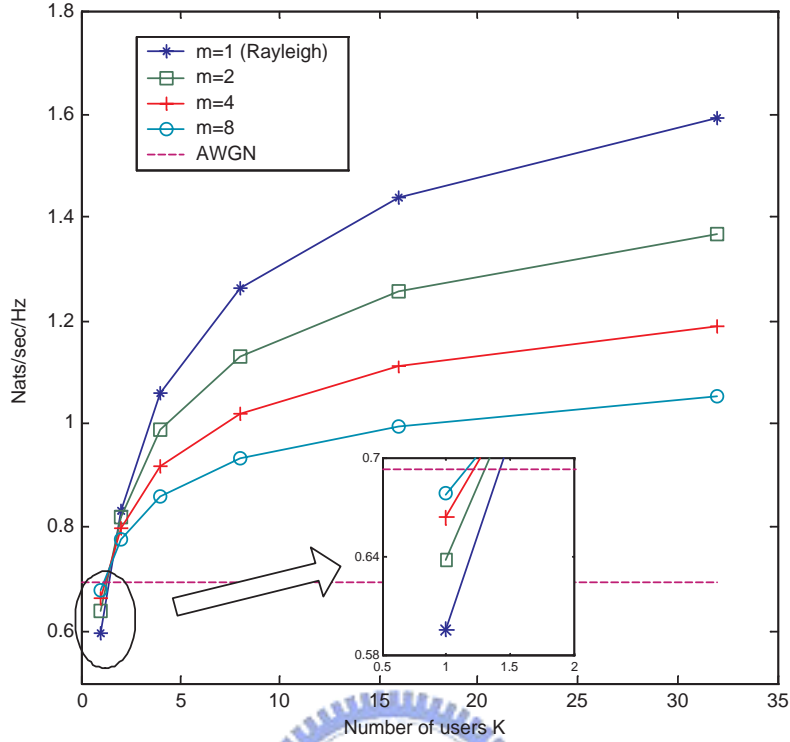
Figure 3.1: Impact of Nakagami-m channel fading on the capacity of the multiuser scheduling system.

based antenna schemes.

3.3 System Capacity with Joint Multiuser Scheduling and Antenna Diversity

Now we extend the capacity analysis to the multiuser MIMO system. To this end, N_t transmit antennas and N_r receive antennas are employed at the base station and each user, respectively. Thus, the link between the base station and any user constitutes a (N_t, N_r) MIMO system. The channel between the base station and user k can be characterized by a $N_r \times N_t$ matrix $\mathbf{H}_k = [h_{ij}^{(k)}]$ where h_{ij} is the channel gain from the jth transmit antenna to the ith receive antenna. We assume that the links between each pair of transmit and receive antennas are subject to independent Nakagami fading. Therefore, $|h_{ij}^{(k)}|^2/\sigma_n^2$ are i.i.d. gamma distributed random variables as defined in $(3.1)^2$. In the following, we consider four fading

---

[2]By letting the fading parameter $m = (1 + K^2)^2/(1 + 2K^2)$ [88], the considered MIMO channel model corresponds to that used in [37, 89] with a K-factor to represent a light of sight component.

mitigation based antenna schemes, including 1) selective transmission/selective combining (ST/SC); 2) maximum ratio transmission/maximum ratio combining (MRT/MRC); 3) selective transmission/maximum ratio combining (ST/MRC) and 4) space-time block codes (STBC). As remarked in Section 2.1.1, all of the four considered antenna schemes are capable of delivering full antenna diversity order over the MIMO channels. For a fair comparison, the total transmit power across all N_t antennas is constrained to the same level for all the antenna schemes.

3.3.1 ST/SC Scheme

Assume that orthogonal pilot signals transmit from N_t spatially separated antennas at the base station. By monitoring the pilot signals, each user can distinguish the link with the strongest SNR from $N_t N_r$ possible transmit and receive antenna pairs at any time slot. Collecting feedback from all K users, the base station can determine the target user and the associated transmit antenna radiating the best link quality. Under this policy, the scheduling rule can be mathematically expressed as

$$k^* = \arg \max_k |h_{ij}^{(k)}|^2 \ . \tag{3.25}$$

Thus, we have $f_{\text{link}}^{k^*}(\gamma) = f_{\gamma_{\max}}(\gamma\,;p,q,KN_tN_r)$ for the ST/SC scheme, where $f_{\gamma_{\max}}(\gamma\,;\cdot,\cdot,\cdot)$ is defined in (3.10). Comparing the conditional PDF $f_{\text{link}}^{k^*}(\gamma)$ associated with the ST/SC scheme and that of the SISO case, we obtain the system capacity with joint multiuser scheduling and the ST/SC antenna scheme in Nakagami fading channels as follows:

$$\langle C \rangle_{\text{st-sc}} = \Lambda_2 \left(m,\ \frac{m}{\rho},\ KN_tN_r \right) \ . \tag{3.26}$$

Expression (3.26) can be interpreted from two folds. On the one hand, from a multiuser system point of view, the base station can see total KN_r antennas at the receiving end rather than only N_r. The additional $K(N_r - 1)$ *virtual antennas* from other users can be exploited to improve system capacity. On the other hand, the multiple antennas in the ST/SC scheme can be viewed as *virtual users* to increase the multiuser diversity order for

30

the considered scheduling algorithm. Thus, we can take a broader view to define the *selection order S* as the size of a set with S i.i.d. gamma random variables, which are provided by the multiple users and/or multiple antennas in the multiuser MIMO system. Consequently, the capacity improvement achieved by the ST/SC MIMO scheme with multiuser scheduling can be explained from the fact that the selection order is indeed increased from $S = K$ to $S = KN_tN_r$.

3.3.2 MRT/MRC Scheme

In [32], the authors proposed an MRT/MRC scheme to deliver full antenna diversity over the MIMO channel, which was later analyzed in [33] under the Rayleigh fading channel in more detail. Given a known channel matrix, this method can maximize the received SNR by applying the specific beamforming weight $\mathbf{w}_t$ at the transmitter and combining weight $\mathbf{w}_r$ at the receiver. It was shown that by setting $\mathbf{w}_t$ and $\mathbf{w}_r$ to be the principle right and left singular vectors of the channel matrix respectively, the optimal received SNR can be attained with the effective output SNR $\gamma_k = \lambda_{\max}(\mathbf{H}_k^H \mathbf{H}_k)/\sigma_n^2$, where $\mathbf{H}_k^H$ is the transpose conjugate of $\mathbf{H}_k$, and $\lambda_{\max}(\mathbf{H}_k^H \mathbf{H}_k)$ is the maximum eigenvalue of $\mathbf{H}_k^H \mathbf{H}_k$. Based on the effective output SNR γ_k, the decision rule for the scheduler is

$$k^* = \arg \max_k \ \lambda_{\max}(\mathbf{H}_k^H \mathbf{H}_k) \ . \tag{3.27}$$

Note that the effective output SNR γ_k is a random variable depending on different realizations of the random channel matrix. Recently, the exact distribution of $\lambda_{\max}(\mathbf{H}_k^H \mathbf{H}_k)$ for Rayleigh channels is given by [33]

$$f_{\lambda_{\max}}(\lambda) = \sum_{i=1}^{N_r} \sum_{j=N_t-N_r}^{(N_t+N_r)i-2i^2} d_{ij} \ i^{j+1} \lambda^j e^{-i\lambda}/j! \ , \tag{3.28}$$

where d_{ij} is the associated coefficient determined by different combinations of N_t and N_r. As one can see from (3.28), it is not easy to derive the conditional PDF $f_{\text{link}}^{k^*}(\gamma)$ directly based on (3.28). However, for generalized Nakagami fading channels, we can utilize the following

inequality [90]

$$\frac{\|\mathbf{H}_k\|_F^2}{\min(N_t, N_r)} \leq \lambda_{\max}(\mathbf{H}_k^H \mathbf{H}_k) \leq \|\mathbf{H}_k\|_F^2 \tag{3.29}$$

to obtain the lower and the upper bound of system capacity. Note that in (3.29) $\|\mathbf{H}_k\|_F$ is the Frobenius matrix norm with $\|\mathbf{H}_k\|_F^2 = \sum_{i=1}^{N_r} \sum_{j=1}^{N_t} |h_{ij}^{(k)}|^2$. Thus, applying Lemmas 3.1 and 3.2 to (3.29), one can utilize $f_{\text{link}}^{k^*}(\gamma) = f_{\gamma_{\max}}(\gamma; pN_t N_r, qN, K)$ and $f_{\text{link}}^{k^*}(\gamma) = f_{\gamma_{\max}}(\gamma; pN_t N_r, q, K)$ to further derive the lower and the upper bound for the system capacity with the MRT/MRC scheme, respectively. By comparing these conditional PDFs with that of the SISO case, we reach

$$\Lambda_2\left(mN_t N_r, \frac{mN}{\rho}, K\right) \leq \langle C \rangle_{\text{mrt-mrc}} \leq \Lambda_2\left(mN_t N_r, \frac{m}{\rho}, K\right) , \tag{3.30}$$

where $\langle C \rangle_{\text{mrt-mrc}}$ is the system capacity achieved by the MRT/MRC scheme with multiuser scheduling.

In the cases of SIMO ($N_t = 1$) and MISO ($N_r = 1$), the channel matrix is reduced to a rank-one vector. Under such conditions, the achieved system capacity in (3.30) is equal to the upper bound expression, i.e., $\langle C \rangle_{\text{mrc}} = \Lambda_2\left(mN_r, \frac{m}{\rho}, K\right)$ for the receive MRC and $\langle C \rangle_{\text{mrt}} = \Lambda_2\left(mN_t, \frac{m}{\rho}, K\right)$ for the transmit MRT, respectively.

3.3.3 ST/MRC Scheme

Here, we study a hybrid scheme, which implements the ST at the transmitter and the MRC at the receiver over the MIMO channel [30]. With the MRC method utilized at the receiver, the effective SNR at the kth user's combiner output with respect to the jth transmit antenna can be written as $\gamma_k = \sum_{i=1}^{N_r} |h_{ij}^{(k)}|^2/\sigma_n^2$ [24]. Similarly, the base station gathers the effective SNR of all users and selects the target user according to the following criterion

$$k^* = \arg\max_k \sum_{i=1}^{N_r} |h_{ij}^{(k)}|^2 . \tag{3.31}$$

Applying Lemma 3.1 to (3.31), we have $f_{\text{link}}^{k^*}(\gamma) = f_{\gamma_{\max}}(\gamma; pN_r, q, KN_t)$ for the ST/MRC scheme. Accordingly, the capacity of the multiuser scheduling system with the ST/MRC

scheme is described as follows:

$$\langle C \rangle_{\text{st-mrc}} = \Lambda_2 \left(mN_r, \frac{m}{\rho}, KN_t \right) \ . \tag{3.32}$$

3.3.4 STBC Scheme

Space-time block codes (STBC) pertain to another category of antenna schemes to provide antenna diversity gain without requiring prior channel knowledge at the transmitter. Here, we focus on the STBC with orthogonal structures, which was introduced in [28] and developed more generally in [29]. Through coding over time as well as transmit antennas, the orthogonal STBC technique can also deliver full antenna diversity order by using simple linear processing at the receiver. From [55, 91], the effective SNR of user k at the output of the STBC decoder is given by $\gamma_k = \frac{1}{N_t} \sum_{i=1}^{N_r} \sum_{j=1}^{N_t} |h_{ij}^{(k)}|^2 / \sigma_n^2$. Thus, the corresponding selection rule for the base station scheduler is

$$k^* = \arg \max_k \frac{1}{N_t} \sum_{i=1}^{N_r} \sum_{j=1}^{N_t} |h_{ij}^{(k)}|^2 \ . \tag{3.33}$$

Again, applying Lemmas 3.1 and 3.2 to (3.33), we have $f_{\text{link}}^{k^*} = f_{\gamma_{\max}}(\gamma\,;pN_tN_r, qN_t, K)$ for the STBC method. Consequently, the capacity of the multiuser scheduling system with the orthogonal STBC can be expressed as

$$\langle C \rangle_{\text{stbc}} = \Lambda_2 \left(mN_tN_r, \frac{mN_t}{\rho}, K \right) \ . \tag{3.34}$$

Notice that the system capacity achieved with joint multiuser scheduling and the orthogonal STBC will in general be lower than (3.34). The reason follows from the fact that only the STBC with full code rate can support the capacity promised by (3.34) while the full code rate STBC are available for a limited number of transmit antennas and signal constellations [29]. Nevertheless, we still can use (3.34) to evaluate the impact of applying the STBC scheme on top of the multiuser scheduling system since it represents an optimistic performance upper bound.

3.3.5 Discussions

Table 3.1 summarizes the system capacity achieved with all the aforementioned antenna diversity schemes in the considered multiuser scheduling system. Comparing $\langle C \rangle_{\mathrm{st}}$ with $\langle C \rangle_{\mathrm{sc}}$ and $\langle C \rangle_{\mathrm{mrt}}$ with $\langle C \rangle_{\mathrm{mrc}}$, one can find that the duality between the transmit and receive diversity methods. However, the practical considerations for implementing these antenna schemes in the multiuser scheduling system are quite different. First of all, the transmit methods have the potential advantage of relieving computation burdens for user terminals. Moreover, the cost (benefit) of adding one more antenna at the base station for the transmit methods can be amortized (shared) by multiple users. Next, the transmit methods generally require additional pilot signals since the receiver would rely on them to estimate the SNR from each corresponding transmit antenna. Finally, the required amount of signalling in the feedback channel is usually larger for the transmit methods than the receive methods. For example, as compared with the receive SC method, using the transmit ST scheme requires the terminal to send back not only the SNR of the strongest channel, but also the signalling to indicate the best serving antenna. The transmit MRT scheme needs even a larger amount of overheads in the feedback channel because the channel magnitude and phase for all transmit antennas are mandatory for the base station to perform the MRT scheme correctly.

3.4 Capacity Revisited: A Change of Coordinate Parameters

So far we have developed a unified capacity formula applicable to the wireless system with joint antenna diversity and multiuser scheduling. However, the closed-form expression (3.16) for integer p and the approximate expression (3.23) for general p may be too involved to clearly explain the interplay of multiuser scheduling and different antenna diversity schemes. For this reason, we further suggest a set of parameter transformations.

We first define the *array gain a* as

$$a \triangleq \frac{\mathrm{E}[\gamma_k]}{\rho} = \frac{p/q}{\rho} \tag{3.35}$$

Table 3.1: Capacity summary of the multiuser scheduling system with various fading mitigation based antenna schemes, where $N_{\min} = \min(N_t, N_r)$.

MIMO antenna schemes	System capacity	Array gain (a)	AF gain (f)	Selection order (S)
$\langle C \rangle_{\text{siso}},\ (1,1)$	$\Lambda_2\left(m, \dfrac{m}{\rho}, K\right)$	1	1	K
$\langle C \rangle_{\text{sc}},\ (1,N_r)$	$\Lambda_2\left(m, \dfrac{m}{\rho}, KN_r\right)$	1	1	KN_r
$\langle C \rangle_{\text{mrc}},\ (1,N_r)$	$\Lambda_2\left(mN_r, \dfrac{m}{\rho}, K\right)$	N_r	$1/N_r$	K
$\langle C \rangle_{\text{st}},\ (N_t,1)$	$\Lambda_2\left(m, \dfrac{m}{\rho}, KN_t\right)$	1	1	KN_t
$\langle C \rangle_{\text{mrt}},\ (N_t,1)$	$\Lambda_2\left(mN_t, \dfrac{m}{\rho}, K\right)$	N_t	$1/N_t$	K
$\langle C \rangle_{\text{st-sc}},\ (N_t,N_r)$	$\Lambda_2\left(m, \dfrac{m}{\rho}, KN_tN_r\right)$	1	1	KN_tN_r
$\langle C \rangle_{\text{st-mrc}},\ (N_t,N_r)$	$\Lambda_2\left(mN_r, \dfrac{m}{\rho}, KN_t\right)$	N_r	$1/N_r$	KN_t
$\langle C \rangle_{\text{mrt-mrc}}^{\text{ub}},\ (N_t,N_r)$	$\Lambda_2\left(mN_tN_r, \dfrac{m}{\rho}, K\right)$	N_tN_r	$1/N_tN_r$	K
$\langle C \rangle_{\text{mrt-mrc}}^{\text{lb}},\ (N_t,N_r)$	$\Lambda_2\left(mN_tN_r, \dfrac{mN}{\rho}, K\right)$	$N_tN_r/N_{\min}$	$1/N_tN_r$	K
$\langle C \rangle_{\text{stbc}},\ (N_t,N_r)$	$\Lambda_2\left(mN_tN_r, \dfrac{mN_t}{\rho}, K\right)$	N_r	$1/N_tN_r$	K

to account for the average increased level of received SNR mainly due to coherent combining relative to the SISO case [92]. Note that in (3.35) $\gamma_k \sim \mathcal{G}(p,q)$ is the effective receive SNR at the combiner output for user k. Next, recall that the amount of fading (AF) associated with the PDF of γ_k is defined as [88]

$$\text{AF}[\gamma_k] = \frac{\text{Var}[\gamma_k]}{\text{E}[\gamma_k]^2} \ , \tag{3.36}$$

where $\text{Var}[\gamma_k]$ denotes the variance of γ_k. The AF parameter can be viewed as a measure of the severity of fading and is independent of the mean power for the Nakagami fading. Also, it can be a measure of the randomness of a random variable, namely, the higher the AF the larger spread the fading distribution [93]. From (3.36), we further define the second parameter f, called the *amount of fading gain*, as

$$f \triangleq \frac{\text{AF}[\gamma_k]}{1/m} = \frac{m}{p} \tag{3.37}$$

35

to capture the relative randomness of γ_k with respect to the SISO case.

In terms of array gain a, amount of fading gain f and the previously defined selection order S, the system capacity then can be described by these three parameters as

$$\Lambda_3(a, f, S) = \Lambda_2 \left(\frac{m}{f}, \frac{m}{af\rho}, S \right) \quad . \tag{3.38}$$

Table 3.1 lists the values of a, f and S corresponding to all the considered antenna schemes. Next, we introduce Lemma 3.3 to further derive an analytical capacity upper bound.

Lemma 3.3 Let $X_1, \cdots, X_S$ be i.i.d. random variables with common mean μ and variance σ^2. Let $Y = \max\{X_1, \cdots, X_S\}$. Then the mean of the random variable Y is upper bounded by

$$\mathrm{E}[Y] \leq \mu + \frac{(S-1)\sigma}{\sqrt{2S-1}} \quad . \tag{3.39}$$

Proof: Please refer to [87, p.59]. □

Applying Lemma 3.3 and Jensen's inequality to (3.38), one can obtain

$$\begin{aligned}
\Lambda_3(a, f, S) &\leq \log\left(1 + a\rho\left[1 + \frac{(S-1)}{\sqrt{2S-1}}\sqrt{\frac{f}{m}}\right]\right) \\
&\simeq \log\left(1 + a\rho\left[1 + \sqrt{\frac{Sf}{2m}}\right]\right), \quad \text{for large } S \quad . \tag{3.40}
\end{aligned}$$

Essentially, (3.40) provides a simple capacity upper bound for effectively assessing the performance improvements attributed to fading characteristics, multiuser scheduling and different antenna diversity schemes in the multiuser MIMO system. Referring to (3.40) together with Table 3.1, we can make the following conjectures:

1. The higher value of Nakagami fading parameter m brings about a detrimental effect on the system capacity jointly achieved by the scheduling algorithm (3.9) and all the considered antenna schemes.

2. The ST/SC scheme can further improve the capacity of the multiuser scheduling system by amplifying multiuser diversity order. If a system already has possessed large selection order provided by inherent user population, it is expected that the attainable capacity gain with the additional ST/SC scheme may be somewhat limited.
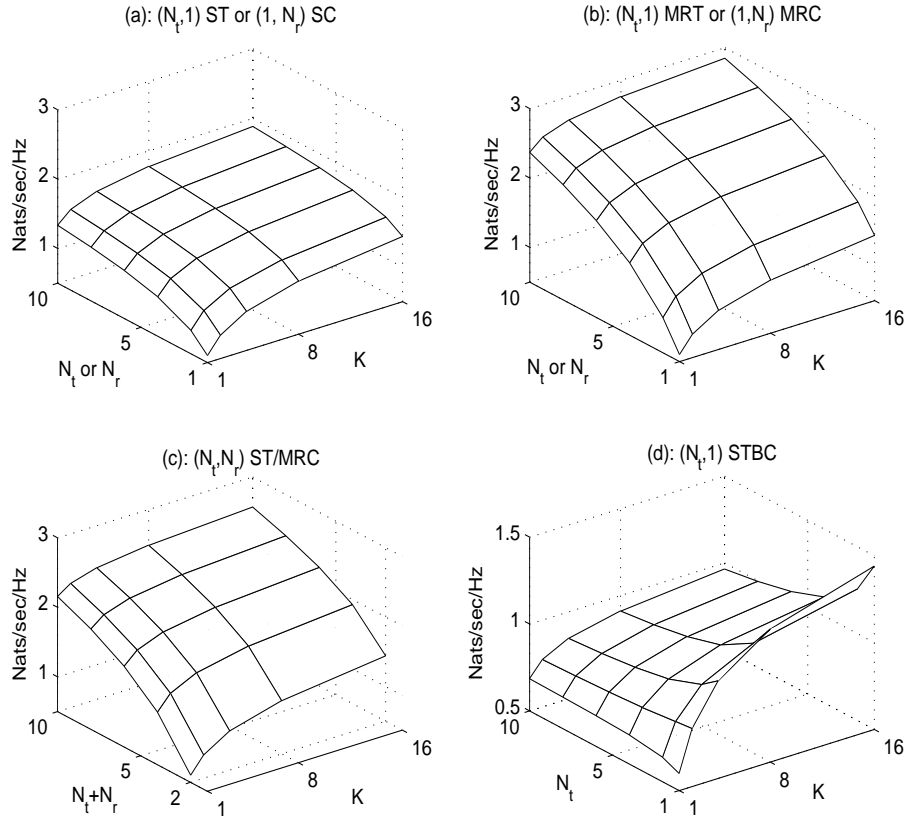
Figure 3.2: Comparison of the achievable system capacity with joint multiuser scheduling and various diversity-based antenna schemes.

3. Although the MRT/MRC scheme reduces the amount of fading gain, the combined effect of the increased array gain and the reduced amount of fading gain can still yield greater system capacity as compared with the ST/SC method.

4. Employing the STBC via N_t transmit antennas can damp the channel fluctuations as though the Nakagami fading parameter changes from m to mN_t but without the supplement of array gain. As a result, the STBC method may cause a negative impact on the capacity of the multiuser system with multiuser diversity. This is consistent with the observations in [11, 55].

These conjectures will be further validated in the next section through numerical evaluations.

37
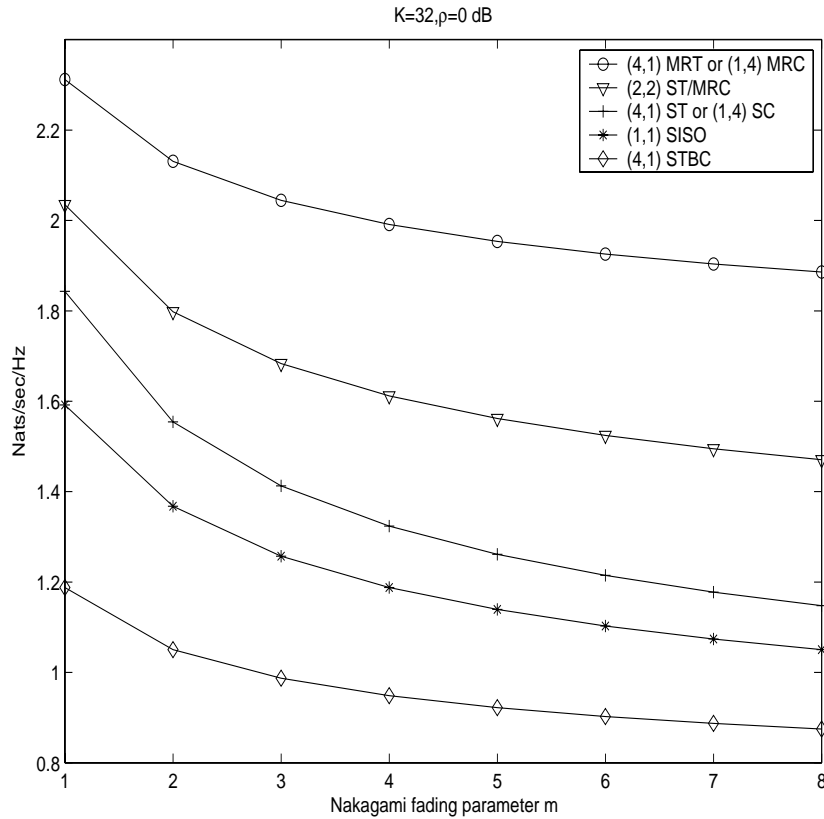
Figure 3.3: Impact of Nakagami-m channel fading on the attainable system capacity with joint multiuser scheduling and antenna diversity schemes.

3.5   Numerical Results

In this section, we give some numerical examples using the derived unified capacity formula. The capacity result and the associated parameters are summarized in Table 3.1, where (N_t, N_r) represents the MIMO system with N_t transmit antennas and N_r receive antennas, and the superscripts ub and lb stand for the upper bound and the lower bound, respectively. In the Figs. 3.2 and 3.3, we let $\rho = 0$ dB for numerical evaluations.

Figure 3.2 compares the achievable system capacity with joint multiuser scheduling and various diversity-based antenna schemes. One can see that the system capacity increases as the number of users K increases for all the Figs. 3.2-(a) to 3.2-(d). However, increasing the number of transmit antennas for the STBC method could degrade the capacity in the presence of multiuser scheduling ($K \geq 2$) as shown in Fig. 3.2-(d). Comparing Figs. 3.2-(a), 3.2-(b) and 3.2-(c), it is observed that the MRT/MRC method provides the highest capacity.
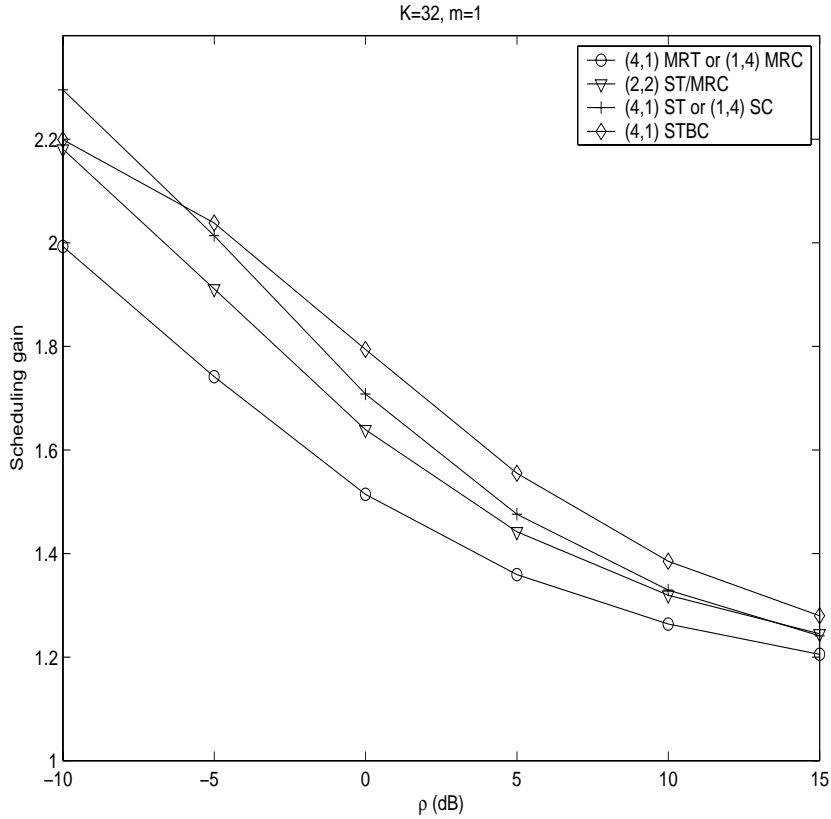
Figure 3.4: Comparison of the achievable scheduling gain with different values of mean SNR.

We note that $N_t = N_r$ is assumed for the ST/MRC case in Fig. 3.2-(c). For the ST/SC method, the marginal benefit of adding additional antennas is more suppressed as compared with the MRT/MRC method, especially when K is large. When comparing the capacity performance of Figs. 3.2-(a), 3.2-(b) and 3.2-(d) over the MISO channel, we may interpret that the MRT schemes achieves the highest capacity at the cost of the highest amount of feedback overheads. On the contrary, in a system with restricted feedback capability, applying the STBC method along with the traditional round-robin scheduling appears to be a feasible solution.

Figure 3.3 shows the impact of Nakagami-m channel fading on the system capacity with joint multiuser scheduling and antenna diversity schemes. In this example, we let $K = 32$. One can see that the higher m causes a negative impact on the capacity for all the studied antenna schemes. When m increases from one to eight, the capacity drops 18.4% for the $(4, 1)$ MRT scheme, 37.7% for the $(4, 1)$ ST scheme and 26.4% for the $(4, 1)$ STBC scheme,

respectively. This implies that the ST/SC scheme is more sensitive to the condition of channel fading than the other schemes.

Figure 3.4 compares the achievable scheduling gain under different mean SNR conditions. We set $K = 32$ and $m = 1$ in this figure. The performance metric of the y-axis is defined as the capacity achieved by joint multiuser scheduling and MIMO antenna schemes normalized to the capacity with multiple antennas only. Given a fixed number of antennas, this metric can indicate the capacity benefit solely resulting from scheduling. From Fig. 3.4, it is shown that the considered scheduling policy provides more capacity gain when ρ is smaller. If a user with a smaller ρ is mainly due to its location far from the base station, this property is relevant to implying that the multiuser diversity can offer more capacity gain for the user with a larger propagation loss.

3.6 Chapter Summary

In this chapter, we have investigated the issue of applying the fading mitigation based antenna technique for the multiuser scheduling system through a capacity analysis. A unified capacity formula connecting multiuser diversity from multiple users, antenna diversity from multiple antenna systems and fading parameter from Nakagami channel models is established. With a set of parameter changes, the new capacity expression is powerful to interpret the interaction between the multiuser scheduling system and various fading mitigation based antenna techniques. As a result, it is concluded in this chapter that it may not be a good strategy for utilizing the diversity-based antenna technique in the multiuser scheduling system due to the following two main reasons. First, the channel damping effect resulting from using the diversity-based antenna technique is intrinsically harmful to the multiuser scheduling system where large channel fluctuations are preferred. Second, from the multiuser MIMO point of view, since the user population has contributed a large amount of multiuser diversity gain, the additional antenna diversity coming from the diversity-based antenna scheme can then only add to limited capacity benefit. In the next chapter, we will move

to consider another category of multiple antenna techniques, i.e. the multiplexing-based antenna technique, for their application in the multiuser scheduling system.

Chapter 4

Throughput Enhancement Based Antenna Techniques for Multiuser Scheduling Systems

This chapter studies the benefit of combining the throughput enhancement based (or multiplexing based) antenna technique with the multiuser scheduling system from both the perspectives of cell coverage extension and system capacity improvement. For a point-to-point MIMO system, recent studies have revealed that the remarkable capacity gain resulting from the spatial multiplexing MIMO system may come at the sacrifice of degrading link reliability. This tradeoff between antenna multiplexing gain against antenna diversity gain may translate into smaller coverage areas. In this chapter, we will demonstrate that using the scheduling technique can effectively replenish the diversity-deficient spatial multiplexing MIMO system with multiuser diversity. In particular, we will introduce a novel scheduling scheme, called the strongest-weakest-normalized-subchannel-first (SWNSF) scheduling, which requires only limited amount of feedback. Analysis and results will indicate that the SWNSF scheduling can significantly increase the coverage of the multiuser MIMO system while further improving the system capacity.

4.1 Channel Model

Consider a multiuser MIMO system where a base station with N_t transmit antennas serves K downlink users each of which is equipped with N_r receive antennas. We assume that the

spatial multiplexing method is used for data transmission between the base station and any target user. For clarifying the effect of multiuser scheduling on the supplement of diversity gain, we assume $N_t = N_r = N$ since in this case all the degrees of freedom in the MIMO system are exhausted for multiplexing gain [3]. Thus, the link between the base station and each individual user constitutes an $N \times N$ MIMO system. Let $\mathbf{x}_k$ and $\mathbf{y}_k$ be the $N \times 1$ transmit and receive signal vectors for user k, respectively, $\mathbf{G}_k$ the $N \times N$ channel matrix between the base station and user k, and $\mathbf{n}_k$ the $N \times 1$ spatially white noise vector with $\mathrm{E}[\mathbf{n}_k\mathbf{n}_k^H] = \sigma_n^2\mathbf{I}$. Thus, the link between $\mathbf{x}_k$ and $\mathbf{y}_k$ is related by [89]

$$\mathbf{y}_k = \mathbf{G}_k\mathbf{x}_k + \mathbf{n_k} = \sqrt{g_k}\,\mathbf{H}_k\mathbf{x}_k + \mathbf{n}_k \ , \tag{4.1}$$

where g_k depicts the large-scale (local average) behavior of the channel gain, and $\mathbf{H}_k$ captures the channel fading characteristics. For user k at a distance of r_k from the base station, g_k can be generally represented by [24]

$$10\log_{10}(g_k) = -10\mu\log_{10}(r_k) + g_0 \ \ [\mathrm{dB}] \ , \tag{4.2}$$

where μ is the path loss exponent and g_0 is a constant subject to certain path loss models. For the $N \times N$ normalized channel matrix $\mathbf{H}_k$, we assume that every entry of $\mathbf{H}_k$ is independent, circular-symmetric complex Gaussian random variable $\mathcal{CN}(0,1)$, meaning that the real and imaginary parts of each entry have uncorrelated Gaussian distributions with zero mean and variance $1/2$. The total transmit power at the base station is constrained by P_t, i.e. $\mathrm{E}[\mathbf{x}_k^H\mathbf{x}_k] \leq P_t$.

With the link model defined in (5.1), the ergodic capacity (nats/sec/Hz) of an open-loop MIMO system with equal power allocation among transmit antennas is given by [1]

$$C_k = \mathrm{E}\left[\log\det\left(I + \frac{\rho_k}{N}\mathbf{H}_k\mathbf{H}_k^H\right)\right] \tag{4.3}$$

where

$$\rho_k = P_t\,g_k/\sigma_n^2 = (P_t/\sigma_n^2)\,r_k^{-\mu}\,10^{g_0/10} \tag{4.4}$$

is the average receive signal-to-noise ratio (SNR) of user k. By applying the singular value decomposition (SVD) to $\mathbf{H}_k$ of (4.3), C_k can be also represented by

$$C_k = \sum_{i=1}^{N} \mathrm{E}\left[\log\left(1 + \frac{\rho_k}{N}\lambda_{k,i}\right)\right] , \qquad (4.5)$$

where $\{\lambda_{k,i}\}_{i=1}^{N}$ are the eigenvalues of the Wishart matrix $\mathbf{H}_k\mathbf{H}_k^{H}$ for user k. Without loss of generality, we arrange $\{\lambda_{k,i}\}_{i=1}^{N}$ in the decreasing order so that $\lambda_{k,N} \geq \lambda_{k,N-1} \geq \cdots \geq \lambda_{k,1} \geq 0$[1]. Comparing to the ergodic capacity of the single-input-single-output (SISO) system, the ergodic capacity of an open-loop MIMO channel is enhanced by forming n parallel subchannels, each of which has effective output SNR $\gamma_{k,i} = \rho_k\lambda_{k,i}/N$ at the receive antenna. In this thesis, we refer to the link capacity as the ergodic capacity of the information theory.

In addition to the link capacity, let's examine the link outage probability of the MIMO system because it reflects how reliable a MIMO channel can support the corresponding capacity. For the SISO system, a common definition of link outage is the probability that the receive SNR is less than a predetermined value γ_{th}, i.e. $P_{\mathrm{out}} = \Pr\{\gamma < \gamma_{\mathrm{th}}\}$ [88]. Based on the insight from [14], the link outage for the spatial multiplexing MIMO system can be generalized as follows. By noting that all the subchannels of the spatial multiplexing MIMO system are used for independent data transmissions in parallel, the link outage for the spatial multiplexing MIMO system can be defined as the event when the receive SNR of any subchannel is less than γ_{th}. That is, for any user k,

$$\begin{aligned}
P_{\mathrm{out}}^{k} &= \Pr\{\gamma_{k,1} < \gamma_{\mathrm{th}} \cup \gamma_{k,2} < \gamma_{\mathrm{th}} \cdots \cup \gamma_{k,N} < \gamma_{\mathrm{th}}\} \\
&= 1 - \Pr\left\{\min_{\forall i}\{\gamma_{k,i}\} = \gamma_{k,1} \geq \gamma_{\mathrm{th}}\right\} \\
&= \Pr\{\gamma_{k,1} < \gamma_{\mathrm{th}}\} .
\end{aligned} \qquad (4.6)$$

Intuitively, the weakest subchannel with the lowest SNR in the MIMO system dominates the outage probability performance since the weakest subchannel is most likely to incur transmission errors. By writing (4.6) as $\Pr\{\gamma_{k,1} \geq \gamma_{\mathrm{th}}\} = 1 - P_{\mathrm{out}}^{k}$, (4.6) can be also interpreted

---

[1]It is shown in [95] that the random Wishart matrix $\mathbf{H}_k\mathbf{H}_k^{H}$ has N distinct eigenvalues with probability one.

as that all the receive SNR in subchannels of the MIMO system are required to be greater than γ_{th} with the probability of $(1 - P_{\text{out}}^k)$. In Section 4.3, we will relate (4.6) to the resulting cell coverage.

4.2 Scheduling Algorithms

Assume that multiple users are served by a base station in a time division multiple access manner. In each time slot, the base station selects a target user according to a certain scheduling policy. For any user k, the channel $\mathbf{H}_k$ is assumed to be fixed during a time slot, but independently varies between different time slots. The variation of $\mathbf{H}_k$ across users is also assumed to be independent. In the following, we introduce two scheduling algorithms. The first one is the traditional round-robin scheduling method, which serves as the baseline performance for comparison. The second one is our proposed strongest-weakest-normalized-subchannel-first scheduling algorithm.

4.2.1 Round-Robin Scheduling

The round-robin (RR) scheduling assigns each time slot to a target user in the circularly sequential manner among K users. The round-robin scheduling is known for its fairness and low implementation cost. In a multiuser system where users can have different near-far locations, the RR scheduling provides a fair allocation scheme for numerous near-far users to access services with equal probability. However, the RR scheduling can not exploit multiuser diversity since it ignores the channel conditions among user population. Next, we study another fair scheduling algorithm that can take advantage of multiuser diversity to offer additional scheduling gain.

4.2.2 Strongest-Weakest-Normalized-Subchannel-First Scheduling

From a multiuser system point of view, the base station can see the total NK antennas at the receive end rather than N. In a diversity-deficient spatial multiplexing MIMO system where all physical antennas are dedicated to capacity enhancement, the additional $(K-1)N$ virtual

receive antennas from the other users can be exploited to improve reliability performance. Per the observation from (4.6), we introduce a scheduling algorithm to take advantage of multiuser diversity to directly cope with the weakest subchannel of the MIMO system. The proposed algorithm, called the strongest-weakest-normalized-subchannel-first (SWNSF) scheduling, selects the target user with the maximum $\lambda_{k,n}$ among K users at each time slot:

$$
\begin{aligned}
k^* &= \arg\max_k \frac{\lambda_{\min}\left(\mathbf{G}_k\mathbf{G}_k^H\right)}{g_k} \tag{4.7} \\
&= \arg\max_k \lambda_{\min}\left(\mathbf{H}_k\mathbf{H}_k^H\right) \\
&= \arg\max_k \lambda_{k,1} \ . \tag{4.8}
\end{aligned}
$$

where $\lambda_{\min}(\cdot)$ denotes the minimum eigenvalue. In (4.7), g_k in the denominator is used to equalize the average SNR among different users due to the near-far effect. In practice, g_k can be estimated based on the long-term measurements at the user side. We assume that each user can accurately estimate the value of $\lambda_{k,1}$ and correctly send it back to the base station without delay.

Let $\tilde{\mathbf{H}}_k$ and $\tilde{\gamma}_{k,1}$ be the normalized channel matrix and the output SNR of the weakest subchannel for user k determined by the SWNSF algorithm, respectively. Accordingly, $\tilde{\lambda}_{k,1} = \tilde{\gamma}_{k,1}N/\rho_k$ is the minimum eigenvalue of $\tilde{\mathbf{H}}_k\tilde{\mathbf{H}}_k^H$. Thus, the following proposition summaries the important properties of the SWNSF scheduling algorithm.

Proposition 4.1 Assume that K users with different ρ_k $(1 \leq k \leq K)$ are served according to the SWNSF scheduling policy defined in (4.8). Let p_k be the probability of user k being served at any time slot. Then we have:

(i) The SWNSF scheduling is fair in the sense $p_k = 1/K$.

(ii) The CDF of $\tilde{\gamma}_{k,1}$ is $F_{\tilde{\gamma}_{k,1}}(\gamma) = \left[F_{\gamma_{k,1}}(\gamma)\right]^K$ for any k, where $F_{\gamma_{k,1}}(\gamma)$ is the CDF of $\gamma_{k,1}$.

Proof: From (4.8), any user k competes for services with the other $(K-1)$ users at each time slot. Because $\{\lambda_{k,1}\}_{k=1}^K$ are i.i.d. random variables, we have $p_k = 1/K$. Furthermore,

the CDF of $\tilde{\lambda}_{k,1}$ is given by

$$F_{\tilde{\lambda}_{k,1}}(\lambda) = \Pr\left\{\max_k\left(\lambda_{k,1}\right) < \lambda\right\} = \left[F_{\lambda_{k,1}}(\lambda)\right]^K \ . \tag{4.9}$$

Since $\tilde{\gamma}_{k,1} = \rho_k\tilde{\lambda}_{k,1}/N$ and $\gamma_{k,1} = \rho_k\lambda_{k,1}/N$, we can have

$$F_{\tilde{\gamma}_{k,1}}(\gamma) = F_{\tilde{\lambda}_{k,1}}\left(\frac{N\gamma}{\rho_k}\right) = \left[F_{\lambda_{k,1}}\left(\frac{N\gamma}{\rho_k}\right)\right]^K = \left[F_{\gamma_{k,1}}(\gamma)\right]^K \ . \tag{4.10}$$

$$\square$$

Proposition 4.1 states that the SWNSF scheduling can capture the variations of independent channel fading to achieve multiuser diversity, while maintaining fairness among users. Next, we investigate how the RR and SWNSF scheduling algorithms affect the coverage and capacity of the multiuser MIMO system.

4.3 Effect of SWNSF Scheduling on Coverage

In this section, we investigate the effect of multiuser scheduling on cell coverage. We consider a single cell with the background noise. Referring to (4.6) and the path loss related link budget (4.4), we shall determine the cell radius by the maximum distance at which the link quality suffices for maintaining a required receive SNR γ_{th} with the probability at least $(1 - P_{\text{out}})$ [96, 97]. Since the user at the cell boundary is the major concern in determining cell coverage, we may omit the user index k to ease notations in this section.

4.3.1 Characteristics of $\lambda_{k,1}$

Now we introduce Proposition 4.2 to characterize the statistical distribution of $\lambda_{k,1}$.

Proposition 4.2 Let $\lambda_{k,N} \geq \lambda_{k,N-1} \geq \cdots \geq \lambda_{k,1} \geq 0$ be the *ordered eigenvalues* of the Wishart matrix $\mathbf{H}_k\mathbf{H}_k^H$, where $\mathbf{H}_k$ is an $N\times N$ channel matrix with each entry $h_{ij} \sim \mathcal{CN}(0,1)$. Then the marginal PDF of the minimum eigenvalue $\lambda_{k,1}$ is exponentially distributed with parameter $1/N$.

Proof: From [98], for an $N \times M$ ($N \geq M$) channel matrix $\mathbf{H}_k$, the joint distribution function

of the ordered eigenvalues of $\mathbf{H}_k\mathbf{H}_k^H$ is

$$f_{\lambda_{k,1},\cdots,\lambda_{k,N}}(\lambda_1,\cdots,\lambda_N) = \frac{\pi^{N(N-1)}}{\Gamma_M(N)\Gamma_N(M)} \exp\left(-\sum_{i=1}^{N}\lambda_i\right) \prod_{i=1}^{N}\lambda_{N-i+1}^{M-N} \prod_{i>j}(\lambda_i-\lambda_j)^2 \ , \quad (4.11)$$

where $\Gamma_a(x)$ is the complex multivariate gamma function defined by

$$\Gamma_a(x) = \pi^{a(a-1)/2} \prod_{i=1}^{a}\Gamma(x-i+1) \ . \quad (4.12)$$

Note that $\Gamma(x)$ is the ordinary gamma function. In the case of $M = N$, (4.11) is reduced to

$$f_{\lambda_{k,1},\cdots,\lambda_{k,N}}(\lambda_1,\cdots,\lambda_N) = \frac{1}{\left[\prod_{i=1}^{N}\Gamma(i)\right]^2} \exp\left(-\sum_{i=1}^{N}\lambda_i\right) \prod_{i>j}(\lambda_i-\lambda_j)^2 \ . \quad (4.13)$$

Therefore, the marginal distribution of $\lambda_{k,1}$ can be obtained by integrating over all the other variables as follows:

$$f_{\lambda_{k,1}}(\lambda_1) = \frac{1}{\left[\prod_{i=1}^{N}\Gamma(i)\right]^2} \int_{\lambda_1}^{\infty}\int_{\lambda_2}^{\infty}\cdots\int_{\lambda_{N-1}}^{\infty} \exp\left(-\sum_{i=1}^{N}\lambda_i\right) \prod_{i>j}(\lambda_i-\lambda_j)^2 \, d\lambda_N\cdots d\lambda_3 d\lambda_2 \ . \quad (4.14)$$

By making the transformation $x_i = \lambda_i - \lambda_1$ for $i = 2,\cdots,N$, (4.14) can be written as

$$\begin{aligned}
f_{\lambda_{k,1}}(\lambda_1) &= e^{-N\lambda_1}\left\{ \frac{1}{\left[\prod_{i=1}^{N}\Gamma(i)\right]^2} \int_{0}^{\infty}\int_{x_2}^{\infty}\cdots\int_{x_{N-1}}^{\infty} \exp\left(-\sum_{i=2}^{N}x_i\right) \prod_{i=2}^{N}x_i^2 \right. \\
&\qquad \left. \cdot \prod_{\substack{i>j \\ i,j\in\{2,\cdots,N\}}}(x_i-x_j)^2 \, dx_N\cdots dx_3 dx_2 \right\} \ . \quad (4.15)
\end{aligned}$$

Since the $(N-1)$ fold integrals in the bracket of (4.15) involve only variables $x_2,\cdots,x_N$ and $f_{\lambda_{k,1}}(\lambda_1)$ is a probability density function, we can have

$$f_{\lambda_{k,1}}(\lambda_1) = Ne^{-N\lambda_1}, \ \lambda_1 \geq 0 \ . \quad (4.16)$$

$\square$

The statistical properties of the minimum eigenvalue for the general $N \times M$ channel matrix can be found in [99].

4.3.2 Cell Radius with RR Scheduling

Since the RR scheduling selects the target user in a statistically random manner, the receive SNR of the target user will not be affected by the RR scheduling algorithm. Thus, according to Proposition 4.2 and $\gamma_{k,1} = \rho_k \lambda_{k,1}/N$, the receive SNR $\gamma_{k,1}$ of any target user under the RR scheduling is an exponentially distributed random variable with the following CDF

$$F_{\gamma_{k,1}}(\gamma) = 1 - \exp\left(-\frac{N^2\gamma}{\rho_k}\right), \quad \gamma \geq 0 \ . \tag{4.17}$$

Suppose that the cell radius is defined by the farthest distance at which the link quality suffices for maintaining a required receive SNR γ_{th} with the probability no less than $(1-P_{\text{out}})$. Thus, by substituting (4.17) and (4.4) into (4.6), the cell radius of the multiuser MIMO system employing the RR scheduling is given by

$$r = \left[\left(\frac{P_t}{\sigma_n^2}\right)\left(\frac{10^{g_0/10}}{N^2\gamma_{\text{th}}}\right)\log\left(\frac{1}{1-P_{\text{out}}}\right)\right]^{1/\mu} \ . \tag{4.18}$$

For $n = 1$ or the SISO case, the cell radius of (4.18) becomes

$$r_{\text{SISO}} = \left[\left(\frac{P_t}{\sigma_n^2}\right)\left(\frac{10^{g_0/10}}{\gamma_{\text{th}}}\right)\log\left(\frac{1}{1-P_{\text{out}}}\right)\right]^{1/\mu} \ . \tag{4.19}$$

Comparing (4.18) and (4.19) under the same total transmit power of a base station P_t and the same link reliability requirements P_{out} and γ_{th}, we have

$$r = \left(\frac{1}{N^2}\right)^{1/\mu} r_{\text{SISO}} \ . \tag{4.20}$$

As a result, the cell radius of the spatial multiplexing multiuser MIMO system shrinks under the RR scheduling. Next, we derive the cell radius of the multiuser MIMO system using the SWNSF scheduling.

4.3.3 Cell Radius with SWNSF Scheduling

When the connection between the base station and the target user is established by the SWNSF scheduling, the receive SNR $\tilde{\gamma}_{k,1}$ is changed according to (4.10). By substituting (4.17) into (4.10), the CDF of $\tilde{\gamma}_{k,1}$ subject to the SWNSF scheduling becomes

$$F_{\tilde{\gamma}_{k,1}}(\gamma) = \left[1 - \exp\left(-\frac{N^2\gamma}{\rho_k}\right)\right]^K, \quad \gamma \geq 0 \ . \tag{4.21}$$

Analogous to (4.18), applying (4.21) and (4.4) to (4.6), we can obtain the cell radius of the multiuser MIMO system with the SWNSF scheduling as follows:

$$\tilde{r} = \left[\left(\frac{P_t}{\sigma_n^2} \right) \left(\frac{10^{g_0/10}}{N^2 \, \gamma_{\text{th}}} \right) \log \left(\frac{1}{1 - \sqrt[K]{P_{\text{out}}}} \right) \right]^{1/\mu} .$$ (4.22)

We can also compare $\tilde{r}$ in (4.22) and r_{SISO} in (4.19) to have

$$\begin{aligned} \tilde{r} &= \left[\frac{1}{N^2} \log \left(\frac{1}{1 - \sqrt[K]{P_{\text{out}}}} \right) \Big/ \log \left(\frac{1}{1 - P_{\text{out}}} \right) \right]^{1/\mu} r_{\text{SISO}} \\ &\simeq \left[\frac{1}{N^2} \left(\frac{1}{P_{\text{out}}} - \frac{1}{2} \right) \log \left(\frac{1}{1 - \sqrt[K]{P_{\text{out}}}} \right) \right]^{1/\mu} r_{\text{SISO}}, \quad \text{for small } P_{\text{out}} . \end{aligned}$$ (4.23)

Unlike (4.20) where r is always smaller than r_{SISO}, $\tilde{r}$ in (4.23) can be possibly greater than r_{SISO} with a sufficient number of users in the system, i.e.

$$K \geq \left\lceil \frac{\log(P_{\text{out}})}{\log \left(1 - \exp \left(-\frac{2N^2 P_{\text{out}}}{2 - P_{\text{out}}} \right) \right)} \right\rceil ,$$ (4.24)

where $\lceil x \rceil$ denotes the smallest integer greater or equal to x. Next, we give a numerical example to compare the resulting cell radius when adopting the RR and SWNSF scheduling policies.

4.3.4   Numerical Example

Figure 4.1 plots the cell radius of the multiuser MIMO system using the RR and SWNSF scheduling according to (4.20) and (4.23). We normalize r_{SISO} to unity and set the path loss exponent $\mu = 4$ in this example. Also, we require the link reliability of the user at the cell boundary to be adequately covered 90% of the time, i.e. $P_{\text{out}} = 0.1$. From Fig. 4.1, it is shown that the cell radius of the spatial multiplexing MIMO system with the RR scheduling reduces as compared with SISO case. However, applying the SWNSF scheduling can enhance the receive SNR, thereby extending the cell radius. When sufficiently many users in the system, e.g. $K = 5$ for $N = 3$ and $K = 12$ for $N = 4$, the cell radius with the SWNSF scheduling is greater than r_{SISO}.
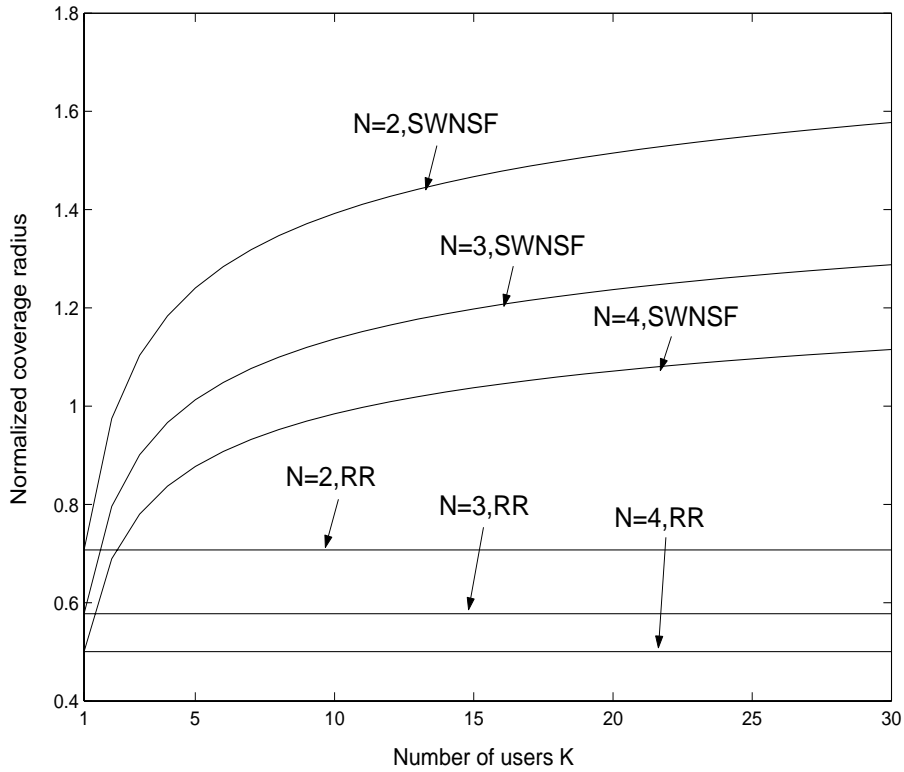
Figure 4.1: Comparison of the cell radius of the multiuser MIMO system using the RR and SWNSF scheduling.

4.4 Effect of SWNSF Scheduling on Capacity

In the previous section, we have demonstrated that the SWNSF scheduling can extend the coverage of the multiuser MIMO system. Now, we proceed to investigate the capacity benefit resulting from the SWNSF scheduling. In order to evaluate the capacity improvement resulting from the SWNSF scheduling, we need to characterize the statistical behavior of all the eigenvalues $\{\tilde{\lambda}_{k,i}\}_{i=1}^{N}$. In what follows, we first derive the mean increment of $(\tilde{\lambda}_{k,1} - \lambda_{k,1})$ due to the SWNSF scheduling. Then, we examine the mean increment of $(\tilde{\lambda}_{k,i} - \lambda_{k,i})$ of all the other ordered eigenvalues $\{\tilde{\lambda}_{k,i}\}_{i=2}^{N}$. Finally, we derive the link and system capacity for the multiuser MIMO system employing the SWNSF scheduling.

4.4.1 Analysis of $\tilde{\lambda}_{k,1}$

Recall from Proposition 4.2 that $\lambda_{k,1}$ is an exponentially distributed random variable with parameter $1/N$. From (4.9), the SWNSF scheduling has changed the CDF of the minimum eigenvalue into

$$F_{\tilde{\lambda}_{k,n}}(\lambda) = \left(1 - e^{-n\lambda}\right)^K \quad . \tag{4.25}$$

By comparing $F_{\tilde{\lambda}_{k,1}}(\lambda)$ and $F_{\lambda_{k,1}}(\lambda)$, one can find that the magnitude of the smallest eigenvalue is boosted for $K > 1$. To be specific, the mean of $\tilde{\lambda}_{k,1}$ can be obtained by

$$
\begin{aligned}
\mathrm{E}[\tilde{\lambda}_{k,1}] &\overset{(a)}{=} \int_0^\infty (1 - F_{\tilde{\lambda}_{k,1}}(\lambda)) d\lambda \\
&\overset{(b)}{=} \int_0^\infty \sum_{k=1}^K \binom{K}{k} (-1)^{k+1} e^{-nk\lambda} d\lambda \\
&= \frac{1}{n} \sum_{k=1}^K \binom{K}{k} \frac{(-1)^{k+1}}{k} \\
&\overset{(c)}{=} \frac{1}{n} \sum_{k=1}^K \frac{1}{k}
\end{aligned}
\tag{4.26}
$$

where (a) relies on $\tilde{\lambda}_{k,1} \geq 0$, (b) uses the binomial expansion and (c) follows from [100, eq. 0.155]. Equivalently, the mean increment of $\tilde{\lambda}_{k,1}$ relative to $\lambda_{k,1}$ can be expressed by

$$\Delta_\lambda \overset{\Delta}{=} \mathrm{E}[\tilde{\lambda}_{k,1}] - \mathrm{E}[\lambda_{k,1}] = \frac{1}{N} [\psi(K+1) + \beta - 1] \quad , \tag{4.27}$$

where $\psi(K+1) = -\beta + \sum_{k=1}^K k^{-1}$ is the psi function for integer K and $\beta \simeq 0.5772$ is the Euler's constant [82]. We note that the psi function $\psi(K+1)$ can be approximated by $\log(K+1) \simeq \log K$ for sufficiently large K [82, eq. 6.3.18].

4.4.2 Analysis of $\{\tilde{\lambda}_{k,i}\}_{i=2}^N$

With the statistical knowledge of $\tilde{\lambda}_{k,1}$, we proceed to investigate the behavior of $\{\tilde{\lambda}_{k,i}\}_{i=2}^N$ when applying the SWNSF algorithm. We introduce a new set of random variables as follows:

$$
\begin{aligned}
S_{k,1} &\overset{\Delta}{=} \lambda_{k,1} \\
S_{k,i} &\overset{\Delta}{=} \lambda_{k,i} - \lambda_{k,1}, \quad \text{for } 2 \leq i \leq N-1 \quad .
\end{aligned}
\tag{4.28}
$$

Obviously, $S_{k,i}$ denote the "spacing" between $\lambda_{k,i}$ and the smallest eigenvalue $\lambda_{k,1}$ for $2 \leq i \leq N - 1$. Through $S_{k,i}$, the following proposition describes some statistical characteristics of $\tilde{\lambda}_{k,i}$.

Proposition 4.3 Let $S_{k,i}$ be the random variables defined in (4.28). Let $\phi_{\tilde{\lambda}_{k,i}}(\omega)$, $\phi_{\lambda_{k,i}}(\omega)$ and $\phi_{S_{k,i}}(\omega)$ denote the Laplace transforms of $\tilde{\lambda}_{k,i}$, $\lambda_{k,i}$ and $S_{k,i}$, respectively. Then we have

(i) The spacing $S_{k,i}$ are independent of $\lambda_{k,1}$ for $2 \leq i \leq N$.

(ii) $\phi_{\tilde{\lambda}_{k,i}}(\omega)$, $\phi_{\lambda_{k,i}}(\omega)$ and $\phi_{S_{k,i}}(\omega)$ are related by

$$\phi_{\tilde{\lambda}_{k,i}}(\omega) = \phi_{\tilde{\lambda}_{k,1}}(\omega)\phi_{S_{k,i}}(\omega) = A(\omega)\phi_{\lambda_{k,i}}(\omega), \quad 2 \leq i \leq N \ . \tag{4.29}$$

where $A(\omega) = \frac{K!\,(1+\omega/N)\,\Gamma(1+\omega/N)}{\Gamma(1+K+\omega/N)}$, $\Gamma(\cdot)$ is the gamma function and $K! = \prod_{i=1}^{K} i$.

(iii) The mean increment between $\tilde{\lambda}_{k,i}$ and $\lambda_{k,i}$ is

$$\mathrm{E}[\tilde{\lambda}_{k,i}] - \mathrm{E}[\lambda_{k,i}] = \Delta_\lambda = \frac{1}{N}\left[\psi(K+1) + \beta - 1\right], \quad 2 \leq i \leq N \ . \tag{4.30}$$

(iv) The sum of $\mathrm{E}[\tilde{\lambda}_{k,i}]$ over all eigenvalues is

$$\sum_{i=1}^{N} \mathrm{E}[\tilde{\lambda}_{k,i}] = N^2 + N\,\Delta_\lambda \ . \tag{4.31}$$

Proof: Please refer to Appendix B. $\square$

By comparing (4.27) and (4.30), it is interesting to find that the mean increment of $\Delta_\lambda = \mathrm{E}[\tilde{\lambda}_{k,1} - \lambda_{k,1}]$ resulting from the SWNSF scheduling has been shifted to all the other ordered eigenvalues. In other words, the SWNSF scheduling can increase the value of $\mathrm{E}[\tilde{\lambda}_{k,1}]$ and subsequently the *repelling property* between $\tilde{\lambda}_{k,i}$ and $\tilde{\lambda}_{k,1}$ (as implied by Proposition 4.3 brings about the same amount of enhancement for $\mathrm{E}[\tilde{\lambda}_{k,i}]$. The effect of the SWNSF scheduling on the movement of $\lambda_{k,i}$ can be best illustrated by the following example.

Example 4.1: Consider a 3×3 MIMO system. Following (4.11), the joint PDF of the ordered eigenvalues of $\mathbf{H}_k\mathbf{H}_k^H$ is given as

$$f_{\lambda_{k,1},\lambda_{k,2},\lambda_{k,3}}(\lambda_1, \lambda_2, \lambda_3) = \frac{1}{4}\,e^{-(\lambda_1+\lambda_2+\lambda_3)}(\lambda_3 - \lambda_2)^2(\lambda_3 - \lambda_1)^2(\lambda_2 - \lambda_1)^2 \ ,$$

$$\lambda_3 \geq \lambda_2 \geq \lambda_1 \geq 0 \ . \tag{4.32}$$
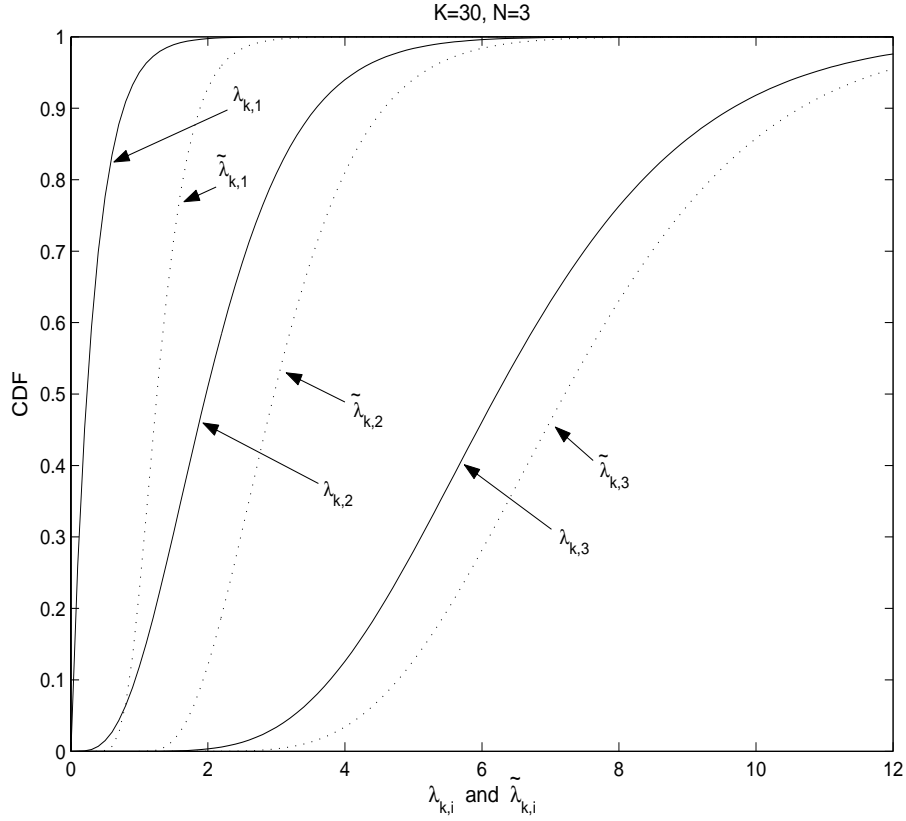
Figure 4.2: The CDFs of $\lambda_{k,i}$ and $\tilde{\lambda}_{k,i}$ for $K = 30$ and $N = 3$.

Then the marginal CDF associated with $\lambda_{k,1}$, $\lambda_{k,2}$ and $\lambda_{k,3}$ can be respectively derived as

$$F_{\lambda_{k,1}}(\lambda) = \int_0^\lambda \left[\int_{\lambda_1}^\infty \int_{\lambda_2}^\infty f_{\lambda_{k,1},\lambda_{k,2},\lambda_{k,3}}(\lambda_1, \lambda_2, \lambda_3) d\lambda_3 d\lambda_2 \right] d\lambda_1 = 1 - e^{-3\lambda} \ , \qquad (4.33)$$

$$\begin{aligned}
F_{\lambda_{k,2}}(\lambda) &= \int_0^\lambda \left[\int_0^{\lambda_2} \int_{\lambda_2}^\infty f_{\lambda_{k,1},\lambda_{k,2},\lambda_{k,3}}(\lambda_1, \lambda_2, \lambda_3) d\lambda_3 d\lambda_1 \right] d\lambda_2 \\
&= 1 + 2e^{-3\lambda} - e^{-2\lambda} \left(3 + 3\lambda^2 + \lambda^3 + \frac{\lambda^4}{4} \right) \ , \qquad (4.34)
\end{aligned}$$

and

$$\begin{aligned}
F_{\lambda_{k,3}}(\lambda) &= \int_0^\lambda \left[\int_0^{\lambda_3} \int_0^{\lambda_2} f_{\lambda_{k,1},\lambda_{k,2},\lambda_{k,3}}(\lambda_1, \lambda_2, \lambda_3) d\lambda_1 d\lambda_2 \right] d\lambda_3 \\
&= 1 - e^{-3\lambda} + e^{-2\lambda} \left(3 + 3\lambda^2 + \lambda^3 + \frac{\lambda^4}{4} \right) \\
&\quad - e^{-\lambda} \left(3 + 3\lambda^2 - \lambda^3 + \frac{\lambda^4}{4} \right) \ . \qquad (4.35)
\end{aligned}$$

On the other hand, from (4.25), the CDF of the smallest eigenvalue with the effect of the SWNSF scheduling becomes

$$F_{\tilde{\lambda}_{k,1}}(\lambda) = \left(1 - e^{-3\lambda}\right)^K \quad . \tag{4.36}$$

By using (4.34) to obtain the Laplace transform of $\lambda_{k,2}$ and invoking (4.29), the Laplace transform of of $\tilde{\lambda}_{k,2}$ is given as

$$\phi_{\tilde{\lambda}_{k,2}}(\omega) = \frac{K!\,(32 + 22\omega + 4\omega^2)\,\Gamma(1 + \omega/3)}{\Gamma(1 + K + \omega/3)(2 + \omega)^5} \quad . \tag{4.37}$$

Similarly, we can have

$$\phi_{\tilde{\lambda}_{k,3}}(\omega) = \frac{K!\,(32 + 42\omega + 14\omega^2)\,\Gamma(1 + \omega/3)}{\Gamma(1 + K + \omega/3)(2 + 3\omega + \omega^2)^5} \quad . \tag{4.38}$$

Then the PDFs and CDFs of $\tilde{\lambda}_{k,2}$ and $\tilde{\lambda}_{k,3}$ can be obtained from (4.37) and (4.38) by using the numerical inversion [101].

Figure 4.2 plots the CDFs of all the eigenvalues with the effect of the SWNSF scheduling for $K = 30$ and $N = 3$. Comparing $F_{\lambda_{k,1}}(\lambda)$ and $F_{\tilde{\lambda}_{k,1}}(\lambda)$, one can see that the SWNSF scheduling causes the CDF of the smallest eigenvalue to move rightward, implying that the link reliability between the base station and the target user is improved. Furthermore, the CDFs of all the other ordered eigenvalues are repelled to move rightward accordingly. Essentially, the property of the rightward shift for all $F_{\lambda_{k,i}}(\lambda)$ enables further capacity improvements for the spatial multiplexing MIMO system. $\diamondsuit$

4.4.3　Scheduling Gain for Mean SNR Improvement

From (4.31) and (B.7), we can further write

$$\frac{\sum_{i=1}^{N} \mathrm{E}[\tilde{\lambda}_{k,i}]}{\sum_{i=1}^{N} \mathrm{E}[\lambda_{k,i}]} = \frac{\sum_{i=1}^{N} \mathrm{E}[\tilde{\gamma}_{k,i}]}{\sum_{i=1}^{N} \mathrm{E}[\gamma_{k,i}]} = 1 + \frac{1}{N^2}\left[\psi(K+1) + \beta - 1\right] \quad . \tag{4.39}$$

The expression (4.39) indicates that the sum of the mean receive SNR at all subchannels of the spatial multiplexing MIMO system is improved thanks to the SWNSF scheduling. Based on (4.39), we can make the comments regarding the SWNSF scheduling gain as follows:

- The SWNSF scheduling can improve the receive SNR for the MIMO system by exploiting multiuser diversity. When user population is large, the improvement of the mean receive SNR due to the SWNSF scheduling grows with $\log(K)/N^2$.

- The large number of antenna elements could attenuate the multiuser diversity gain resulting from the SWNSF scheduling. This phenomenon can be intuitively explained as follows. Generally speaking, scheduling is a media access layer (MAC) technique to deliver multiuser diversity gain by utilizing independent channel fluctuations among users. Therefore, the larger the channel variations among users, the higher the performance gain from scheduling. In this regard, it is shown in (4.16) that the number of antennas reduces the variance of $\lambda_{k,1}$ to $1/N^2$. Thus, the damped channel fluctuation reduces the scope that the SWNSF scheduling can exploit, thereby diluting the scheduling gain. A recent work [102] also observed the phenomenon of diminishing scheduling gain with the increased number of antennas. Fortunately, with the antenna number of practical interests, the SWNSF scheduling can still provide considerable scheduling gain.

4.4.4 Capacity Analysis

Now we precede to derive the link capacity and system capacity with the SWNSF scheduling. We define the system capacity as the sum of the link capacity delivered to each user on average. Therefore, the system capacity with the SWNSF scheduling can be written as

$$\langle C \rangle_{\text{SWNSF}} = \sum_{k=1}^{K} p_k \tilde{C}_k = \frac{1}{K} \sum_{k=1}^{K} \tilde{C}_k \ , \tag{4.40}$$

where $p_k = 1/K$ follows Proposition 4.1 and

$$\tilde{C}_k = \sum_{i=1}^{N} \mathrm{E}\left[\log(1 + \tilde{\gamma}_{k,i})\right] = \sum_{i=1}^{N} \mathrm{E}\left[\log\left(1 + \frac{\rho_k}{N}\tilde{\lambda}_{k,i}\right)\right] \tag{4.41}$$

is the link capacity of user k subject to the SWNSF scheduling. When user k is at the low SNR regime, (4.41) can be approximated by using (4.31), that is,

$$\tilde{C}_k \simeq \frac{\rho_k}{N} \sum_{i=1}^{N} \mathrm{E}[\tilde{\lambda}_{k,i}] = \rho_k \left[N + \frac{1}{N}\left(\psi(K+1) + \beta - 1\right)\right], \quad \text{for small } \rho_k \ . \tag{4.42}$$

When user k is at high SNR regime, $\tilde{C}_k$ in (4.41) can be upper bounded by

$$\tilde{C}_k \leq N \log \left(\frac{\rho_k}{N} \right) + N \log \left[N + \frac{1}{N} \left(\psi(K+1) + \beta - 1 \right) \right], \quad \text{for large } \rho_k \ , \qquad (4.43)$$

where the derivation is in Appendix C.

For comparison, we also express the system capacity with the RR scheduling as

$$\langle C \rangle_{\text{RR}} = \sum_{k=1}^{K} p_k C_k = \frac{1}{K} \sum_{k=1}^{K} C_k \ , \qquad (4.44)$$

where C_k is the link capacity of user k under the RR scheduling. Again, since the RR algorithm dose not alter the statistics of the receive SNR for any target user, C_k in (4.44) is the same as (4.5). In [103], a closed-form expression for C_k is given as

$$C_k = e^{N/\rho_k} \sum_{i=0}^{N-1} \sum_{j=0}^{i} \sum_{l=0}^{2j} \left\{ \frac{(-1)^l}{2^{2i-l}} \binom{2i-2j}{i-j} \binom{2j}{j} \binom{2j}{l} \sum_{r=0}^{l} E_{r+1} \left(\frac{N}{\rho_k} \right) \right\} \ , \qquad (4.45)$$

where $E_r(\cdot)$ is the exponential integral function of order r, defined as [82]

$$E_r(z) = \int_1^{\infty} e^{-zt} t^{-r} dt \ . \qquad (4.46)$$

Next, we evaluate the capacity gain of $\tilde{C}_k$ over C_k when applying the SWNSF scheduling.

4.4.5 Numerical Example

Here, we give some numerical examples to demonstrate the capacity benefits brought by the SWNSF scheduling. We divide the total K users equally into five groups. The users in the same group have the same value of average SNR ρ. The values of ρ from the first group to the fifth group are set to $[30, 20, 10, 0, -10]$ dB, respectively. In the following, we apply the low SNR approximation of (4.42) and the high SNR upper bound of (4.43) to evaluate the link capacity of the users in groups $\{4, 5\}$ and that in groups $\{1, 2, 3\}$, respectively.

Figure 4.3 shows the capacity improvement accomplished by the SWNSF scheduling for the users in different groups. The performance metric is the ratio of the link capacity achieved by the SWNSF scheduling to that by the RR scheduling, i.e. $\tilde{C}_k/C_k$. We assume $K = 50$ and $N = 3$ in this example. As one can see from Fig. 4.3, the SWNSF scheduling
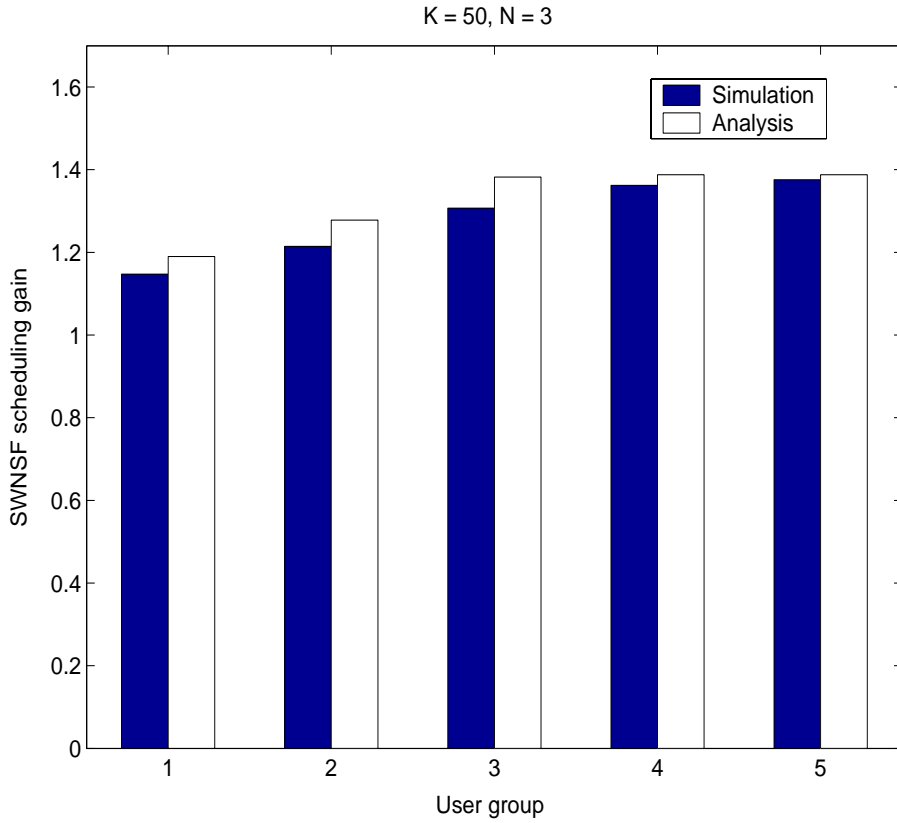
Figure 4.3: Capacity improvement with the SWNSF scheduling for the users in different user groups.

can provide 15% to 38% capacity gain over the RR scheduling for the users in the groups 1 to 5, respectively. This implies that the SWNSF scheduling tends to bring about higher capacity gain for the users with lower ρ.

Figure 4.4 shows the average capacity gain resulting from the SWNSF scheduling with different numbers of users in the system. The performance metric shown in the y-axis is the average capacity gain defined by $\frac{1}{K}\sum_{k=1}^{K}\frac{\tilde{C}_k}{C_k}$. One can see from Fig. 4.4 that the capacity gain increases as K increases. Furthermore, the average capacity gain achieved by the SWNSF scheduling diminishes due to the effect of channel damping when a larger number of antenna elements is employed.
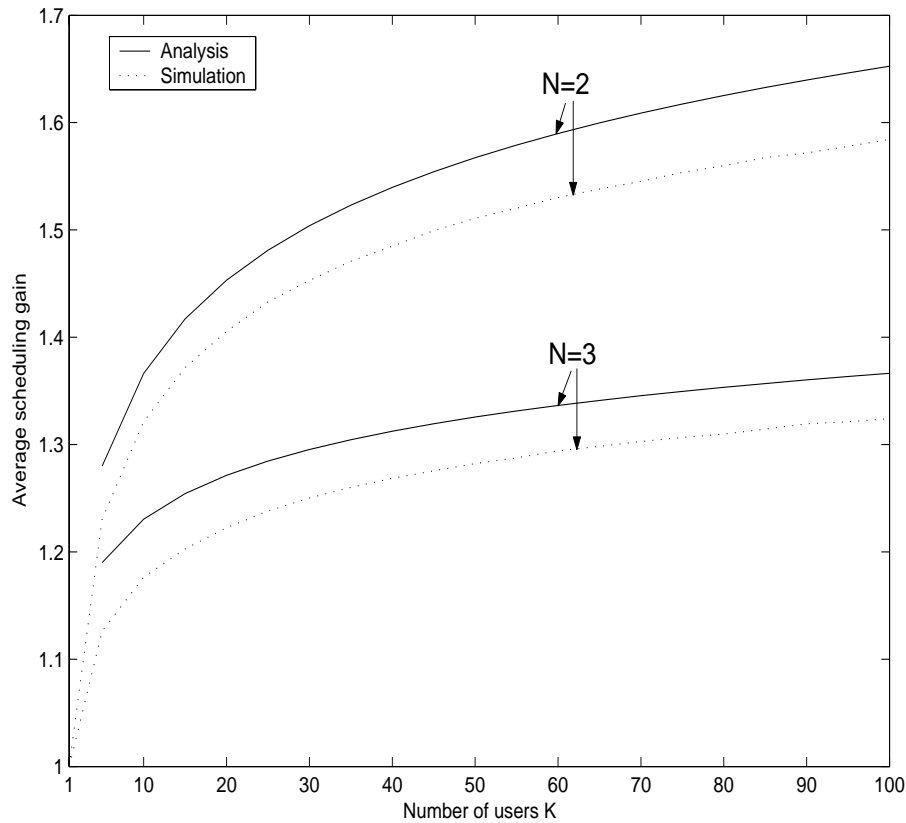
Figure 4.4: Average capacity gain resulting from the SWNSF scheduling with different numbers of users in the system.

4.5 Chapter Summary

The whole idea of this chapter is to promote a novel notion of using the multiuser diversity: one can devote the physical antennas to gaining capacity with the multiplexing-based MIMO scheme while taking advantage of multiuser diversity to compensate the degraded link quality for the multiplexing-based MIMO system. To be specific, we have proposed a SWNSF scheduling algorithm, which requires only scalar feedback, to demonstrate the merit of combining the multiplexing-based antenna technique with the multiuser scheduling system from both the perspectives of cell coverage extension and system capacity improvement.

Table 4.1 presents a quantitative sketch of how the proposed SWNSF scheduling enhances the coverage and capacity of the multiuser MIMO system. We normalize both the cell radius and link capacity for the SISO system to unity. The cell radius and link capacity for $K = 20, 50$ and $N = 2, 3$ are shown in Table 4.1 in comparison with the SISO

Table 4.1: Coverage and capacity enhancements with the SWNSF scheduling for $K = 20, 50$ and $N = 1, 2, 3$

| Multiuser MIMO systems | | $K = 20$ | | $K = 50$ | |
		Relative Cell Radius	Relative Capacity Gain	Relative Cell Radius	Relative Capacity Gain
$N = 1$	SISO	1	1	1	1
$N = 2$	MIMO with RR scheduling	0.71	1.94	0.71	1.94
$N = 2$	MIMO with SWNSF scheduling	1.52	2.74	1.65	2.94
$N = 3$	MIMO with RR scheduling	0.58	2.89	0.58	2.89
$N = 3$	MIMO with SWNSF scheduling	1.24	3.54	1.35	3.72

case. From the coverage performance aspect, the large number of antennas for the spatial multiplexing MIMO system can result in coverage shrinkage because of link reliability degradation. However, the SWNSF scheduling can virtually extend coverage by improving the receive SNR quality. From the capacity performance aspect, one can see that, as expected, the capacity of the spatial multiplexing MIMO system grows linearly with the number of antennas. Moreover, applying the SWNSF scheduling can further improve the capacity for the MIMO system. In the next chapter, we continue to explore the advantage of applying the multiplexing-based antenna technique for the multiuser MIMO system.

Chapter 5

Throughput Enhancement Based Antenna Techniques for Multiuser Scheduling Systems with Zero-Forcing Receivers

In this chapter, we revisit the topic of combining the multiplexing-based antenna technique with the multiuser scheduling system. In contrast with Chapter 4 where the optimal receiver is assumed, this chapter considers the zero-forcing receiver. Although the zero-forcing receiver is known to suffer from noise enhancement in a point-to-point (or single-user) MIMO system, the inherent property of poor channel quality avoidance from multiuser scheduling provides a natural way to overcome this drawback. To probe the merit of such cross-layer cooperation, this chapter introduces an analytical framework to evaluate the performance of the zero-forcing receiver operating in the multiuser MIMO system with scheduling. Furthermore, a number of scheduling algorithms that require different amounts of feedback information will be studied to assess the impact of feedback on the resulting performance.

5.1 The Zero-Forcing Receiver for a Single-User MIMO System

To begin with, we consider a point-to-point (single-user) MIMO system consisting of N_t transmit and N_r receive antennas. Let $\mathbf{x}$ and $\mathbf{y}$ be $N_t \times 1$ and $N_r \times 1$ signal vectors at the transmitter and the receiver, respectively. Let $\mathbf{n}$ denote the $N_r \times 1$ spatially white noise

with the covariance matrix $\mathrm{E}[\mathbf{n}\mathbf{n}^H] = \sigma^2 \mathbf{I}_{N_r}$, where $(\cdot)^H$ is the complex conjugate transpose operation . Then, the link between $\mathbf{x}$ and $\mathbf{y}$ is modelled by

$$\mathbf{y} = \mathbf{G}\mathbf{x} + \mathbf{n} = \sqrt{g}\mathbf{H}\mathbf{x} + \mathbf{n} \ , \tag{5.1}$$

where $\sqrt{g}$ depicts the large-scale (local average) behavior of the channel gain, and the $N_r \times N_t$ normalized channel matrix $\mathbf{H}$ characterizes the channel fading. We consider the flat Rayleigh fading such that every entry of $\mathbf{H}$ is independent, circular-symmetric complex Gaussian random variables $\mathcal{CN}(0,1)$. The total transmit power across all N_t antennas is constrained by $\mathrm{E}[\mathbf{x}^H\mathbf{x}] \leq P_t$.

Assume that at the transmitter the spatial multiplexing with equal power allocation method is applied to send N_t parallel data streams over the MIMO channel. Meanwhile, at the receiver the zero-forcing algorithm is used to recover the received spatially multiplexed signals. By multiplying $\mathbf{y}$ with $\mathbf{H}^\dagger/\sqrt{g}$, where $\mathbf{H}^\dagger = (\mathbf{H}^H\mathbf{H})^{-1}\mathbf{H}^H$ is the pseudo-inverse of $\mathbf{H}$, the received signal vector is decoded as

$$\hat{\mathbf{x}} = \mathbf{H}^\dagger\mathbf{y}/\sqrt{g} = \mathbf{x} + \mathbf{H}^\dagger\mathbf{n}/\sqrt{g} \ . \tag{5.2}$$

The output SNR at the n-th subchannel after the zero-forcing processing in (5.2) can be expressed by

$$\gamma_n = \frac{\rho}{N_t \left[(\mathbf{H}^H\mathbf{H})^{-1}\right]_{nn}} \ , \quad n = 1, \cdots, N_t \tag{5.3}$$

where $[\mathbf{A}]_{ij}$ is the (i,j)-th entry of $\mathbf{A}$ and $\rho = P_t g/\sigma^2$ is the mean received SNR. From [104] and [105], we know that γ_n in (5.3) is a Chi-squared distributed random variable with $2(N_r - N_t + 1)$ degrees of freedom and all $\{\gamma_n\}_{n=1}^{N_t}$ are independent and identically distributed (i.i.d.). Thus, the probability density function (PDF) of γ_n can be written as

$$f_{\gamma_n}(\gamma_n) = \frac{N_t \, e^{-N_t\gamma_n/\rho}}{\rho \, (N_r - N_t)!} \left(\frac{N_t}{\rho}\gamma_n\right)^{N_r - N_t}, \quad \gamma_n \geq 0 \ . \tag{5.4}$$

Note that the assumption of $N_r \geq N_t$ has been implicitly made for the spatial multiplexing MIMO system. Next, we utilize (5.4) to derive the achievable throughput and the outage probability for the zero-forcing receiver.

5.1.1 Achievable Throughput

Since the MIMO channel has been decomposed to N_t parallel, non-interfering single-input-single-output (SISO) subchannels from (5.4), the achievable throughput of the zero-forcing receiver can be obtained by summing up the throughput contributed from all subchannels. That is,

$$C_{\mathrm{zf}} = \sum_{n=1}^{N_t} \mathrm{E}\left[\log\left(1 + \gamma_n\right)\right] \tag{5.5}$$

$$= N_t \int_0^\infty \log(1 + \gamma_n) f_{\gamma_n}(\gamma_n) d\gamma_n \tag{5.6}$$

$$= \frac{N_t \, e^{N_t/\rho} \, N_t^{N_r - N_t + 1}}{\rho^{N_r - N_t + 1}} \sum_{n=1}^{N_r - N_t + 1} \left(\frac{\rho}{N_t}\right)^n \Gamma\left(n - N_r + N_t - 1, \frac{N_t}{\rho}\right) , \tag{5.7}$$

where (5.6) follows from the i.i.d. property of γ_n and (5.7) is obtained from the integral identity of (A.2). Note that $\Gamma(\cdot, \cdot)$ in (5.7) is the incomplete gamma function defined in (A.4). In addition, recall that the theoretical ergodic capacity of an open-loop MIMO system with $N_r \geq N_t$ is given as [1, 103]

$$C_{\mathrm{opt}} = \mathrm{E}\left[\log\det\left(\mathbf{I}_{N_r} + \frac{\rho}{N_t}\mathbf{H}\mathbf{H}^H\right)\right] \tag{5.8}$$

$$= e^{N_t/\rho} \sum_{i=0}^{N_t-1} \sum_{j=0}^{i} \sum_{l=0}^{2j} \left\{ \frac{(-1)^l (2j)! (N_r - N_t + l)!}{2^{2i-l} j! l! (N_r - N_t + j)!} \right.$$

$$\left. \cdot \binom{2i - 2j}{i - j}\binom{2j + 2N_r - 2N_t}{2j - l} \sum_{r=0}^{N_r - N_t + l} E_{r+1}\left(\frac{N_t}{\rho}\right) \right\} , \tag{5.9}$$

where $E_r(\cdot)$ is the exponential integral function of order r defined in (4.46). By comparing (5.7) and (5.9) under the same power constraint as well as the same number of transmit and receive antennas, we define the "efficiency" of the zero-forcing receiver as

$$\eta_1 = \frac{C_{\mathrm{zf}}}{C_{\mathrm{opt}}} \tag{5.10}$$

to gauge the performance of the zero-forcing receiver in extracting the multiplexing gain of the MIMO system.

Figure 5.1 plots the efficiency of the zero-forcing receiver defined in (5.10) for different numbers of transmit and receive antennas with various values of ρ. First, one can see
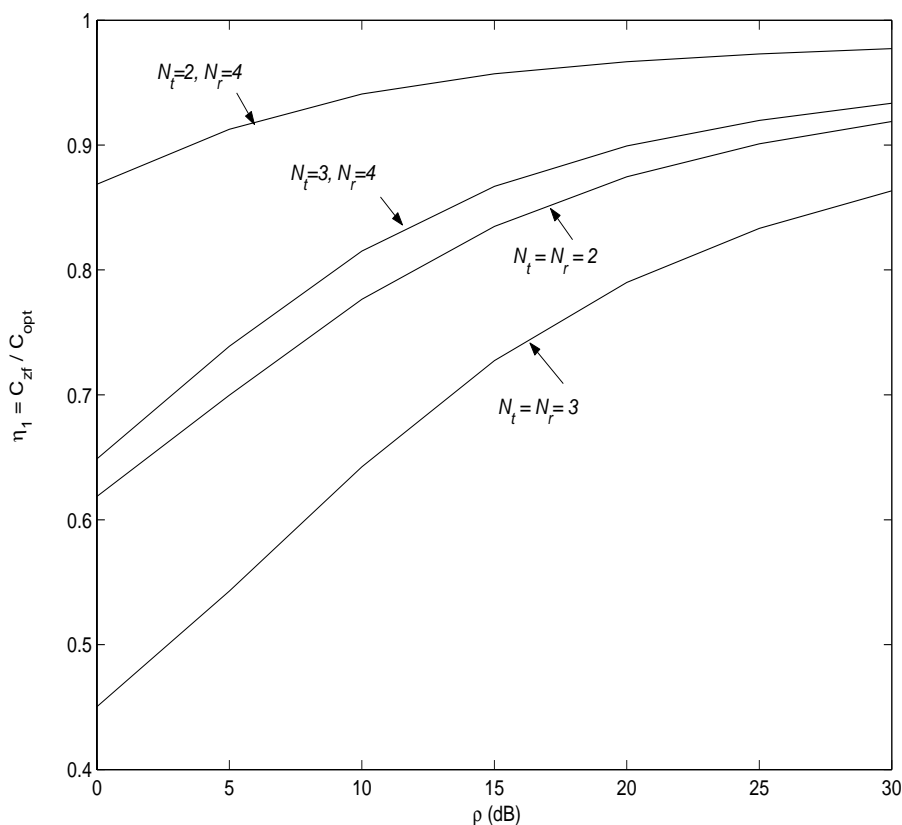
Figure 5.1: Achievable throughput for the zero-forcing receiver in a single-user MIMO system.

that the zero-forcing receiver can only achieve the comparable capacity with the optimal receiver at the high SNR region. The low SNR condition would exacerbate the effect of noise enhancement and significantly degrade the performance of the zero-forcing receiver. Second, for the case of equal number of transmit and receive antennas (i.e., $N_t = N_r = 2$ and $N_t = N_r = 3$), the more the antennas, the lower the efficiency. Third, by comparing the case $N_t = N_r = 2$ to $N_t = 2$ and $N_r = 4$, it is observed that adding more receive antennas can significantly improve the efficiency of the zero-forcing receiver to offer multiplexing gain because the diversity provided by the additional receive antenna can alleviate the effect of noise enhancement.

5.1.2 Outage Probability

As discussed in Section 4.1, the outage probability for a spatial multiplexing MIMO system can be defined as the event when the output SNR of any subchannel is less than a
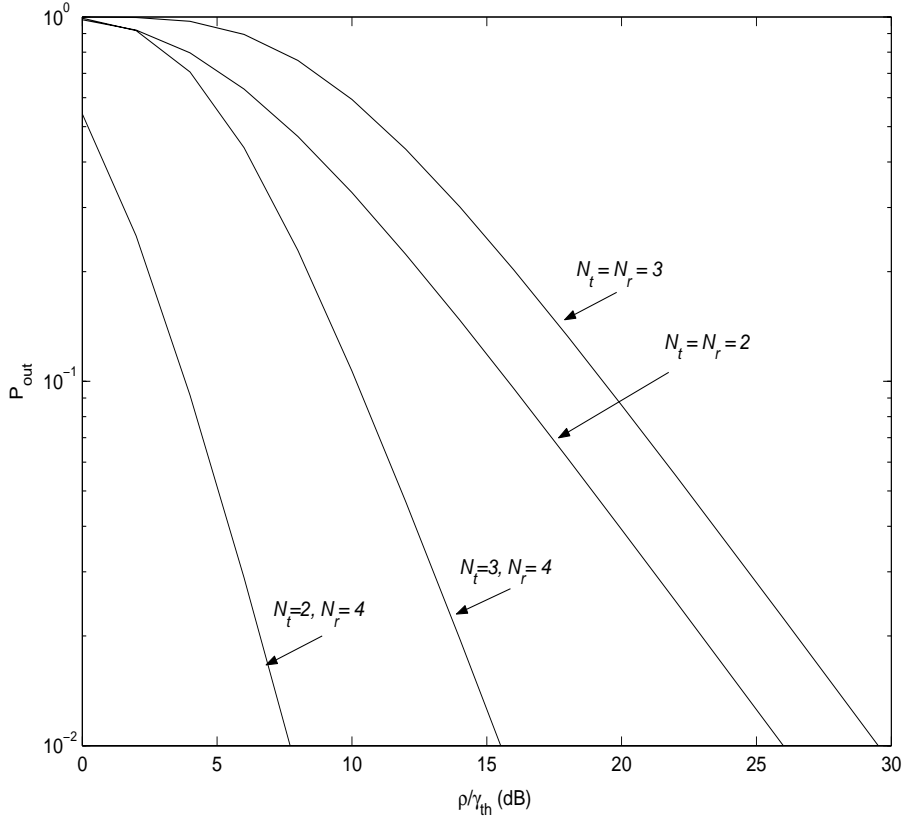
Figure 5.2: Outage probability for the zero-forcing receiver in a single-user MIMO system.

predetermined value γ_{th}. That is,

$$
\begin{aligned}
P_{\text{out}} &= \Pr\{\gamma_1 < \gamma_{\text{th}} \ \cup \ \gamma_2 < \gamma_{\text{th}} \ \cdots \ \cup \ \gamma_{N_t} < \gamma_{\text{th}}\} \\
&= \Pr\left\{\min_{\forall i}\{\gamma_i\} \triangleq \gamma_{\min} < \gamma_{\text{th}}\right\} \\
&= 1 - \Pr\left\{\gamma_{\min} \geq \gamma_{\text{th}}\right\} \ .
\end{aligned}
\tag{5.11}
$$

Substituting (5.4) into (5.11) and denoting the CDF of γ_n by $F_{\gamma_n}(\cdot)$, we can obtain the outage probability for the MIMO system using the zero-forcing receiver as [106]

$$
\begin{aligned}
P_{\text{out}} &= 1 - \left[1 - F_{\gamma_n}(\gamma_{\text{th}})\right]^{N_t} \\
&= 1 - \left[\Gamma\left(N_r - N_t + 1, \frac{N_t\gamma_{\text{th}}}{\rho}\right) \bigg/ (N_r - N_t)!\right]^{N_t} \ .
\end{aligned}
\tag{5.12}
$$

Figure 5.2 plots the outage probability of the zero-forcing receiver versus ρ/γ_{th} for various numbers of transmit and receive antennas according to (5.12). One can find that increasing the number of receive antennas and/or working the zero-forcing receiver at the high SNR

regime are two crucial factors for the zero-forcing receiver to have the satisfactory outage probability performance.

5.1.3 The Effect of Noise Enhancement

Two important effects resulting from the scheduling technique can essentially help to improve the achievable throughput and the outage probability performances of the zero-forcing receiver. First, the multiuser selection diversity extracted by a proper scheduling algorithm can prevent the user from being served under ill channel conditions. Second, taking the view from the whole multiuser MIMO system, one can find that the scheduling algorithm can virtually increase the number of receive antennas to the sum of all the users' receive antennas. Therefore, while the low efficiency of the zero-forcing receiver may disqualify its use in a pure point-to-point single user MIMO system, a practical and interesting question arises: given an underlying scheduling system such as IS-856, how well the multiuser diversity can be utilized to mitigate the adverse noise enhancement effect of the zero-forcing receiver so that it can become a viable option to restore the spatially multiplexed signals over the MIMO system? Towards this end, the resulting performance of the multiuser MIMO system using the zero-forcing receiver and a variety of scheduling algorithms will be analyzed in the rest of this chapter.

5.2 The Multiuser MIMO System with Zero-Forcing Receivers

Now we shift the focus from the single user MIMO system to the multiuser MIMO system. In this section, we describe the system model, illustrate the feedback schemes for multiuser scheduling and define performance metrics.

5.2.1 System Model

Consider a multiuser MIMO system where the base station with N_t transmit antennas serves K downlink users, each of which is equipped with N_r receive antennas. For the purpose of

decoupling the benefits of the multiuser scheduling from the extra receive antennas, we shall restrict our analysis to the worse case $N_t = N_r$. The channel between the base station and user k $(k = 1, \cdots, K)$ is represented by the channel matrix $\mathbf{G}_k = \sqrt{g_k}\mathbf{H}_k$ as defined in (5.1). As we have shown in Proposition 4.1 of Chapter 4, the near-far effect due to different ρ_k can be compensated by using the normalization technique for scheduling algorithms. Therefore, we can focus on $g_k = g$ for all k. Again, the channel variations of $\mathbf{H}_k$ are assumed to be fixed during a time slot, but independently vary from time slot to time slot. The variations of $\mathbf{H}_k$ across users are also assumed to be independent. Thus, from (5.3), the PDF of the output SNR at the n-th subchannel of user k becomes

$$f_{\gamma_n^k}(\gamma_n) = \frac{N}{\rho} e^{-N\gamma_n/\rho} \ . \tag{5.13}$$

That is, γ_n^k for $n \in \{1, \cdots, N\}$ and $k \in \{1, \cdots, K\}$ are i.i.d. exponentially distributed random variables with parameter ρ/N.

To tackle the total NK variates in the multiuser MIMO system from (5.13), order statistics is a convenient tool to analyze the performance when the scheduling algorithm selects a part of the total variates as the subchannels for data transmissions. We introduce the notation about order statistics that will be used extensively in the remaining part of this chapter. Let $X_1, X_2, \cdots, X_L$ be a random sample from a continuous random variable with PDF $f_X(x)$ and CDF of $F_X(x)$. Let $X_{1:L} \leq X_{2:L} \leq \cdots \leq X_{L:L}$ be the order statistics obtained by arranging the preceding sample in increasing order of magnitude. Then $X_{l:L}$ $(1 \leq l \leq L)$ is called the l-th order statistic and its PDF and CDF can be respectively expressed by [106]

$$f_{X_{l:L}}(x_l) = \frac{L!}{(l-1)!(L-l)!} \left[F_X(x_l)\right]^{l-1} \left[1 - F_X(x_l)\right]^{L-l} f_X(x_l) \ , \tag{5.14}$$

and

$$F_{X_{l:L}}(x_l) = \sum_{i=l}^{L} \binom{L}{i} \left[F_X(x_l)\right]^i \left[1 - F_X(x_l)\right]^{L-i} \ . \tag{5.15}$$

Following this notation, the subchannel output SNR $\{\gamma_n^k\}_{n=1}^N$ for any user k can be arranged to have $\gamma_{1:N}^k \leq \cdots \leq \gamma_{N:N}^k$.

5.2.2   Feedback Schemes for Scheduling

The base station is assumed to have the knowledge of channel quality through the instantaneous feedback of subchannel output SNR from all users. We consider two feedback schemes that provide the base station with different amounts of channel quality information:

- *Scalar feedback:* For scalar feedback it means that only a scalar value of one subchannel output SNR selected from the N subchannels is sent back from each user. In Section 5.3, we will analyze two extreme cases wherein the maximum or minimum value of each user's subchannel output SNR (i.e. $\gamma_{N:N}^k$ or $\gamma_{1:N}^k$) is available at the base station. According to this feedback information, the base station selects one target user to serve. Such a scalar feedback scheduling requires only a low-rate feedback channel and can be applicable to the current IS-856 cellular system, where a feedback channel of 800 Hz is supported in the reverse link [4].

- *Vector feedback:* In this case, the base station has the complete knowledge of γ_n^k for all n and k. Therefore, this scheme requires a vector of $\{\gamma_n^k\}_{n=1}^N$ be sent back from each user. Since $\{\gamma_n^k\}$ are i.i.d. over n and k, the base station then can exploit the full knowledge of $\{\gamma_n^k\}$ to achieve better performance by performing scheduling in the spatial (antenna) domain as well [59, 63]. Unlike the scalar feedback scheduling which dedicates all transmit antennas to one user, the vector feedback scheduling allows transmit antennas to independently bear data streams for different target users so that the base station may service multiple users at the same time slot. Obviously, compared with the scalar feedback scheduling, the vector feedback scheduling increases the available selection order in the multiuser MIMO system from K to NK. However, the vector feedback scheduling would consume more reverse link capacity due to higher feedback overhead.

5.2.3 Performance Metrics

Now we derive the achievable throughput ($\tilde{C}_{\text{zf}}$) and outage probability ($\tilde{P}_{\text{out}}$) of the zero-forcing receiver operating in the multiuser MIMO system with scheduling. Represent $\{\tilde{\gamma}_n\}_{n=1}^N$ as the subchannel output SNRs for the data streams transmitting from the base station to the target user(s) after applying the scheduling technique. Also, let $\tilde{\gamma}_{1:N} \leq \cdots \leq \tilde{\gamma}_{N:N}$ be the ordered version of $\{\tilde{\gamma}_n\}_{n=1}^N$ and $f_{\tilde{\gamma}_{n:N}}(\gamma_n)$ denote the PDF of $\tilde{\gamma}_{n:N}$. Therefore, the achievable throughput of the zero-forcing receiver in the multiuser MIMO system can be expressed by modifying (5.5) as

$$\tilde{C}_{\text{zf}} = \sum_{n=1}^N \text{E}[\log(1 + \tilde{\gamma}_{n:N})] = \sum_{n=1}^N \int_0^\infty \log(1 + \gamma_n) f_{\tilde{\gamma}_{n:N}}(\gamma_n) d\gamma_n \quad . \tag{5.16}$$

Analogous to (5.11), the outage probability in the presence of multiuser scheduling then can be written as

$$\tilde{P}_{\text{out}} = \Pr\{\tilde{\gamma}_{1:N} < \gamma_{\text{th}}\} = \int_0^{\gamma_{\text{th}}} f_{\tilde{\gamma}_{1:N}}(\gamma_1) d\gamma_1 \quad . \tag{5.17}$$

5.3 Analysis for Scalar Feedback Scheduling

This section analyzes the performance of the multiuser MIMO system with scalar feedback scheduling. We investigate two scheduling polices that select the target user based on the extreme order statistic of $\gamma_{N:N}^k$ or $\gamma_{1:N}^k$. The other scheduling policies that use the order statistic of $\gamma_{n:N}^k$ for $n \in \{2, \cdots, N-1\}$ can be also analyzed by similar procedures presented in the following.

5.3.1 Max-Max Scheduling

With the information of $\{\gamma_{N:N}^k\}_{k=1}^K$ from all users, the base station chooses the target user according to

$$k^* = \arg\max_k \gamma_{N:N}^k \quad . \tag{5.18}$$

We call the scheduling policy of (5.18) the *max-max scheduling*. Obviously, once the target user k^* is determined, we have

$$\tilde{\gamma}_{n:N}^{\text{ma}} = \gamma_{n:N}^{k^*} \qquad \text{for } n = 1, \cdots, N \tag{5.19}$$

where the superscript *ma* denotes the max-max scheduling. Recall from (5.13) that γ_n^k are i.i.d. random variables across n and k. Therefore, $\tilde{\gamma}_{N:N}^{\text{ma}}$ (the highest order of $\tilde{\gamma}_{n:N}^{\text{ma}}$) in (5.19) can be equivalently generated by selecting the largest one from the total KN i.i.d. random variables given in (5.13). Representing X as an exponentially distributed random variable with parameter ρ/N, it is then followed that

$$\tilde{\gamma}_{N:N}^{\text{ma}} = X_{KN:KN} \ . \tag{5.20}$$

Thus, applying (5.20) to (5.14), the PDF of $\tilde{\gamma}_{N:N}^{\text{ma}}$ is obtained as

$$f_{\tilde{\gamma}_{N:N}^{\text{ma}}}(\gamma_N) = \frac{KN^2}{\rho} e^{-N\gamma_N/\rho} \left(1 - e^{-N\gamma_N/\rho}\right)^{KN-1} \ . \tag{5.21}$$

Next, we proceed to derive the PDF of $\tilde{\gamma}_{n:N}^{\text{ma}}$ for $n = 1, \cdots, N-1$ through the derived $f_{\tilde{\gamma}_{N:N}^{\text{ma}}}(\gamma_N)$ in (5.21).

Let $f_{\gamma_{n:N}^{k^*}, \gamma_{N:N}^{k^*}}(\gamma_n, \gamma_N)$ denote the joint PDF of $\gamma_{n:N}^{k^*}$ and $\gamma_{N:N}^{k^*}$. Then the marginal PDF of $\tilde{\gamma}_{n:N}^{\text{ma}}$ can be obtained by

$$f_{\tilde{\gamma}_{n:N}^{\text{ma}}}(\gamma_n) = \int_{\gamma_n}^{\infty} f_{\gamma_{n:N}^{k^*}, \gamma_{N:N}^{k^*}}(\gamma_n, \gamma_N) \, d\gamma_N, \quad n = 1, \cdots, N-1 \ . \tag{5.22}$$

Using the conditional probability property, we can write

$$f_{\gamma_{n:N}^{k^*}, \gamma_{N:N}^{k^*}}(\gamma_n, \gamma_N) = f_{\gamma_{n:N}^{k^*} | \gamma_{N:N}^{k^*}}(\gamma_n | \gamma_N) f_{\gamma_{N:N}^{k^*}}(\gamma_N) \ , \tag{5.23}$$

where $f_{\gamma_{N:N}^{k^*}}(\gamma_N) = f_{\tilde{\gamma}_{N:N}^{\text{ma}}}(\gamma_N)$ is given in (5.21), and the conditional PDF $f_{\gamma_{n:N}^{k^*} | \gamma_{N:N}^{k^*}}(\gamma_n | \gamma_N)$ can be obtained with the help of the following lemma.

Lemma 5.1 Let $X_{1:L} \leq \cdots \leq X_{L:L}$ be the order statistics of a sample of size L from a random variable with PDF $f_X(x)$ and CDF $F_X(x)$. Given that $X_{j:L} = x_j$ for $j > i$, the

conditional PDF of $X_{i:L}$ is

$$f_{X_{i:L}}\left(x_i \mid X_{j:L} = x_j\right) = \frac{(j-1)!}{(i-1)!(j-i-1)!} \left\{\frac{F_X(x_i)}{F_X(x_j)}\right\}^{i-1}$$
$$\cdot \left\{\frac{F_X(x_j) - F_X(x_i)}{F_X(x_j)}\right\}^{j-i-1} \frac{f_X(x_i)}{F_X(x_j)}, \quad x_i \le x_j \qquad (5.24)$$

Proof: Please refer to [106, Theorem 2.4.2]. □

By substituting (5.24) into (5.23) and using the binomial expansion $(1-x)^n = \sum_{i=0}^{n} \binom{n}{i}(-1)^i x^i$, (5.22) can be derived as

$$f_{\tilde{\gamma}_{n:N}^{\mathrm{ma}}}(\gamma_n) = \frac{KN^2(N-1)!}{\rho(n-1)!(N-n-1)!} \sum_{i_1=0}^{n-1} \binom{n-1}{i_1} \sum_{i_2=0}^{N(K-1)} \binom{N(K-1)}{i_2}$$
$$\cdot e^{-(i_1+i_2+1+N-n)N\gamma_n/\rho} \sum_{i_3=0}^{N-n-1} \binom{N-n-1}{i_3} \frac{(-1)^{i_1+i_2+i_3}}{i_2+i_3+1} . \qquad (5.25)$$

As a result, from (5.21) and (5.25), we obtain all the PDFs of $\tilde{\gamma}_{n:N}^{\mathrm{ma}}$ for $n = 1, \cdots, N$. In the following, we use these PDFs to derive the achievable throughput and outage probability of the zero-forcing receiver operating in the multiuser MIMO system with scheduling. First, the outage probability defined in (5.17) under the max-max scheduling can be computed by integrating $f_{\tilde{\gamma}_{1:N}^{\mathrm{ma}}}(\gamma_1)$ from 0 to γ_{th}. Specifically, we have

$$\tilde{P}_{\mathrm{out}}^{\mathrm{ma}} = KN(N-1) \sum_{i_1=0}^{N(K-1)} \binom{NK-N}{i_1} \frac{1 - e^{-(i_1+N)N\gamma_{\mathrm{th}}/\rho}}{(i_1+N)}$$
$$\cdot \sum_{i_2=0}^{N-2} \binom{N-2}{i_2} \frac{(-1)^{i_1+i_2}}{(i_1+i_2+1)} . \qquad (5.26)$$

Furthermore, applying (5.21) and (5.25) to (5.16), we obtain the achievable throughput of the zero-forcing receiver subject to the max-max scheduling as follows:

$$\tilde{C}_{\mathrm{zf}}^{\mathrm{ma}} = C_{\tilde{\gamma}_{N:N}^{\mathrm{ma}}} + \sum_{n=1}^{N-1} C_{\tilde{\gamma}_{n:N}^{\mathrm{ma}}} \qquad (5.27)$$

where

$$C_{\tilde{\gamma}_{N:N}^{\mathrm{ma}}} = \frac{KN^2}{\rho} \sum_{i=0}^{KN-1} (-1)^i \binom{KN-1}{i} h\left(\frac{N(i+1)}{\rho}\right) \qquad (5.28)$$

71

and

$$C_{\tilde{\gamma}_{n:N}^{\mathrm{ma}}} = \frac{KN^2(N-1)!}{\rho(n-1)!(N-n-1)!} \sum_{i_1=0}^{n-1} \binom{n-1}{i_1} \sum_{i_2=0}^{N(K-1)} \binom{N(K-1)}{i_2}$$

$$\cdot h\left(\frac{(i_1+i_2+1+N-n)N}{\rho}\right) \sum_{i_3=0}^{N-n-1} \binom{N-n-1}{i_3} \frac{(-1)^{i_1+i_2+i_3}}{i_2+i_3+1} \qquad (5.29)$$

for $n = 1, \cdots, N-1$. Note that $h(\cdot)$ in (5.28) and (5.29) is defined as

$$h(x) \triangleq \int_0^\infty e^{-xt} \log(1+t)dt = \frac{e^x E_1(x)}{x} \quad . \qquad (5.30)$$

5.3.2   Max-Min Scheduling

Now we investigate another scalar feedback scheduling wherein the base station arranges transmissions according to $\{\gamma_{1:N}^k\}_{k=1}^K$. Note that $\gamma_{1:N}^k$ represents the minimum output SNR among N antennas for user k. During each time slot, the base station selects the target user by the following *max-min scheduling* policy[1]:

$$k^* = \arg\max_k \gamma_{1:N}^k \quad . \qquad (5.31)$$

Similar to (5.19), given the selected user k^*, we have

$$\tilde{\gamma}_{n:N}^{\mathrm{mi}} = \gamma_{n:N}^{k^*} \qquad \text{for } n = 1, \cdots, N \qquad (5.32)$$

where the superscript *mi* denotes the max-min scheduling. From (5.13) and (5.14), it is easy to find that the feedback information $\gamma_{1:N}^k$ has an exponential distribution with parameter ρ/N^2. Therefore, applying the scheduling rule of (5.31) to select the maximum from K i.i.d. $\{\gamma_{1:N}^k\}_{k=1}^K$, we represent $\tilde{\gamma}_{1:N}^{\mathrm{mi}}$ in (5.32) as

$$\tilde{\gamma}_{1:N}^{\mathrm{mi}} = X_{K:K} \qquad (5.33)$$

where X is an exponentially distributed random variable with parameter ρ/N^2. Thus, applying (5.14) to (5.33) yields the PDF of $\tilde{\gamma}_{1:N}^{\mathrm{mi}}$

$$f_{\tilde{\gamma}_{1:N}^{\mathrm{mi}}}(\gamma_1) = \frac{KN^2}{\rho} \sum_{i=0}^{K-1} (-1)^i \binom{K-1}{i} e^{-N^2(i+1)\gamma_1/\rho} \quad . \qquad (5.34)$$

---

[1]The max-min scheduling algorithm considered in this chapter corresponds to the SWNSF scheduling introduced in Chapter 4.

Also, applying (5.15) and (5.33) to (5.17), we get the outage probability under the max-min scheduling as

$$\tilde{P}_{\text{out}}^{\text{mi}} = \left(1 - e^{-N^2\gamma_{\text{th}}/\rho}\right)^K .$$ (5.35)

The following lemma gives the conditional distribution of a higher order statistic conditioned on a lower order statistic.

Lemma 5.2 Let $X_{1:L} \leq \cdots \leq X_{L:L}$ be the order statistics of a sample of size L from a random variable with PDF $f_X(x)$ and CDF $F_X(x)$. Given that $X_{i:L} = x_i$ for $i < j$, the conditional PDF of $X_{j:L}$ is

$$f_{X_{j:L}}(x_j \mid X_{i:L} = x_i) = \frac{(L-i)!}{(n-j)!(j-i-1)!} \left\{ \frac{F_X(x_j) - F_X(x_i)}{1 - F_X(x_i)} \right\}^{j-i-1}$$

$$\cdot \left\{ \frac{1 - F_X(x_j)}{1 - F_X(x_i)} \right\}^{i-j} \frac{f_X(x_j)}{1 - F_X(x_i)}, \quad x_i \leq x_j$$ (5.36)

Proof: Please refer to [106, Theorem 2.4.1]. □

With $f_{\tilde{\gamma}_{1:N}^{\text{mi}}}(\gamma_1)$ in (5.34), one can utilize Lemma 5.2 to derive the other higher order PDFs of $\tilde{\gamma}_{n:N}^{\text{mi}}$ for $n = 2, \cdots, N$ as we obtained the lower order PDFs of $\tilde{\gamma}_{n:N}^{\text{ma}}$ for $n = 1, \cdots, N-1$ by using $f_{\tilde{\gamma}_{N:N}^{\text{ma}}}(\gamma_N)$ and Lemma 5.1 in Section 5.3.1. Here, we adopt Lemma 5.3 to take advantage of the additive Markov chain property for the order statistics of a random sample from an exponential distribution. The result of Lemma 5.3 was originally proved in [107] and has been applied in many problems involving the order statistics from an exponential distribution.

Lemma 5.3 Let $X_{1:L} \leq \cdots \leq X_{L:L}$ be the order statistics of a random sample of size L from an exponential distribution with parameter λ. Define a new set of random variables to denote the spacings between $X_{l:L}$ and $X_{l-1:L}$ as follows:

$$\begin{cases} S_1 = X_{1:L}, \\ S_l = X_{l:L} - X_{l-1:L}, \quad l = 2, \cdots, L \end{cases}$$ (5.37)

Then, S_l are independent exponentially distributed random variables with parameter $\lambda/(L-l+1)$ for $1 \leq l \leq L$. Hence, the PDF of S_l is given by

$$f_{S_l}(s_l) = \frac{L-l+1}{\lambda} \exp\left(-\frac{L-l+1}{\lambda}s_l\right), \quad l = 1, 2, \cdots, L$$ (5.38)

73

Proof: Please refer to [106, Theorem 4.6.1]. □

Since the spacings S_l ($2 \leq l \leq L$) are independent of $X_{1:L}$ according to Lemma 5.3, we can capture the statistics of $\tilde{\gamma}_{n:N}^{\text{mi}}$ for $n = 2, \cdots, N$ by writing

$$\tilde{\gamma}_{n:N}^{\text{mi}} = \tilde{\gamma}_{1:N}^{\text{mi}} + S_2 + \cdots + S_n \ . \tag{5.39}$$

Representing $\phi_{\tilde{\gamma}_{1:N}^{\text{mi}}}(\omega)$ and $\phi_{S_l}(\omega)$ as the Laplace transform of $\tilde{\gamma}_{1:N}^{\text{mi}}$ and S_l, respectively, we have

$$f_{\tilde{\gamma}_{n:N}^{\text{mi}}}(\gamma_n) = \mathcal{L}^{-1} \left\{ \phi_{\tilde{\gamma}_{1:N}^{\text{mi}}}(\omega) \prod_{l=2}^{n} \phi_{S_l}(\omega) \right\}, \quad n = 2, \cdots, N \tag{5.40}$$

where $\mathcal{L}^{-1}(\cdot)$ denotes the inverse Laplace transform. By using $\phi_{\tilde{\gamma}_{1:N}^{\text{mi}}}(\omega) = \frac{N^2/\rho}{\omega + N^2/\rho}$, $\phi_{S_l}(\omega) = \frac{(L-l+1)/\lambda}{\omega + (L-l+1)/\lambda}$ and applying the partial fractional technique [82], (5.40) can be derived as

$$f_{\tilde{\gamma}_{n:N}^{\text{mi}}}(\gamma_n) = \frac{KN^2 \prod_{j=2}^{n}(N-j+1)}{\rho(n-2)!} \sum_{i_1=0}^{K-1} \sum_{i_2=2}^{n} \frac{(-1)^{n+i_1+i_2} \binom{K-1}{i_1} \binom{n-2}{i_2-2}}{(N + Ni_1 + i_2 - N - 1)}$$
$$\cdot \left[e^{-\gamma_n (N-i_2+1)N/\rho} - e^{-\gamma_n(N+i_1N)N/\rho} \right] \ . \tag{5.41}$$

Finally, substituting the PDFs of $\tilde{\gamma}_{n:N}^{\text{mi}}$ in (5.34) and (5.41) into (5.16), we obtain the achievable throughput when using the max-min scheduling policy as

$$\tilde{C}_{\text{zf}}^{\text{mi}} = C_{\tilde{\gamma}_{1:N}^{\text{mi}}} + \sum_{n=2}^{N} C_{\tilde{\gamma}_{n:N}^{\text{mi}}} \tag{5.42}$$

where

$$C_{\tilde{\gamma}_{1:N}^{\text{mi}}} = \frac{KN^2}{\rho} \sum_{i=0}^{K-1} (-1)^i \binom{K-1}{i} h\left(\frac{N^2(i+1)}{\rho} \right) \tag{5.43}$$

and

$$C_{\tilde{\gamma}_{n:N}^{\text{mi}}} = \frac{KN^2 \prod_{j=2}^{n}(N-j+1)}{\rho(n-2)!} \sum_{i_1=0}^{K-1} \sum_{i_2=2}^{n} \frac{(-1)^{n+i_1+i_2} \binom{K-1}{i_1} \binom{n-2}{i_2-2}}{(N + Ni_1 + i_2 - N - 1)}$$
$$\cdot \left[h\left(\frac{(N-i_2+1)N}{\rho} \right) - h\left(\frac{(N+i_1N)N}{\rho} \right) \right] \tag{5.44}$$

for $n = 2, \cdots, N$.

5.4 Analysis for Vector Feedback Scheduling

In this section, we analyze the performance of the multiuser MIMO system using vector feedback scheduling. We first study the spatially-independent scheduling algorithm introduced in [59] and then consider a spatially-greedy scheduling strategy that can fully exploit the selection diversity provided by the multiple users and antennas in the whole network.

5.4.1 Spatially-Independent Scheduling

As remarked in Section 5.2.2, the ample information from vector feedback enables the base station to perform scheduling across multiple antennas. The spatially-independent scheduling policy allows each transmit antenna independently to select its target user. Specifically, for the nth transmit antenna, the target user k_n^* associated with this antenna is determined according to

$$k_n^* = \arg\max_k \gamma_n^k \ , \tag{5.45}$$

where γ_n^k is the output SNR of the nth receive antenna for user k. From (5.45), the resulting output SNR for the data sent from the nth antenna is

$$\tilde{\gamma}_n^{\text{si}} = X_{K:K} \tag{5.46}$$

where X is exponentially distributed with parameter ρ/N and the superscript si denotes the spatially-independent scheduling. Therefore, the PDF of $\tilde{\gamma}_n^{\text{si}}$ in (5.46) can be given by

$$f_{\tilde{\gamma}_n^{\text{si}}}(\gamma_n) = \frac{KN}{\rho} \left(1 - e^{-N\gamma_n/\rho}\right)^{K-1} e^{-N\gamma_n/\rho}, \quad n = 1, \cdots, N \ . \tag{5.47}$$

Since $\tilde{\gamma}_n^{\text{si}}$ in (5.47) are i.i.d. with respect to n, the achievable link throughput of the zero-forcing under the spatially-independent scheduling can be obtained by

$$\tilde{C}_{\text{zf}}^{\text{si}} = N \int_0^\infty \log(1 + \gamma_n) f_{\tilde{\gamma}_n^{\text{si}}}(\gamma_n) d\gamma_n$$

$$= \frac{KN^2}{\rho} \sum_{i=0}^{K-1} \binom{K-1}{i} (-1)^i h\left(\frac{(k+1)N}{\rho}\right) \ . \tag{5.48}$$

75

Furthermore, we can also obtain the PDF or CDF of the ordered version $\tilde{\gamma}_{n:N}^{\mathrm{si}}$ by simply applying (5.14) or (5.15) to (5.46). Consequently, the resulting outage probability subject to the spatially-independent scheduling can be calculated by invoking the CDF of $\tilde{\gamma}_{1:N}^{\mathrm{si}}$ as

$$\tilde{P}_{\mathrm{out}}^{\mathrm{si}} = 1 - \left[1 - \left(1 - e^{-N\gamma_{\mathrm{th}}/\rho} \right)^K \right]^N . \tag{5.49}$$

5.4.2   Spatially-Greedy Scheduling

Another scheduling policy which can fully exploit the knowledge of vector feedback is the *spatially-greedy scheduling*. Given γ_n^k for all $n \in \{1, \cdots, N\}$ and $k \in \{1, \cdots, K\}$, the base station can sort the total NK samples (denoted as $X_{1:KN} \leq \cdots \leq X_{KN:KN}$) by magnitude across all users and antennas. The spatially-greedy scheduling then assigns the transmissions over the N transmit antennas to the data streams that yield the top N highest output SNR. Following this policy, we have

$$\tilde{\gamma}_{n:N}^{\mathrm{sg}} = X_{KN-N+n:KN}, \quad n = 1, \cdots, N \tag{5.50}$$

where X is exponentially distributed with parameter ρ/N and the superscript sg denotes the spatially-greedy scheduling. Accordingly, applying (5.14) to (5.50) gives the PDF of $\tilde{\gamma}_{n:N}^{\mathrm{sg}}$ for all n as follows:

$$f_{\tilde{\gamma}_{n:N}^{\mathrm{sg}}}(\gamma_n) = \frac{N \prod_{j=0}^{KN-n}(KN-j)}{\rho\,(KN-n)!} \sum_{i=0}^{KN-n} \binom{KN-n}{i} (-1)^{KN-n+i}\, e^{-N(KN-i)\gamma_n/\rho} . \tag{5.51}$$

Finally, substituting (5.51) into (5.16) and (5.17), we obtain the achievable link throughput

$$\tilde{C}_{\mathrm{zf}}^{\mathrm{sg}} = \frac{N}{\rho} \sum_{n=1}^{N} \frac{\prod_{j=0}^{KN-n}(KN-j)}{(KN-n)!} \sum_{i=0}^{KN-n} (-1)^{KN-n+i} \binom{KN-n}{i} h\left(\frac{(KN-i)N}{\rho} \right) \tag{5.52}$$

and the outage probability

$$\tilde{P}_{\mathrm{out}}^{\mathrm{sg}} = \sum_{i=KN-N+1}^{KN} \binom{KN}{i} e^{-(KN-i)N\gamma_{\mathrm{th}}/\rho} \left(1 - e^{-N\gamma_{\mathrm{th}}/\rho} \right)^i \tag{5.53}$$

for the zero-forcing receiver operating in the multiuser MIMO system with the spatially-greedy scheduling.

We note that the scheduling gain disappears for $K = 1$. Under such circumstances, the achievable throughput expressions of (5.27), (5.42), (5.48) and (5.52) with the various scheduling policies all reduce to

$$C_{\text{zf}} = N \, \exp\left(\frac{N}{\rho}\right) E_1\left(\frac{N}{\rho}\right) \ , \tag{5.54}$$

which is the achievable throughput for the single-user MIMO system as given in (5.7) with $N_t = N_r = N$. In the context of multiuser MIMO systems, (5.54) also corresponds to the achievable throughput of the zero-forcing receiver in the multiuser MIMO system using the round-robin scheduling. Similarly, the outage probability expressions of (5.26), (5.35), (5.49) and (5.53) all simplify to

$$P_{\text{out}} = 1 - e^{-N^2\gamma_{\text{th}}/\rho} \ , \tag{5.55}$$

which is the outage probability for the single-user MIMO system as given in (5.12) with $N_t = N_r = N$.

5.5 Discussions

5.5.1 Effect of Scheduling on Output SNR Distributions

To gain more insights into how the various scheduling algorithms affect the achievable throughput and outage probability performances, we compare the CDFs of $\gamma_{n:N}$ and $\tilde{\gamma}_{n:N}$ as illustrated in Fig. 5.3. The dashed curves in this figure represent the CDFs of $\gamma_{n:N}$ while the solid curves from Fig. 5.3-(a) to Fig. 5.3-(d) correspond to $\tilde{\gamma}_{n:N}$ of using the max-max, max-min, spatially-independent and spatially-greedy policies, respectively. The effect of scheduling on the outage probability performance can be reflected from the movement of the lowest order statistic of $\gamma_{1:N}$. On the other hand, we can assess the improvement of the achievable throughput performance due to scheduling by observing the enhancement of all order statistics of $\{\gamma_{n:N}\}_{n=1}^{N}$. We set $N = 3$, $K = 16$ and $\rho = 0$ dB in this example. From Fig. 5.3, some observations are made as follows:

- In Fig. 5.3-(a), the highest order statistic of $\gamma_{3:3}$ gains a significant boost while the lowest order statistic of $\gamma_{1:3}$ only improves slightly under the max-max scheduling. By
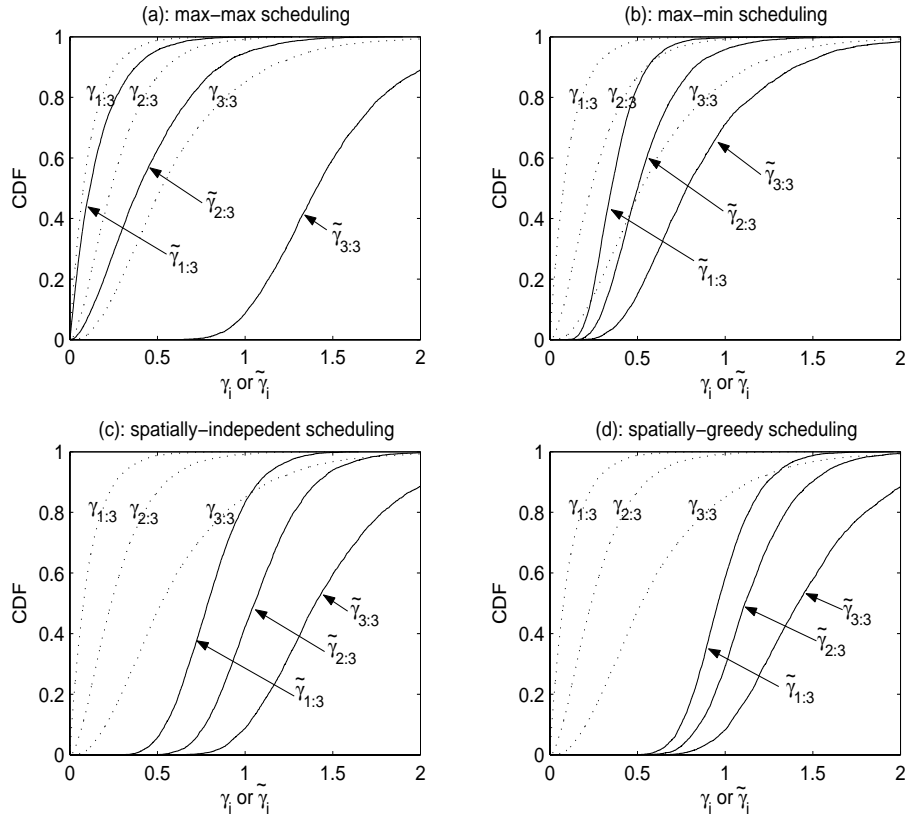
Figure 5.3: The CDFs of the output SNR subject to various scheduling algorithms in the multiuser MIMO system with $N = 3$, $K = 16$ and $\rho = 0$ dB.

comparison, the improvement of $\gamma_{1:3}$ due to the max-min scheduling in Fig. 5.3-(b) is apparently greater than that in Fig. 5.3-(a) while the enhancement of $\gamma_{3:3}$ is less significant than that in Fig. 5.3-(a).

- Observing Fig 5.3-(d), one can find that $\{\gamma_{n:3}\}_{n=1}^{3}$ are all best enhanced as compared with the other three figures, indicating that the spatially-greedy scheduling can achieve the optimal performance for both outage probability and achievable throughput. As for Fig. 5.3-(c), the spatially-independent scheduling can also enable $\gamma_{3:3}$ to capture the full selection diversity order NK as the spatially-greedy scheduling in Fig. 5.3-(d). However, the improvements of the lower order statistics of $\gamma_{3:1}$ and $\gamma_{3:2}$ in Fig. 5.3-(c) are worse than that in Fig. 5.3-(d) but still much better than that in Figs. 5.3-(a) and 5.3-(b).

- Comparing the scalar feedback scheduling cases of Figs. 5.3-(a) and 5.3-(b) with the

vector feedback scheduling cases of Figs. 5.3-(c) and 5.3-(d), one can see that the amount of feedback information plays an essential role for scheduling techniques to effectively enhance the output SNR of *all* subchannels. In other words, one can design the scheduling scheme to trade the reverse-link feedback rate for improving the downlink performance of the multiuser MIMO system.

5.5.2 Asymptotic Optimality of the ZF Receiver

It is instructive to compare the result of this chapter using the zero-forcing with that of the previous chapter using the optimal receiver under the same max-min scheduling algorithm. Fig. 5.1 have shown that the performance of the zero-forcing is far from optimal at the low SNR regime due to noise enhancement. However, in the multiuser MIMO system, the scheduling technique can virtually create a high SNR environment and thus reduce the occurrence of noise enhancement for the zero-forcing receiver. The following proposition explores the advantage of operating the zero-forcing receiver in the multiuser scheduling system.

Proposition 5.1 Let $\tilde{C}_{\text{opt}}^{\text{mi}}$ and $\tilde{C}_{\text{zf}}^{\text{mi}}$ be the achievable throughput for the optimal receiver and the zero-forcing receiver operating in the same multiuser MIMO system with the max-min scheduling policy. For any finite N, we have

(i) At the low SNR regime,

$$\lim_{K \to \infty} \frac{\tilde{C}_{\text{zf}}^{\text{mi}}}{\tilde{C}_{\text{opt}}^{\text{mi}}} = 1, \quad \text{for small } \rho \ . \tag{5.56}$$

(ii) At the high SNR regime,

$$\lim_{\rho \to \infty} \frac{\tilde{C}_{\text{zf}}^{\text{mi}}}{\tilde{C}_{\text{opt}}^{\text{mi}}} = 1, \quad \text{for any finite } K \ . \tag{5.57}$$

Proof: Please refer to Appendix D. □

Somewhat surprisingly, Proposition 5.1 indicates that the efficiency of the zero-forcing receiver in recovering the spatially multiplexed signals can approach that of the optimal receiver as the number of users goes to infinity. More generally, it also implies that in
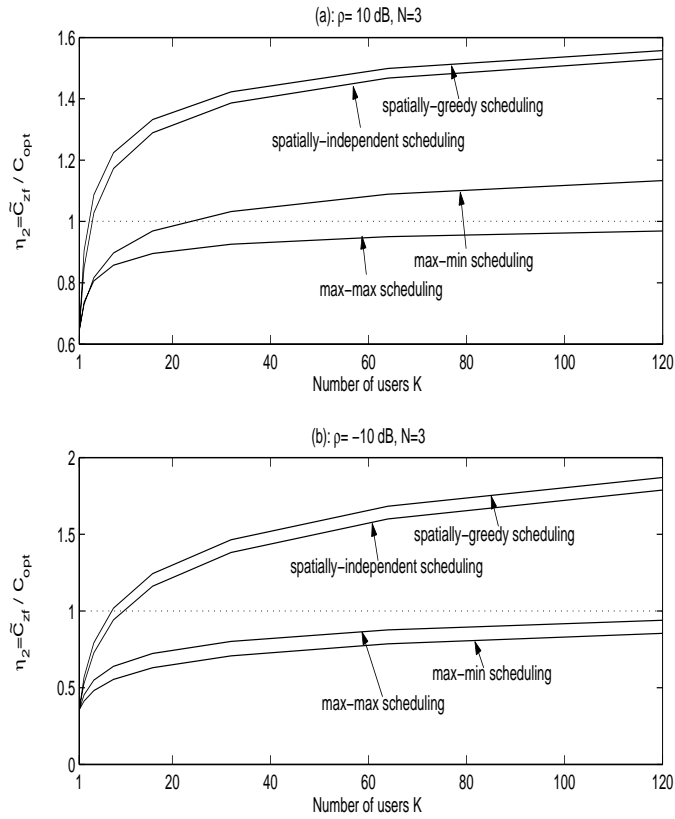
Figure 5.4: Achievable throughput for the zero-forcing receiver in the multiuser MIMO system with various scheduling algorithms.

the multiuser MIMO environment with scheduling the receiver design requirement may be relaxed due to the effect of noise enhancement avoidance. Numerical comparisons of $\tilde{C}_{\mathrm{zf}}^{\mathrm{mi}}$ and $\tilde{C}_{\mathrm{opt}}^{\mathrm{mi}}$ are provided in the next section.

5.6   Numerical Results

Figure 5.4 compares the achievable throughput of $\tilde{C}_{\mathrm{zf}}$ and C_{opt}. Analogous to the definition of η_1 in (5.10), we define

$$\eta_2 = \frac{\tilde{C}_{\mathrm{zf}}}{C_{\mathrm{opt}}} \tag{5.58}$$

to evaluate the efficiency of the zero-forcing receiver in the multiuser scheduling system to deliver the multiplexing gain. In (5.58), $\tilde{C}_{\mathrm{zf}}$ corresponding to the max-max, max-min, spatially-independent and spatially-greedy scheduling algorithms are derived in (5.27), (5.42), (5.48)
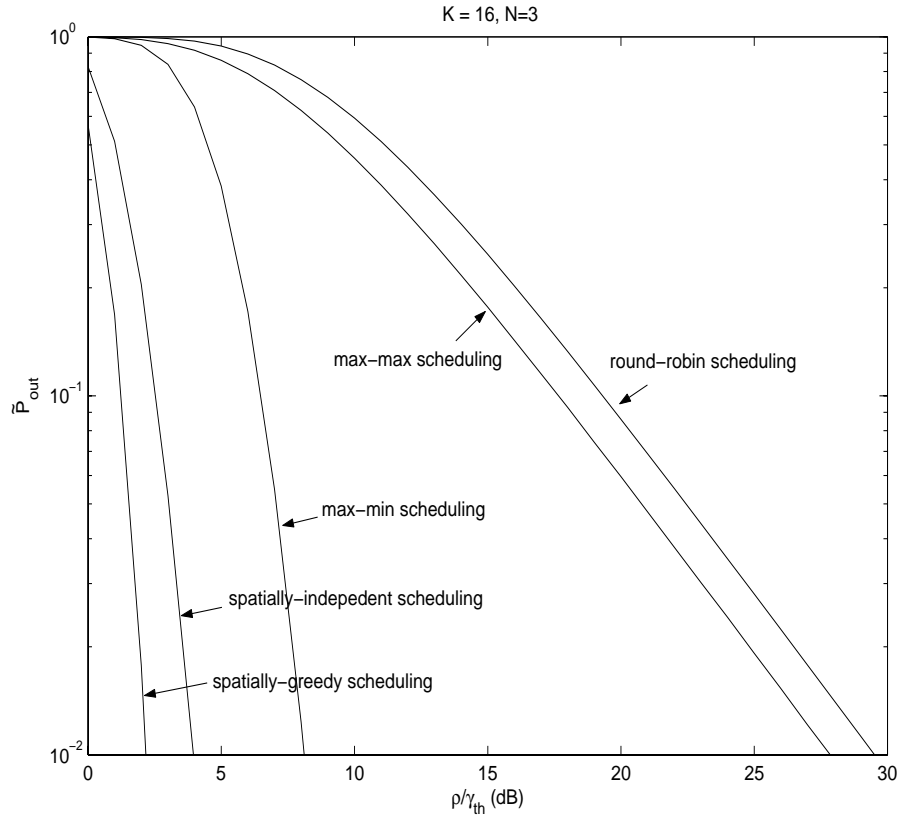
Figure 5.5: Outage probability for the zero-forcing receiver in the multiuser MIMO system with various scheduling algorithms.

and (5.52), respectively. Figs. 5.4-(a) and (b) provide the result of η_2 for a high SNR condition at $\rho = 10$ dB and a low SNR condition at $\rho = -10$ dB, respectively. One can observe that $\tilde{C}_{zf}$ can be greater than C_{opt} with only a small number of K by using the spatially-greedy and spatially-independent scheduling algorithms. As for the scalar feedback scheduling, the achievable throughput $\tilde{C}_{zf}$ can approach C_{opt} with the increasing K for both the max-max and max-min scheduling algorithms. Furthermore, applying the max-min scheduling policy and operating the zero-forcing receiver at a high SNR condition can even result in a higher $\tilde{C}_{zf}$ than C_{opt} with a mediate number of K.

Figure 5.5 presents the outage probability of $\tilde{P}_{out}$ with the various scheduling algorithms for $K = 16$ and $N = 3$. The outage probability subject to the round-robin scheduling is also plotted for comparison. It is shown that the vector feedback scheduling including the spatially-greedy and spatially-independent scheduling can significantly improve the outage
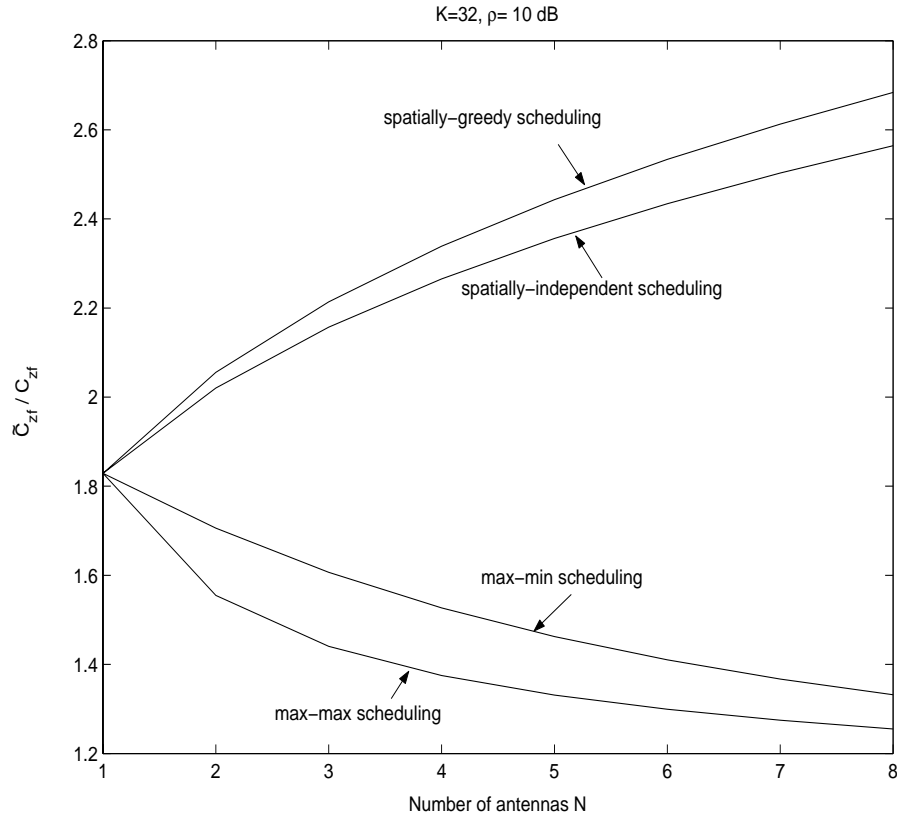
Figure 5.6: The impact of the number of antennas on the scheduling gain defined by $\tilde{C}_{\text{zf}}/C_{\text{zf}}$.

probability performance. As for the scalar feedback scheduling, the max-min scheduling can always yield a much better outage probability performance than the max-max scheduling. Considering the outage probability and the achievable throughput as shown in Fig. 5.4, the max-min scheduling would be a more feasible strategy as compared with the max-max scheduling policy when only scalar feedback is available.

Figure 5.6 illustrates the impact of the number of antennas on the achievable scheduling gain defined by $\tilde{C}_{\text{zf}}/C_{\text{zf}}$. Although the achievable link throughput of the zero-forcing receiver increases for all the studied scheduling algorithms as shown in Fig. 5.4, one can see from Fig. 5.6 that the scheduling gain reduces with the increasing N for the scalar feedback scheduling. The phenomena of diminishing scheduling gain for the scalar feedback scheduling may be attributed to the insufficient feedback information as compared with the vector feedback scheduling.
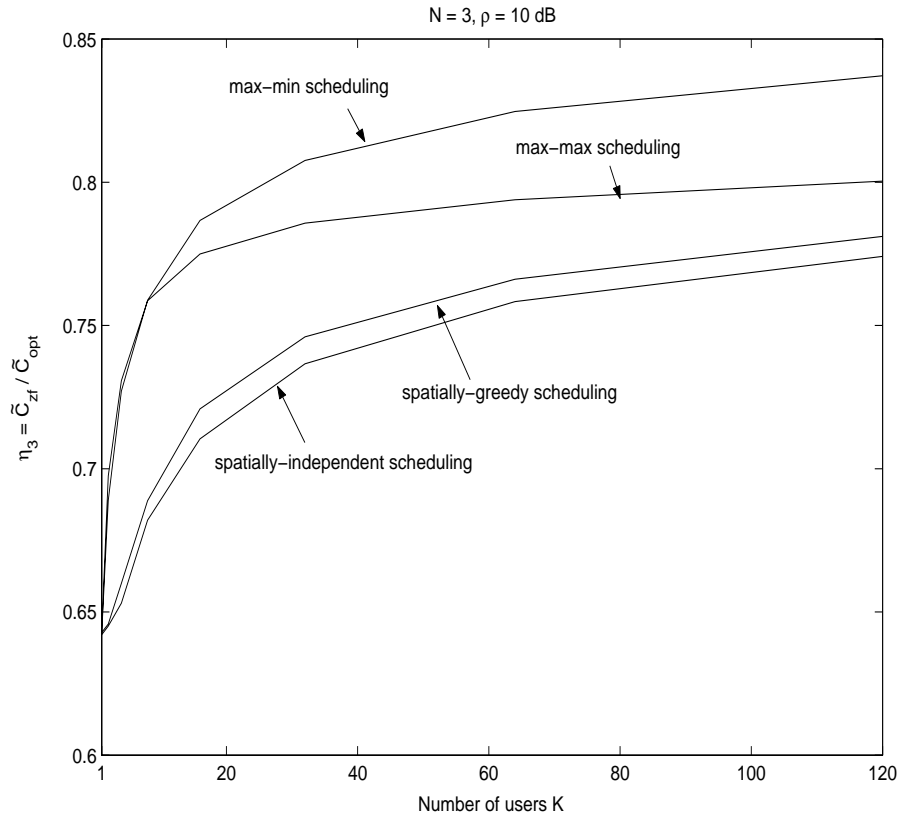
Figure 5.7: Comparison of the achievable throughput for the zero-forcing receiver and the optimal receiver operating in the same multiuser MIMO system.

In the final experiment, we compare the achievable throughput for the zero-forcing receiver ($\tilde{C}_{\mathrm{zf}}$) and the optimal receiver ($\tilde{C}_{\mathrm{opt}}$) operating in the multiuser MIMO system under the same scheduling policy. Recall from (4.5) in Chapter 4 that the subchannel output SNR for the optimal receiver can be represented by $\lambda_n \rho / N$. Therefore, by simply replacing γ_n in (5.18), (5.31), (5.45) and (5.50) with $\lambda_n \rho / N$, $\tilde{C}_{\mathrm{opt}}$ subject to the max-max, max-min, spatially-independent and spatially-greedy scheduling algorithms can be obtained via computer simulations. Fig. 5.7 presents the comparison of $\tilde{C}_{\mathrm{zf}}$ and $\tilde{C}_{\mathrm{opt}}$ by plotting η_3 against the number of users, where η_3 is defined as

$$\eta_3 = \frac{\tilde{C}_{\mathrm{zf}}}{\tilde{C}_{\mathrm{opt}}} \ . \tag{5.59}$$

One can see that the achievable throughput for the zero-forcing receiver and the optimal receiver becomes closer with the increasing number of users in the multiuser scheduling system. This implies a nice cross-layer synergy that employing the simple zero-forcing receiver

83

on top of the multiuser scheduling system can deliver the remarkable multiplexing gain of the MIMO channel in a cost-effective manner.

5.7   Chapter Summary

In this chapter, we have presented an analytical framework to evaluate the performance of the zero-forcing receiver operating in the multiuser MIMO system with a variety of scheduling algorithms. Using the order statistics technique, we derive closed-form expressions for the achievable throughput and outage probability that facilitate efficient numerical comparisons among the various scheduling strategies. Our results indicate that the cross-layer cooperation between the simple zero-forcing receiver and scheduling technique can achieve the full capacity of the MIMO system. Furthermore, it is demonstrated that with the increasing number of users in the multiuser MIMO system, the efficiency of the zero-forcing receiver in recovering the spatially multiplexed data can approach that of the optimal receiver. This result further endorses the strength of combining the multiplexing-based antenna scheme with the multiuser scheduling system.
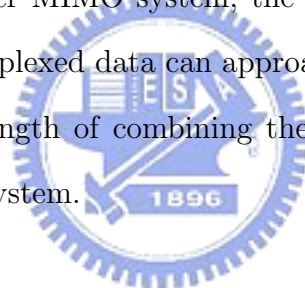
Chapter 6

Interference Suppression Based Antenna Techniques for TDD/CDMA Systems

This chapter shifts the focus to the TDD/CDMA system. As introduced in Section 2.3, the TDD system is flexible to deliver asymmetric traffic services by allocating different numbers of time slots for uplink and downlink transmissions. However, in a TDD/CDMA system, asymmetric traffic may result in severe opposite direction interference because downlink transmitted signals from neighboring base stations may interfere with the uplink received signals of the home cell. In this chapter, we investigate the effect of antenna beamforming techniques from the perspective of suppressing the opposite direction interference. Particularly, four antenna beamforming schemes will be considered in this chapter, including

- The uplink receive beam-steering method is employed at base stations (Scheme I);

- The uplink receive MVDR beamformer is employed at base stations (Scheme II);

- The beam-steering method is jointly applied in both the downlink transmission and uplink reception at all base stations (Scheme III);

- The downlink transmit beam-steering and the uplink receive MVDR beamformer are jointly employed at all base stations (Scheme IV).
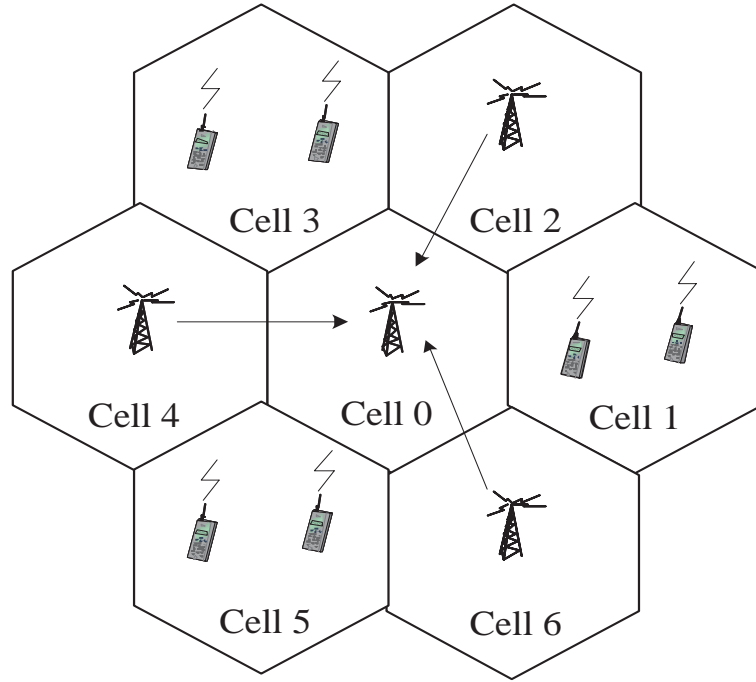
Figure 6.1: An example to illustrate the interference scenario in the TDD/CDMA system, where $\mathcal{B}_{od} = \{2, 4, 6\}$ represents the set of the neighboring cells generating the opposite direction interference and $\mathcal{B}_{sd} = \{1, 3, 5\}$ represents the cells generating the same direction interference.

6.1 System Model

Consider a TDD/CDMA cellular system with seven cells as shown in Fig. 6.1, where the home cell is indexed with $j = 0$ and six adjacent cells are labelled with 1 to 6. Assume that cell 0 in the center is in the uplink mode during a particular time slot t_o. Let $\mathcal{B}_{od}$ and $\mathcal{B}_{sd}$ denote the set of the neighboring cells during time slot t_o operating in the downlink mode and those operating in the uplink mode, respectively. Figure 6.1 illustrates an example with $\mathcal{B}_{od} = \{2, 4, 6\}$ and $\mathcal{B}_{sd} = \{1, 3, 5\}$. In this example, downlink transmissions of cells 2, 4, and 6 will cause the opposite direction interference (i.e., the base stations to base stations interference) to the uplink receiving signals of cell 0, while cells 1, 3, and 5 result in the same direction interference (i.e., the mobile stations to base stations interference).

In our model, we consider propagation loss and log-normal distributed shadowing. Then the link gain $G(r, \alpha)$ between the transmitter and receiver is described as

$$G(r, \alpha) = \kappa_0 r^{-\mu} 10^{\alpha/10} \ , \tag{6.1}$$

where r is the propagation distance, κ_0 is a constant, μ is the path loss exponent and α is a normal distributed random variable with zero mean and standard deviation of σ_s dB. Let P_t be the total transmit power of a base station, and d_j the distance from cell j ($j \in \mathcal{B}_{od}$) to the home cell. Then the total opposite direction interference introduced by the adjacent cells is equal to

$$I_{od} = \sum_{j \in \mathcal{B}_{od}} P_t G(d_j, \alpha_j) \ . \tag{6.2}$$

Assume that uplink power control is ideally executed so that the received signal power of each mobile user is maintained at a constant level P_r at base stations. Then the same direction interference introduced by mobile k_j of $\mathcal{B}_{sd}$ ($j \in \mathcal{B}_{sd}$) is equal to

$$\begin{aligned} I_{k_j} &= P_r G(r_0, \alpha_0)/G(r_{k_j}, \alpha_{k_j}) \\ &= P_r \left(\frac{r_{k_j}}{r_0}\right)^\mu 10^{(\alpha_0 - \alpha_{k_j})/10} \ , \end{aligned} \tag{6.3}$$

where r_0 and r_{k_j} are the distance from mobile k_j of $\mathcal{B}_{sd}$ to cell 0 and that to cell j ($j \in \mathcal{B}_{sd}$), respectively. For ease of notation, let

$$\xi_{k_j} = \left(\frac{r_{k_j}}{r_0}\right)^\mu 10^{(\alpha_0 - \alpha_{k_j})/10}. \tag{6.4}$$

Note that the term $(\alpha_0 - \alpha_{k_j})$ in (6.4) can be represented by another normal distributed random variable with a modified standard deviation [76]. Let K_j denote the number of active mobile users in cell j ($j \in \mathcal{B}_{sd}$) that are in their uplink transmission cycles during a particular time slot t_o. Then from (6.3) and (6.4), the total same direction interference introduced by adjacent cells can be expressed by

$$\begin{aligned} I_{sd} &= \sum_{j \in \mathcal{B}_{sd}} \sum_{k_j=1}^{K_j} I_{k_j} \\ &= \sum_{j \in \mathcal{B}_{sd}} \sum_{k_j=1}^{K_j} P_r \xi_{k_j} \ . \end{aligned} \tag{6.5}$$

In addition to the opposite direction and the same direction interfering signals, there still exists the intracell interference in the TDD/CDMA system, denoted as I_{ic}. Since power

control is assumed to be ideal, the received signal power of all users in a cell will be maintained at a constant level P_r. Thus, I_{ic} can be expressed as

$$I_{ic} = P_r(K_0 - 1) \ ,$$ (6.6)

where K_0 is the number of active mobile users in the home cell that are transmitting uplink signals in time slot t_o. Thus, based on the definitions of I_{od}, I_{sd}, and I_{ic} corresponding to (6.2), (6.5) and (6.6), respectively, the uplink received bit energy-to-interference density ratio γ_k for a target mobile k in the home cell can be written as

$$\gamma_k = \frac{LP_r}{I_{od} + I_{sd} + I_{ic} + \sigma_n^2} \ ,$$ (6.7)

where L is the processing gain and σ_n^2 is the white thermal noise power. In the next section, we will further derive the expression of γ_k with consideration of the effect of antenna beamforming.

6.2   Interference Analysis with Beamforming

In this section, we investigate how antenna beamforming can improve the performance of TDD/CDMA systems. We consider the conventional beam-steering method and the minimum variance distortionless response (MVDR) beamformer. The reasons why these two beamformers are studied are explained as follows. From the viewpoint of implementation, the beam-steering technique is the most economical and practical solution because of its simplicity. In [45], the authors demonstrated that remarkable capacity gain can be achieved for FDD/CDMA systems by using this kind of beamformer. The beam-steering technique is evaluated to provide the baseline performance for comparison. As for the MVDR beamformer, it is well known for its capability of suppressing strong interference [41]. In [112], it is shown that the MVDR criterion can lead to the optimal solution in the sense of maximizing the output signal to interference plus noise ratio. Thus, the MVDR beamformer is evaluated to give a performance upper bound for the TDD/CDMA system with antenna beamforming techniques.

6.2.1 Generic Interference Analysis

To begin with, we first derive the expression of the received bit energy-to-interference density ratio with a generic antenna beamformer. Assume an N-element uniform circular array (UCA) is employed at a base station. The array manifold vector (or steering vector) of an UCA is written as [41]

$$
\mathbf{a}(\theta, \phi) = \frac{1}{\sqrt{N}}
\begin{bmatrix}
e^{j2\pi l/\lambda_c \sin\phi \cos\theta} \\
e^{j2\pi l/\lambda_c \sin\phi \cos(\theta - 2\pi/N)} \\
\vdots \\
e^{j2\pi l/\lambda_c \sin\phi \cos(\theta - 2\pi(N-1)/N)}
\end{bmatrix}, \tag{6.8}
$$

where l is the radius of the circular antenna array, λ_c the wavelength, θ the azimuth angle, and ϕ the vertical angle. The factor $1/\sqrt{N}$ in (6.8) is a normalization factor such that $\mathbf{a}^H\mathbf{a} = 1$. We assume that l is equal to half the wavelength and the vertical angle ϕ is equal to $\pi/2$.

Let $\mathbf{x}(t) = [x_1(t), x_2(t), \cdots, x_N(t)]^T$ be the received signal vector at an N-element antenna array. Then $\mathbf{x}(t)$ can be written as

$$
\mathbf{x}(t) = \mathbf{x}_k(t) + \mathbf{x}_{od}(t) + \mathbf{x}_{sd}(t) + \mathbf{x}_{ic}(t) + \mathbf{n}(t) \ , \tag{6.9}
$$

where $\mathbf{x}_k(t)$ is the desired signal for user k, $\mathbf{x}_{od}(t)$ is the opposite direction interference, $\mathbf{x}_{sd}(t)$ is the same direction interference, $\mathbf{x}_{ic}(t)$ is the intracell interference and $\mathbf{n}(t)$ is the white noise. Specifically, $\mathbf{x}_{od}(t)$ in (6.9) is given by

$$
\mathbf{x}_{od}(t) = \sum_{j \in \mathcal{B}_{od}} \sqrt{P_t G(d_j, \alpha_j)} \mathbf{b}_j \ , \tag{6.10}
$$

where $\mathbf{b}_j$ is the array manifold vector for the signals arriving from cell j ($j \in \mathcal{B}_{od}$). Meanwhile, $\mathbf{x}_{sd}(t)$, $\mathbf{x}_{ic}(t)$ and $\mathbf{x}_k(t)$ can be respectively expressed as

$$
\mathbf{x}_{sd}(t) = \sum_{j \in \mathcal{B}_{sd}} \sum_{k_j=1}^{K_j} \sqrt{P_r \xi_{k_j}} u_{k_j} \left(\left\lfloor \frac{t - \tau_{k_j}}{T} \right\rfloor \right) c_{k_j}(t - \tau_{k_j}) \mathbf{a}_{k_j} \ , \tag{6.11}
$$

89
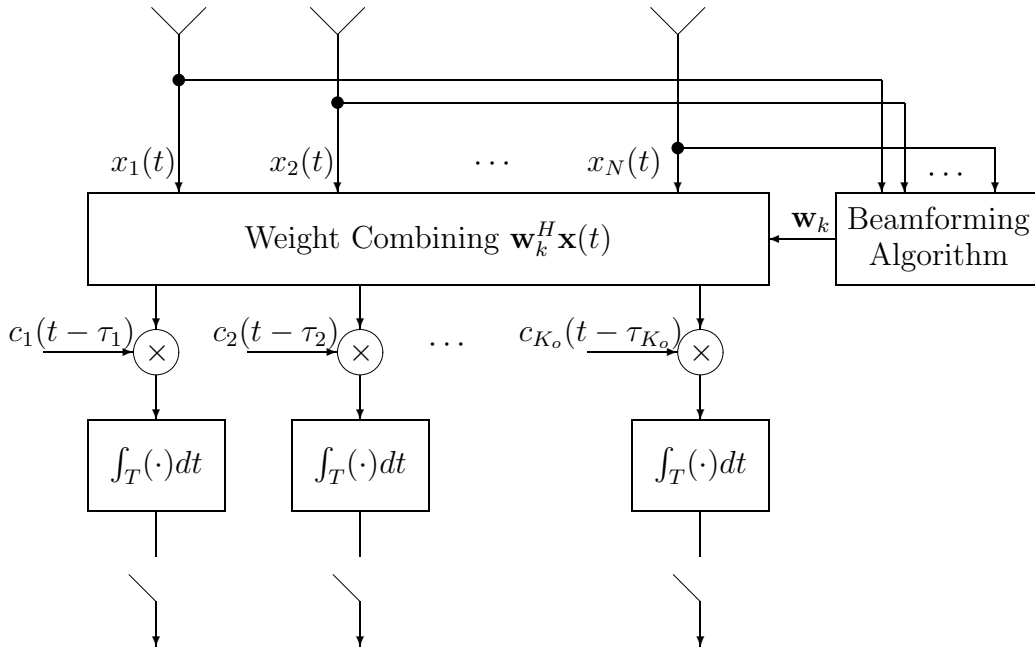
Figure 6.2: A receiver block diagram with antenna beamformers.

$$\mathbf{x}_{ic}(t) = \sum_{k_0 \neq k}^{K_0} \sqrt{P_r} u_{k_0} \left(\left\lfloor \frac{t - \tau_{k_0}}{T} \right\rfloor \right) c_{k_0}(t - \tau_{k_0}) \mathbf{a}_{k_0} \ , \tag{6.12}$$

and

$$\mathbf{x}_k(t) = \sqrt{P_r} u_i \left(\left\lfloor \frac{t - \tau_i}{T} \right\rfloor \right) c_i(t - \tau_i) \mathbf{a}_k \ . \tag{6.13}$$

In (6.11)–(6.13), $\mathbf{a}_{k_j}$ is the array manifold vector for the signals arriving from mobile k_j of cell j; $u_{k_j}(\cdot)$ is the bit waveform with a period T; τ_{k_j} is the propagation delay; $c_{k_j}(\cdot)$ is the spreading code; P_r and ξ_{k_j} are already defined in (6.3) and (6.4). Figure 6.2 shows the receiver block diagram of an antenna beamformer. In Fig. 6.2 the received signal $\mathbf{x}(t)$ for a target user k $(k = 1, \cdots, K_0)$ is first combined with the beamformer weights $\mathbf{w}_k$. After weight combining, the output signal $\mathbf{w}_k^H \mathbf{x}(t)$ is connected to the despreader with processing gain L. Assume that the code sequences of different users are mutually uncorrelated. Then the opposite direction interference I_{od} in (6.2), the same direction interference I_{sd} in (6.5) and the intracell interference I_{ic} in (6.6) become

$$I_{od} = \sum_{j \in \mathcal{B}_{od}} P_t G(d_j, \alpha_j) |\mathbf{w}_k^H \mathbf{b}_j|^2 \ , \tag{6.14}$$

90

$$I_{sd} = \sum_{j \in \mathcal{B}_{sd}} \sum_{k_j=1}^{K_j} P_r \xi_{k_j} |\mathbf{w}_k^H \mathbf{a}_{k_j}|^2 \ , \tag{6.15}$$

and

$$I_{ic} = \sum_{k_0 \neq k}^{K_0} P_r |\mathbf{w}_k^H \mathbf{a}_{k_0}|^2 \ , \tag{6.16}$$

respectively.

By substituting (6.14), (6.15) and (6.16) into (6.7), the bit energy-to-interference density ratio of mobile k with antenna beamforming becomes

$$\gamma_k = LP_r \left\{ \sum_{j \in \mathcal{B}_{od}} P_t G(d_j, \alpha_j) |\mathbf{w}_k^H \mathbf{b}_j|^2 + \sum_{j \in \mathcal{B}_{sd}} \sum_{k_j=1}^{K_j} P_r \xi_{k_j} |\mathbf{w}_k^H \mathbf{a}_{k_j}|^2 + \sum_{k_0 \neq k}^{K_0} P_r |\mathbf{w}_k^H \mathbf{a}_{k_0}|^2 + \sigma_n^2 \right\}^{-1} . \tag{6.17}$$

Next we will investigate the effect of two specific beamformer algorithms, i.e., the beam-steering method and the MVDR beamformer.

6.2.2   Conventional Beam-Steering Technique (Scheme I)

Scheme I adopts the conventional beam-steering algorithm. According to the beam-steering method, we know that the beamformer weight $\mathbf{w}_{bs}$ for user k is equal to its array manifold vector [41], i.e.,

$$\mathbf{w}_{bs} = \mathbf{a}_k \ , \tag{6.18}$$

where $\mathbf{a}_k$ is defined in (6.8). As a result, the bit energy-to-interference density ratio after applying beam-steering (denoted as γ_{bs}) becomes

$$\gamma_{bs} = LP_r \left\{ \sum_{j \in \mathcal{B}_{od}} P_t G(d_j, \alpha_j) |\mathbf{a}_k^H \mathbf{b}_j|^2 + \sum_{j \in \mathcal{B}_{sd}} \sum_{k_j=1}^{K_j} P_r \xi_{k_j} |\mathbf{a}_k^H \mathbf{a}_{k_j}|^2 + \sum_{k_0 \neq k}^{K_0} P_r |\mathbf{a}_k^H \mathbf{a}_{k_0}|^2 + \sigma_n^2 \right\}^{-1} . \tag{6.19}$$

The effect of utilizing the conventional beam-steering technique (Scheme I) is equivalent to steering a beam of signals concentrating at the desired direction. By controlling the direction of the receive beam to track the position of the target mobile station, the beam-steering technique can reduce the effective interference thanks to a lesser number of interferers falling within the angle of the established receive beam. Assume that the interfering mobiles

are uniformly distributed in a cell and W is the effective beamwidth in radian formed by the beam-steering technique. Then the terms $|\mathbf{a}_k^H \mathbf{b}_j|^2$ and $|\mathbf{a}_k^H \mathbf{a}_{k_j}|^2$ in (6.19) can be approximated by a Bernoulli random variable with a successful probability $W/2\pi$. Because the opposite direction interference I_{od} and the same direction interference I_{sd} are reduced by the factors $|\mathbf{a}_k^H \mathbf{b}_j|^2$ and $|\mathbf{a}_k^H \mathbf{a}_{k_j}|^2$, respectively, the received γ_{bs} can be improved.

It has been demonstrated that the beam-steering method can significantly improve the performance of FDD/CDMA systems [45]. However, we conjecture that this kind of beam-steering technique may not be good enough to suppress the opposite direction interference in the TDD/CDMA system. Take Fig. 6.3 as an example. Figures 6.3-(a) and 6.3-(b) illustrate a beam pattern formed by the beam-steering technique from the viewpoints of the whole system and the antenna beam pattern, respectively. In these two figures, a triangle-shaped target mobile is located in the center cell. Cells 2, 4, and 6 surround the center cell and generate the opposite direction interference. From Fig. 6.3-(b), one can see that the conventional beamformer can establish a narrow beam pattern directing toward the target mobile at the angle of 150^0. However, this beamformer can only reduce the impact of the opposite direction interference by smaller antenna gains ranged from 10 dB, 5.6 dB, and 16 dB at the angles of 60^0 and 180^0 and 300^0, respectively. Therefore, the beam pattern of Scheme I may not be good enough to resolve the opposite direction interference issue for TDD/CDMA systems. This is because the beam-steering technique only directs the main beam towards the desired mobile instead of suppressing the opposite direction interference from the side lobe. Based on this observation, in the TDD/CDMA system we prefer the MVDR beamformer to the beam-steering technique.

6.2.3 MVDR Beamformer (Scheme II)

It is well known that the MVDR beamformer can direct the main receive beam toward the desired user, while cancelling the strong interference simultaneously. Therefore, we expect that the MVDR beamformer is more suitable to resolve the issue of the opposite
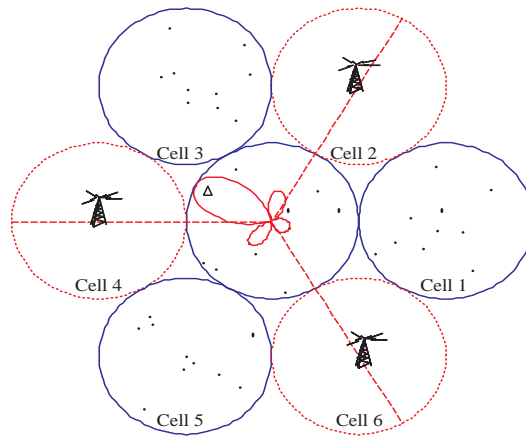
(a) : Beamforming with beam-steering technique
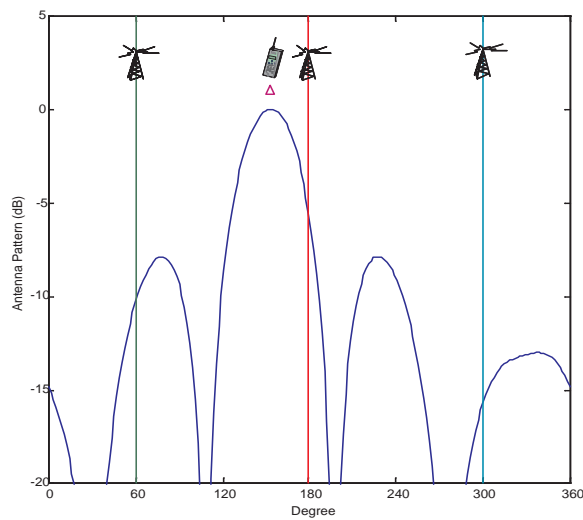
(b) : Antenna pattern with beam-steering technique

Figure 6.3: An illustrative example for a TDD/CDMA system with Scheme I, where $\mathcal{B}_{od} = \{2, 4, 6\}$.

direction interference in the TDD/CDMA system compared with the conventional beam-steering technique. In the following, we will incorporate the effect of the MVDR beamformer into the analysis of the uplink received signals in the TDD/CDMA system.

The goal of the MVDR criteria is to minimize the output power, while maintaining signal strength equal to one in the desired direction. That is, the MVDR beamformer will determine

the weight factor $\mathbf{w}_{mv}$ of the combining scheme according to the following criteria:

$$\mathbf{w}_{mv} = \arg \min_{\mathbf{w}_k} \mathrm{E}[\,|\mathbf{w}_k^H \mathbf{x}|^2\,]$$

$$\text{s.t.} \quad \mathbf{w}_k^H \mathbf{a}_k = 1 \ . \tag{6.20}$$

In (6.20) the term $\mathrm{E}[\,|\mathbf{w}_k^H \mathbf{x}|^2\,]$ can be expressed as

$$\mathrm{E}[\,|\mathbf{w}_k^H \mathbf{x}|^2\,] = \mathbf{w}_k^H \Phi_x \mathbf{w}_k \ , \tag{6.21}$$

where Φ_x is the sampled covariance matrix of the received signal $\mathbf{x}(t)$, i.e., $\Phi_x = \mathrm{E}[\,\mathbf{x}(t)\mathbf{x}(t)^H\,]$. Referring to (6.9), Φ_x can be written as

$$\Phi_x = P_r \mathbf{a}_k \mathbf{a}_k^H + \Phi_{od} + \Phi_{sd} + \Phi_{ic} + \sigma_n^2 \mathbf{I} \tag{6.22}$$

where

$$\Phi_{od} = \sum_{j \in \mathcal{B}_{od}} P_t G(d_j, \alpha_j) \mathbf{b}_j \mathbf{b}_j^H \ , \tag{6.23}$$

$$\Phi_{sd} = \sum_{j \in \mathcal{B}_{sd}} \sum_{k_j=1}^{K_j} P_r \xi_{k_j} \mathbf{a}_{k_j} \mathbf{a}_{k_j}^H \ , \tag{6.24}$$

and

$$\Phi_{ic} = \sum_{k_0 \neq k}^{K_0} P_r \mathbf{a}_{k_0} \mathbf{a}_{k_0}^H \ . \tag{6.25}$$

Here Φ_{od}, Φ_{sd}, and Φ_{ic} denote the signal covariance matrices of the opposite direction interference, the same direction interference, and the intracell interference, respectively.

Applying the Lagrange multiplier approach, one can obtain the MVDR beamformer weight $\mathbf{w}_{mv}$ as follows [41]

$$\mathbf{w}_{mv} = \frac{\Phi_x^{-1} \mathbf{a}_k}{\mathbf{a}_k^H \Phi_x^{-1} \mathbf{a}_k} \ . \tag{6.26}$$

According to [41], the total output power after the MVDR beamforming is equal to

$$\mathrm{E}[\,|\mathbf{w}_{mv}^H \mathbf{x}|^2\,] = (\mathbf{a}_k^H \Phi_x^{-1} \mathbf{a}_k)^{-1} \ . \tag{6.27}$$

Then similar to the derivation of (6.19), we can first substitute the weight $\mathbf{w}_{mv}$ of (6.26) into (6.17) and then refer to (27) to obtain the bit energy-to-interference density ratio γ_{mv} with

94

the MVDR beamformer (Scheme II) as follows:

$$\gamma_{mv} = \frac{LP_r}{(\mathbf{a}_k^H \Phi_x^{-1} \mathbf{a}_k)^{-1} - P_r} \ . \tag{6.28}$$

Defining

$$\Phi_k = (\Phi_{od} + \Phi_{sd} + \Phi_{ic} + \sigma_n^2 \mathbf{I})/P_r \tag{6.29}$$

as the normalized covariance matrix of the received interference plus noise signals, we can further simplify γ_{mv} in (6.28) as

$$\gamma_{mv} = L(\mathbf{a}_k^H \Phi_k^{-1} \mathbf{a}_k) \ , \tag{6.30}$$

where the derivations are detailed in Appendix E.

Since it is not easy to further derive the closed-form expression for γ_{mv}, we will evaluate γ_{mv} numerically to demonstrate the advantage of using the MVDR beamformer in TDD/CDMA systems later in Section 6.4. Now we use Fig. 6.4 to explain intuitively why the MVDR beamformer outperforms the beam-steering technique in TDD/CDMA systems. Figures 6.4-(a) and 6.4-(b) show a beam pattern of the MVDR beamformer with the same scenario as Fig. 6.3. Compared to Fig. 6.3, one can observe that the MVDR beamformer not only directs the beam towards the target mobile at the angle of 150°, but also nullifies the opposite direction interference at the arrival angles of 60°, 180°, and 300°. Note that to obtain the weights of the MVDR beamformer, it only requires the knowledge of the direction of arrival (DOA) from the target mobile. We assume that the information of DOA of the target mobile is available, which can be obtained by the DOA estimation algorithms such as in [111] and [44].

The superiority of MVDR beamforming in suppressing strong interference requires that the signal and interference are uncorrelated. In the multipath environment, the correlation between the desired signal and its multipath arrivals (regarded as interference) may seriously degrade the output signal-to-interference ratio performance. Several techniques to desensitize the correlation of the signal and interference in the received covariance matrix can be found in [44]. Fortunately, in the CDMA system, the delayed arrivals of the desired signal can
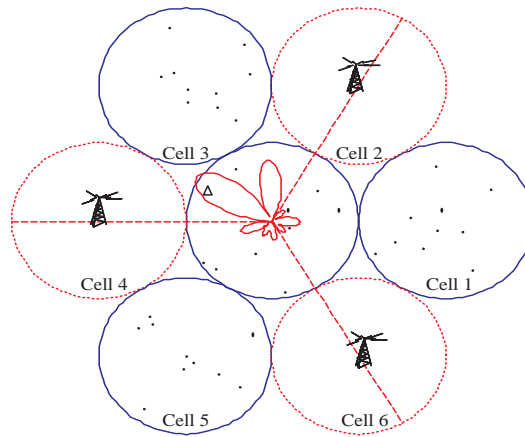
(a) : Beamforming with MVDR beamformer
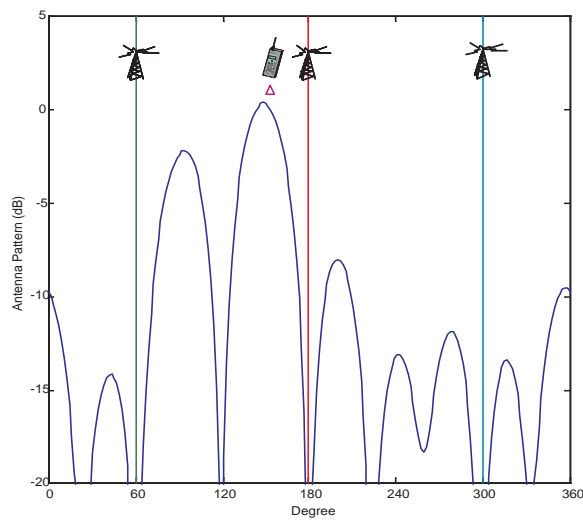
(b) : Antenna pattern with MVDR beamformer

Figure 6.4: An illustrative example for a TDD/CDMA system with Scheme II, where $\mathcal{B}_{od} = \{2, 4, 6\}$.

be resolved by temporal filtering of Rake receivers. Thus, using a two-dimensional spatial-temporal architecture with each branch for an individual delayed path, the MVDR algorithm can still work well and even capture more energy of the desired signal in the multipath environment [23, 113, 114].

6.3 Downlink Beamforming

In this section, we discuss how to improve the performance of the TDD/CDMA system further by exploiting the synergy of adopting both the downlink transmit and uplink receive beamforming simultaneously. Note that in TDD systems, due to channel reciprocity between the downlink and uplink, downlink beamforming can be easily implemented by taking advantage of the estimated parameters from uplink signals. The benefits of incorporating downlink transmit beamforming can be illustrated by an example shown in Fig. 6.5. In the figure, the beam pattern of the center cell is for the uplink reception, while the beam patterns of the neighboring cells are for the downlink transmission. Assume that a simple downlink beam-steering technique has been adopted at the base stations of cells 2, 4 and 6. Obviously, the impacts of the opposite direction interference signals from cells 2, 4, and 6 are alleviated because of weaker power radiating toward the direction of the home cell.

6.3.1 Joint Downlink and Uplink Beam-Steering (Scheme III)

Now we evaluate the effect of Scheme III, where the beam-steering method is adopted for both the downlink transmission and uplink reception at base stations. With downlink transmit beamforming, the opposite direction interference $\tilde{\mathbf{x}}_{od}(t)$ [1] introduced by the neighboring cells can be modified from (6.10). That is,

$$
\begin{aligned}
\tilde{\mathbf{x}}_{od}(t) &= \sum_{j \in \mathcal{B}_{od}} \sum_{k_j=1}^{\tilde{K}_j} \sqrt{p_{k_j} G(d_j, \alpha_j)} |\tilde{\mathbf{w}}_{k_j}^H \tilde{\mathbf{b}}_j| \\
&\quad u_{k_j}\left(\left\lfloor \frac{t - \tau_{k_j}}{T} \right\rfloor\right) c_{k_j}(t - \tau_{k_j}) \mathbf{b}_j \ ,
\end{aligned}
\tag{6.31}
$$

where $\tilde{\mathbf{b}}_j$ is the array manifold vector of the signal transmitting from cell j ($j \in \mathcal{B}_{od}$), $\tilde{\mathbf{w}}_{k_j}$ is the downlink beamformer weight of mobile k_j, $\tilde{K}_j$ is the number of active mobile users in the downlink cycle, and p_{k_j} is the transmission power allocated to the mobile k_j from a base station. Then, the opposite direction interference I_{od} at the output of the receive

---

[1]The superscript $\tilde{[\cdot]}$ in this chapter denotes the case when downlink beam-steering is applied.

beamformer can be modified from (6.14) as follows:

$$\tilde{I}_{od} = \sum_{j \in \mathcal{B}_{od}} \sum_{k_j=1}^{\tilde{K}_j} p_{k_j} G(d_j, \alpha_j) |\tilde{\mathbf{w}}_{k_j}^H \tilde{\mathbf{b}}_j|^2 |\mathbf{w}_k^H \mathbf{b}_j|^2 \quad . \tag{6.32}$$

Note that $P_t = \sum_{k_j=1}^{\tilde{K}_j} p_{k_j}$ is the total transmit power of a base station. Comparing (6.32) with (6.14), one can observe that after incorporating downlink transmit beamforming, the effective radiation power that causes the opposite direction interference from cell j ($j \in \mathcal{B}_{od}$) can be reduced from P_t to a smaller value

$$\tilde{P}_t = \sum_{k_j=1}^{\tilde{K}_j} p_{k_j} |\tilde{\mathbf{w}}_{k_j}^H \tilde{\mathbf{b}}_j|^2 \quad . \tag{6.33}$$

From (6.18), we know that the downlink beamformer weight for mobile k_j of cell j ($j \in \mathcal{B}_{od}$) is given by

$$\tilde{\mathbf{w}}_{k_j} = \tilde{\mathbf{a}}_{k_j} , \tag{6.34}$$

where $\tilde{\mathbf{a}}_{k_j}$ is the array manifold vector of the signal transmitting from cell j to its serving mobile k_j ($j \in \mathcal{B}_{od}$). Due to the reciprocity of TDD channels, $\tilde{\mathbf{a}}_{k_j}$ can be approximated by modifying $\mathbf{a}_{k_j}$ which is already obtained in the uplink beamforming. Replacing P_t of (6.19) with the effective radiated power $\tilde{P}_t$ of (6.33), we can obtain the bit energy-to-interference density ratio $\tilde{\gamma}_{bs}$ of Scheme III as follows:

$$\begin{aligned} \tilde{\gamma}_{bs} &= LP_r \left\{ \sum_{j \in \mathcal{B}_{od}} \sum_{k_j=1}^{\tilde{K}_j} p_{k_j} G(d_j, \alpha_j) |\tilde{\mathbf{a}}_{k_j}^H \tilde{\mathbf{b}}_j|^2 |\mathbf{a}_k^H \mathbf{b}_j|^2 + \right. \\ &\quad \left. \sum_{j \in \mathcal{B}_{sd}} \sum_{k_j=1}^{K_j} P_r \xi_{k_j} |\mathbf{a}_k^H \mathbf{a}_{k_j}|^2 + \sum_{k_0 \neq k}^{K_0} P_r |\mathbf{a}_k^H \mathbf{a}_{k_0}|^2 + \sigma_n^2 \right\}^{-1} . \end{aligned} \tag{6.35}$$

6.3.2 Joint Downlink Beam-Steering and Uplink MVDR Beamformer (Scheme IV)

In the following, we derive the bit energy-to-interference density ratio $\tilde{\gamma}_{mv}$ for Scheme IV. In Scheme IV, a base station transmits downlink signals through the beam-steering process, while in the uplink reception the MVDR beamformer is applied. Let $\tilde{\Phi}_{od}$ represent the
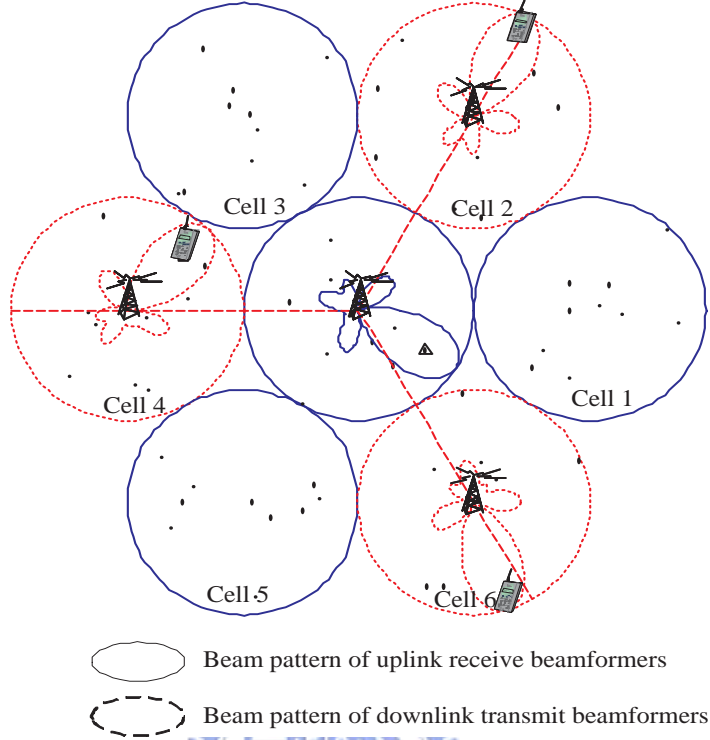
Figure 6.5: An illustrative example for a TDD/CDMA system with Scheme III, where the beam pattern in the center cell is for the uplink reception and those in the neighboring cells $\mathcal{B}_{od} = \{2, 4, 6\}$ are for the downlink transmission.

signal covariance matrix of the opposite direction interference. Then $\tilde{\Phi}_{od}$ can be obtained by replacing P_t of (6.23) with $\tilde{P}_t$ of (6.33). That is,

$$\tilde{\Phi}_{od} = \sum_{j \in \mathcal{B}_{od}} \sum_{k_j=1}^{\tilde{K}_j} p_{k_j} G(d_j, \alpha_j) |\tilde{\mathbf{w}}_{k_j}^H \tilde{\mathbf{b}}_j|^2 \mathbf{b}_j \mathbf{b}_j^H \ . \tag{6.36}$$

Substituting (6.36) into (6.29), we can obtain the normalized covariance matrix $\tilde{\Phi}_k$ of the total interference plus noise as follows:

$$\tilde{\Phi}_k = (\tilde{\Phi}_{od} + \Phi_{sd} + \Phi_{ic} + \sigma_n^2 \mathbf{I})/P_r \ . \tag{6.37}$$

Finally replacing Φ_k of (6.30) with $\tilde{\Phi}_k$ of (6.37), we can obtain $\tilde{\gamma}_{mv}$ for Scheme IV as follows:

$$\tilde{\gamma}_{mv} = L(\mathbf{a}_k^H \tilde{\Phi}_k^{-1} \mathbf{a}_k) \ . \tag{6.38}$$

Note that in both Schemes III and IV, the conventional beam-steering technique is used for downlink transmit beamforming. One may wonder why the MVDR beamforming is not

99

applied in the downlink transmit beamforming. We will discuss this issue in the following. Unlike the uplink receive beamformer, which does not impose any negative impacts on other users, the downlink transmit beamformer may possibly exacerbate the downlink performance of other users. For example, consider the receive MVDR beam pattern of Fig. 6.4, where the main beam is directing to the desired user at the angle of 150° and three nulls at the angles of 60°, 180°, and 300°. It is noteworthy that compared to the conventional beam-steering technique, the uplink MVDR beamformer place the nulls at the directions of interfering sources at the cost of increasing the magnitude of side lobes. Thus, because of higher amplitude in the side lobes, the downlink MVDR transmit beamforming may cause strong interference to other mobiles, e.g., the mobile at the angle of 93° in Fig. 6.4. From this observation, we believe that it is not feasible to apply the weight obtained in the uplink MVDR beamforming straightforwardly for downlink transmit beamforming. To determine the optimal weights of downlink transmit beamforming is a complicated issue [47, 46] and beyond the scope of this thesis. Here, we only consider the suboptimal beam-steering technique for downlink beamforming. In the next section, we will show that even with this kind of simple downlink beam-steering technique, the performance of the TDD/CDMA system can be significantly improved.

6.4   Numerical Results

This section demonstrates the performance results of the aforementioned four different beam-forming techniques. We consider a TDD/CDMA multicellular system, where all cells provide asymmetric traffic services based on their own traffic requirements. Through simulation, we evaluate the bit energy-to-interference density ratio γ for Schemes I, II, III and IV according to (6.19), (6.30), (6.35) and (6.38), respectively. The number of active users in every cell is set to 20 during one time slot, i.e. $K_j = \tilde{K}_j = 20$. In all simulations, we assume mobiles are uniformly distributed and the other system parameters used in simulation are listed in Table 6.1.

Table 6.1: Simulation parameters for the TDD/CDMA system.

Processing gain	$L = 128$
COST-231 propagation model	$10 \log(\kappa_0) = -128.1,\ \mu = 3.76$
Shadowing standard deviation	$\sigma_s = 8$ dB
Cell radius	$R = 1$ Km
Total transmit power of a base station	$P_t = 8$ W
Base station transmit power allocated for each mobile	$p_{k_j} = 0.4$ W
Thermal noise	$\sigma_n^2 = -112$ dBm
Power control level	$P_r/\sigma_n^2 = -1$ dB [96]

6.4.1 Performance of Uplink Beamforming

Figure 6.6 compares the uplink performance of Schemes I and II. In Scheme I beam-steering is applied to suppress the opposite direction interference, while Scheme II adopts the MVDR beamformer. We define the reliability function p as the complementary cumulative distribution function of γ, i.e., $p = 1 - \text{Prob}\{\gamma \leq \gamma_{th}\}$, where γ_{th} is the required bit energy-to-interference density ratio. In the figure, curves (a)$\sim$(d) show the performances of the MVDR beamformer with different number of antenna elements, whereas curve (e) shows the performance of the beam-steering technique. For comparison, the performance without using any beamforming technique is shown in curve (f). In this figure and hereafter, $B = |\mathcal{B}_{od}|$ denotes the number of surrounding cells generating the opposite direction interference. Let's focus on the case when $\gamma_{th} = 7$ dB and $p = 90\%$. From curves (a), (b) and (c), one can find that the uplink MVDR beamformer with antenna elements $N = 9, 7$ and 5 can have satisfactory performance. Because in our simulation scenario there are three neighboring cells generating the strong opposite direction interference, it is necessary to have at least four antenna elements in the MVDR beamformer to place enough nulls to suppress the three strong interfering signals. By contrast, from curve (e) one can see that even with nine antenna elements, Scheme I still cannot yield any feasible solution to overcome the opposite direction interference
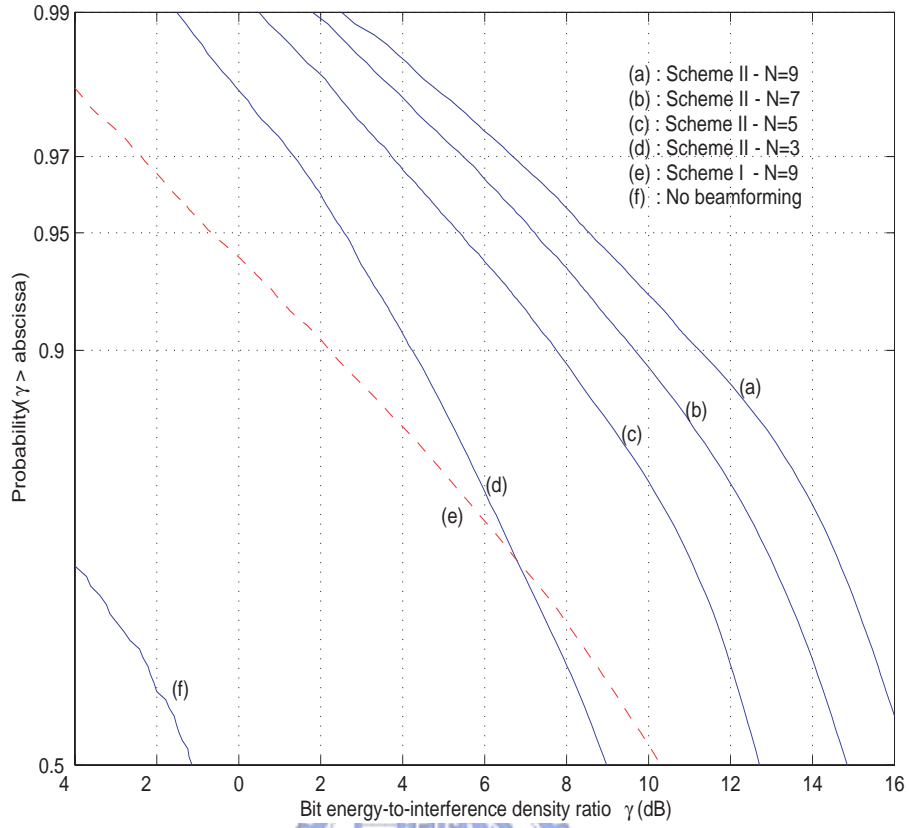
Figure 6.6: Uplink performance comparison of Schemes I and II with different numbers of antenna elements (denoted as N in the figure), where the number of cells generating the opposite direction interference is equal to three.

Figure 6.7 compares the performances of Schemes I and II with different numbers of cells generating the opposite direction interference. With nine antenna elements ($N = 9$), curves (e)∼(g) and curves (a)∼(d) show the performances of Schemes I and II, respectively. Assume that the required reliability p is equal to 90%. We find that when we increase the number of neighboring cells generating the opposite direction interference from one to three, the 90th percentile of γ in Scheme II degrades 3 dB, whereas in Scheme I the 90th percentile of γ degrades 6 dB. Thus, we can conclude that as compared to the conventional beam-steering method, the MVDR beamformer is less sensitive to the increase of the number of cells generating the opposite direction interference.
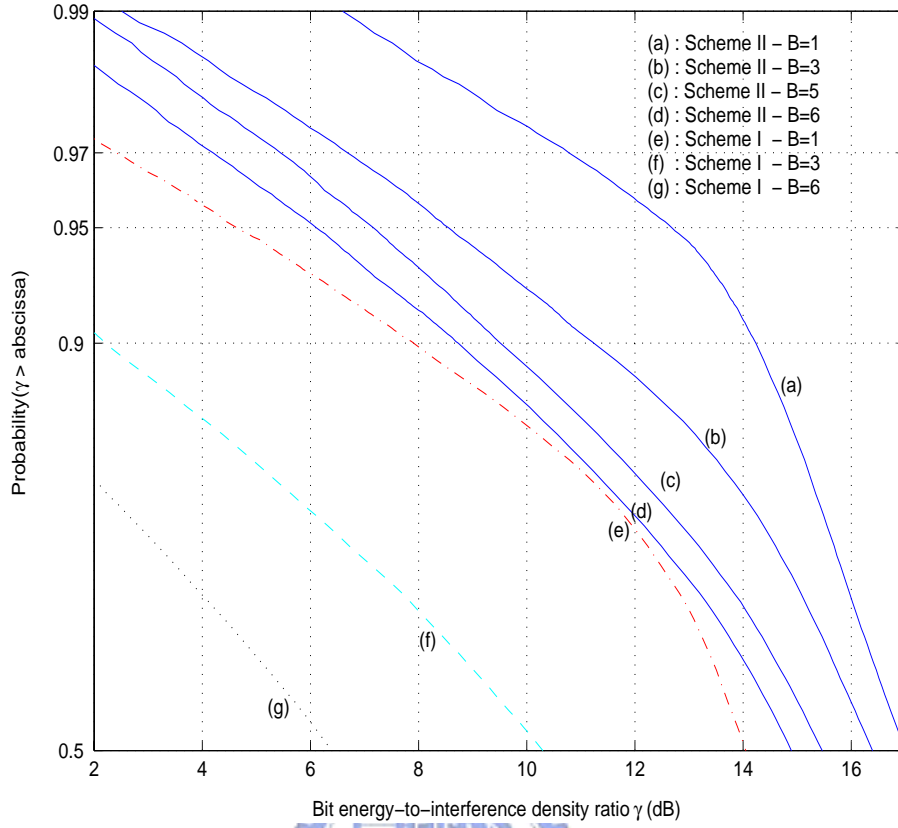
Figure 6.7: Uplink performance comparison of Schemes I and II with different numbers of cells generating the opposite direction interference (denoted as B in the figure), where the number of antenna elements is equal to nine.

6.4.2 Performance of Downlink Beamforming

Figure 6.8 demonstrates the performance improvements by adopting downlink transmit beamforming. One can find that when the downlink transmit beam-steering method is employed, both Schemes III and IV improve the performance of the TDD/CDMA system significantly as compared to Schemes I and II, respectively. Compared to Scheme II (curve (b)), Scheme IV can improve the 90th percentile of γ from 8.74 dB to 11.94 dB (curve (d)). Note that Scheme IV adopts both the downlink transmit beam-steering and uplink receive MVDR beamformers, while Scheme II only utilizes the MVDR beamformer in the uplink reception. For Scheme I the 90th percentile of γ is -0.76 dB (curve (a)), while for Scheme III the 90th percentile of γ is improved to 5.36 dB (curve (c)).

Figure 6.9 demonstrates the impacts of the four aforementioned beamforming techniques
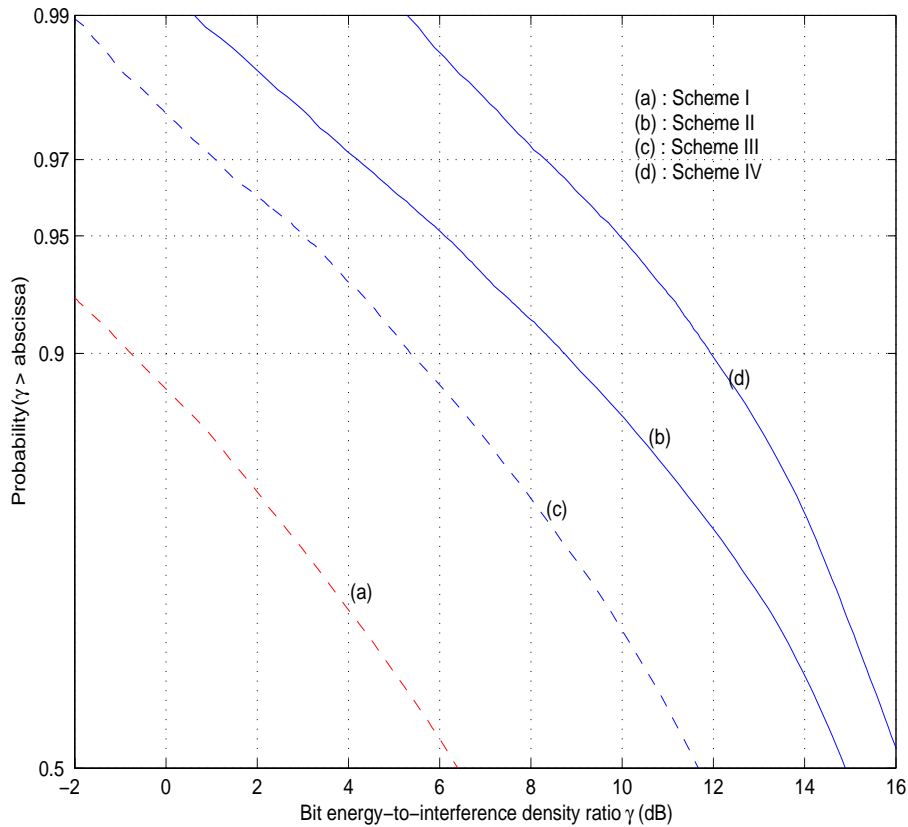
Figure 6.8: Performance improvements by implementing downlink transmit beamformer in the surrounding base stations, where the number of cells generating the opposite direction interference equal to six and the number of antenna elements equal to nine.

in TDD/CDMA systems against the increase of the number of cells generating the opposite direction interference. One can see that Scheme IV is least sensitive to the increase of the number of cells causing the opposite direction interference. Let's consider the case when the required γ_{th} is equal to 7 dB. One can observe that the reliability function with Scheme IV is slightly degraded to 98% as B increases from zero to six. However, for Scheme III the reliability function is degraded to 84%. Note that Scheme II can also be an effective approach to suppress the opposite direction interference since its reliability is still higher than 90%.

6.4.3 Discussion

To determine which beamforming scheme should be used in TDD/CDMA systems is a complicated tradeoff issue between performance improvements and implementation costs.
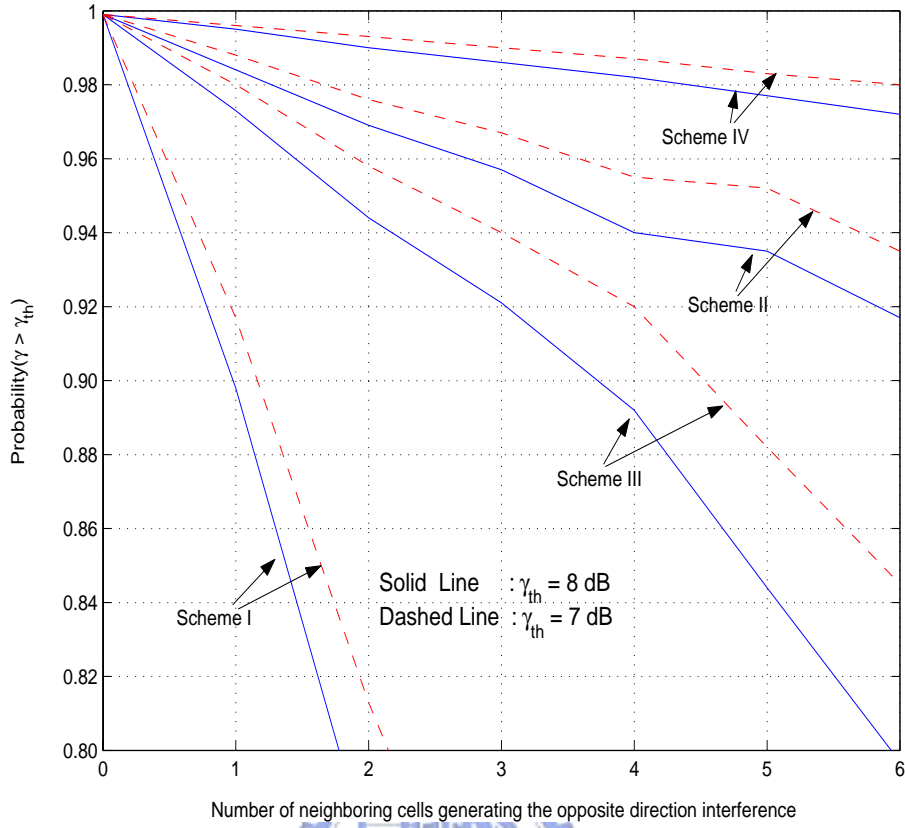
Figure 6.9: Performance comparison of four beamforming schemes with different numbers of cells generating the opposite direction interference, where an antenna array with nine elements is deployed at base stations.

Scheme IV, using the uplink MVDR beamforming and downlink transmit beam-steering, can effectively suppress the opposite direction interference, thereby providing greater flexibility in delivering asymmetric traffic services. In Scheme IV every TDD/CDMA cell can *independently* designate traffic patterns for either uplink modes or downlink modes in every time slot according to its own rate of traffic asymmetry. On the other hand, using a simpler beam-steering method in both the uplink reception and downlink transmission, Scheme III provides satisfactory performance only when the number of cells generating the opposite direction interference is not large. Thus, it is suggested to combine Scheme III with other sectorization or channel assignment techniques to reduce the number of cells generating the opposite direction interference.

Scheme II is another effective technique to reduce the impact of the opposite direction interference. Recall that Scheme II utilizes the MVDR beamforming only in the uplink.

Note that the performance of Scheme II is better than Scheme III but worse than Scheme IV. As remarked earlier, the extra cost of implementing downlink transmit beam-steering may not be very high. If so, Scheme IV will be a better choice than Scheme II provided that the MVDR beamformer has already been adopted in the uplink. As for Scheme I, it is shown that only using beam-steering in the uplink can not provide acceptable performance.

Although we concentrate on the uplink performance of TDD/CDMA systems, antenna beamforming can also be exploited to improve the downlink performance. For example, by taking advantage of the reciprocity of TDD channels, downlink transmit beamforming from neighboring base stations can lower the effective interfering power to the mobile station in the home cell. Furthermore, when the mobile station is employed with a small number of array sizes [108, 47], the downlink performance can be further enhanced with the beamforming techniques similar to the Schemes III and IV.

6.5 Chapter Summary

This chapter have investigated the effect of four antenna beamforming schemes on rejecting the opposite direction interference in the TDD/CDMA system. From the network view to exploit the multiple antennas at the base stations of adjacent cells, we propose a simultaneous downlink transmit beamforming and uplink receive beamforming scheme to alleviate the negative impact of the opposite direction interference with a low implementation cost. Based on the numerical results in this chapter, we can make the following summary:

- Schemes IV, which adopts the MVDR beamformer in the uplink and the beam-steering in the downlink, can effectively suppress the strong opposite direction interference of TDD/CDMA systems, thereby allowing every cell to provide asymmetric traffic services with different rates of traffic asymmetry.

- Scheme III, which adopts the beam-steering method in both the downlink transmission and uplink reception, can provide satisfactory performance when the number of cells generating the opposite direction interference is not large. When combined with other

sectorization or channel assignment techniques, Scheme III can be a very effective mechanism to overcome the opposite direction interference in the TDD/CDMA system with lower implementation costs.

- If only the uplink beamforming is considered, the MVDR beamformer (Scheme II) instead of the conventional beamforming method (Scheme I) should be adopted since the conventional beam-steering can not effectively suppress the opposite direction interference.

As a result, even with the severe impact of the opposite direction interference, a feasible and economical beamforming mechanism (e.g. Scheme III) can be found, which can enable the TDD/CDMA system to deliver asymmetric traffic services within the entire service area with greater flexibility.

Chapter 7

Concluding Remarks

7.1 Dissertation Summary

The story is coming to an epilogue. In the dissertation, it has been seen that the marriage of the multiplexing-based antenna technique with the multiuser scheduling system is finally proved to a wonderful ending due to their complementary diversity-multiplexing characteristics. Another marriage of the diversity-based antenna technique with the multiuser scheduling system, however, may lead to a pitfall due to the intrinsic conflict – one prefers fluctuations while the other makes tranquility. In the third marriage, a happy ending follows when the tough opposite direction interference in the TDD/CDMA systems is tamed by an appropriate match of beamforming techniques.

To sum up, through the lens of the network perspective to exploit the interaction between the multiple antenna technique and its underlying communication system, this dissertation has developed effective strategies to apply the MIMO technique for the multiuser scheduling and TDD/CDMA systems. The dissertation includes the following research topics:

1. The fading mitigation based antenna technique (or diversity-based antenna technique) for the multiuser scheduling system.

2. The throughput enhancement based antenna technique (or multiplexing-based antenna technique) for the multiuser scheduling system.

3. The throughput enhancement based antenna technique for the multiuser scheduling

system with the zero-forcing receiver.

4. The interference suppression based antenna technique (or beamforming technique) for the TDD/CDMA system.

Contributions from this research are listed as follows.

1. Developed an analytical framework to investigate the interaction of antenna diversity and multiuser scheduling. Through a unified capacity analysis, the chaotic interplay among fading characteristics, multiuser diversity and various diversity-based antenna schemes is unraveled.

2. Suggested an innovative strategy to replenish the diversity-deficient spatial multiplexing MIMO system with multiuser diversity. With only scalar feedback, the proposed SWNSF scheduling can significantly improve the cell coverage and system capacity of the multiuser MIMO system.

3. Leveraged the cross-layer cooperation between the simple zero-forcing receiver and multiuser scheduling to achieve the full theoretical capacity of the MIMO system. Also, a proof is given to illustrate the asymptotic optimality of the zero-forcing in a scheduling environment with many users.

4. Invented a cross-cell cooperation among the multiple antennas of adjacent base stations. The exploitation of such a cooperation along with the TDD channel reciprocity enables an effective and economical beamforming solution to resolve the opposite direction interference issue for the TDD/CDMA system.

The following summaries the results from the above contributions.

7.1.1 Fading Mitigation Based Antenna Techniques for Multiuser Scheduling Systems

Chapter 3 and [116] presented a cross-layer analytical framework to jointly investigate antenna diversity and multiuser scheduling under the generalized Nakagami fading channels.

We derive a unified capacity formula for the multiuser scheduling system with different MIMO antenna schemes, including (1) selective transmission/selective combining (ST/SC), (2) maximum ratio transmission/maximum ratio combining (MRT/MRC), (3) ST/MRC and (4) space-time block codes (STBC). Our analytical results lead to the following four observations regarding the interplay of multiuser scheduling and antenna diversity. First, the higher the Nakagami fading parameter, the lower the scheduling gain for all the considered antenna schemes. Second, from the standpoint of multiuser scheduling, the multiple antennas with the ST/SC method can be viewed as virtual users to amplify multiuser diversity order. Third, the boosted array gain of the MRT/MRC scheme can compensate the detrimental impact of the reduced amount of fading gain on multiuser scheduling, thereby resulting in greater capacity than the ST/SC method. Last, employing the STBC scheme together with multiuser diversity may cause a capacity loss due to the reduced amount of fading gain but without the supplement of array gain.

7.1.2 Throughput Enhancement Based Antenna Techniques for Multiuser Scheduling Systems

Chapter 4 and [117] demonstrated the advantage of using multiuser diversity to enhance the degraded link quality of the diversity-deficient spatial multiplexing MIMO system. In particular, a novel SWNSF scheduling algorithm is proposed for the multiuser MIMO system with low-rate feedback channels. The SWNSF scheduling is a fair scheduling policy for near-far users and requires only scalar feedback. Through a tractable eigenvalue analysis, it is shown that the SWNSF scheduling can enhance the receive SNR of all subchannels for any selected user so that better link reliability (and thus coverage extension) and higher link throughput (and thus system capacity improvement) are achieved. It is also observed that a large number of antennas could attenuate the scheduling gain due to the effect of channel damping .

7.1.3 Throughput Enhancement Based Antenna Techniques for Multiuser Scheduling Systems with Zero-Forcing Receivers

Chapter 5 and [118] studied the performance of the zero-forcing receiver operating in the multiuser MIMO system with various scheduling policies. The motivation is to exploit the inherent property of poor channel avoidance from a multiuser scheduling system to overcome the drawback of noise enhancement for the zero-forcing receiver. It is shown that the cross-layer cooperation between the simple zero-forcing receiver and the scheduling technique can achieve the full theoretical capacity of the MIMO system. Moreover, it is shown that with the increasing number of users in the multiuser MIMO system the efficiency of the zero-forcing receiver in recovering the spatially multiplexed data can approach that of the optimal receiver operating under the same scheduling algorithms. An important implication from this result is that the multiuser diversity gain can be used to simultaneously improve system performances as well as reduce receiver implementation complexity. Another important observation from comparing the performance of implementing the scalar feedback and vector feedback scheduling is that the amount of feedback information plays a curial role to enhance the downlink performance of the multiuser MIMO system.

7.1.4 Interference Suppression Based Antenna Techniques for TDD/CDMA Systems

Chapter 6 and [119] investigated the effect of beamforming techniques from the perspective of suppressing the opposite direction interference in TDD/CDMA systems. Four antenna beamforming schemes are studied to alleviate the impact of the strong opposite direction interference from adjacent cells. With only uplink beamforming, it is shown that the MVDR beamformer (Scheme II) instead of the conventional beamforming method (Scheme I) should be adopted since the beam-steering can not effectively suppress the opposite direction interference. However, by exploiting the reciprocal property of TDD channels and the synergy of combining the downlink transmit and uplink receive beamforming, the low-cost Scheme III which adopts the beam-steering method in both the downlink transmission and uplink

reception can also provide satisfactory performance.

7.2 Suggestions For Future Research

The research in this dissertation covers a wide variety of multiple antenna techniques for their applications in contemporary multiuser scheduling and TDD/CDMA wireless systems with the network perspective emphasis. Other research topics related to or inspired by this research are addressed as follows.

- **The impact of imperfections**

  As a first step to explore the relationship of the antenna technique with the multiuser scheduling and TDD/CDMA communication systems, this dissertation has made ideal assumptions in system modelling. For instant, it is assumed that the base station can always have the correct and instantaneous feedback information to perform scheduling. Also the perfect DOA information and channel reciprocity of TDD channels are assumed for antenna beamforming. Considering the inevitable channel estimation error or feedback delay in practical systems, it is worth further investigating the impact of channel uncertainty on the resulting system performance.

- **Optimal scheduling design with feedback rate/delay constraints**

  It has been known that in a point-to-point MIMO system the full channel side information at the transmitter can only add to limited capacity gain (especially at the high SNR condition) as compared with the case of no channel side information. However, in the multiuser MIMO system with scheduling, it is shown in this dissertation that the amount of feedback plays a curial role to enhance the downlink capacity. The difference mainly comes from the fact that in the multiuser MIMO scenario the receive antennas among multiple users can not "really" cooperate so that the joint decoding among them is not possible. Since the higher feedback rate consumes more reverse link capacity, how to design an optimal scheduling algorithm to enhance the downlink

capacity as much as possible while maintaining a low-rate feedback turns out to be an important research topic.

Another important research topic is the optimal scheduling design for the data traffic with delay constraints. This dissertation has implicitly assumed that all the users can wait for services with no delay constraints. Under such circumstances, the mean delay time for any serviced user would increase with the number of users in the system. For the data traffic with stringent delay constraints, how to design an optimal scheduling strategy to meet the delay constraints while enhancing the system performance still remains an important research direction.

- **Antenna beamforming for the multiuser scheduling system**

  From the complementary diversity-multiplexing point of view, this dissertation has demonstrated the superiority of the multiplexing-based antenna schemes over the diversity-based antenna schemes as applied in the multiuser scheduling system. However, the issue of using the beamforming technique for the multiuser scheduling system has not been discussed in the dissertation. A recent study [115] revealed that it is possible for the beamforming technique to deliver degree-of-freedom gains in the MIMO system under certain propagation conditions. Consequently, the pro and con study of combining the antenna beamforming technique with the multiuser scheduling system still remains an open issue.

- **Cross-layer optimization issues**

  This dissertation has exemplified a nice cross-layer cooperation that leverages the combination of the scheduling technique in the MAC layer with the spatial multiplexing MIMO technique in the physical layer. As we remarked in the introduction, it is possible to find more good examples of cross-layer cooperations by using the network perspective methodology. One possible research topic following this philosophy is the joint design of the DCA technique and the antenna beamforming technique for the TDD/CDMA system. Due to the huge calculation in solving the DCA optimization

problem, [18] asserted that it is almost impossible to resolve the opposite direction interference issue by using the DCA method. On the other hand, this dissertation has demonstrated that using the beamforming technique can effectively cancel the number of strong opposite direction interference. Therefore, the cross-layer design of DCA and antenna beamforming techniques may open up a possibility to simultaneously reduce the complexity of the DCA algorithm and lower the implementation requirement for antenna beamforming.

Appendix A

Derivation of Equation (3.16)

For integer values of p, the PDF of (3.10) can be written as [94]

$$f_{\gamma_{\max}}(\gamma\,;p,q,K) = \frac{K}{(p-1)!}\sum_{k=0}^{K-1}\sum_{i=0}^{k(p-1)}(-1)^k\binom{K-1}{k}a_i^k q^{p+i}e^{-(k+1)q\gamma}\gamma^{p+i-1}\ ,\qquad\text{(A.1)}$$

where the coefficient a_i^k is defined in (3.17). Substituting (A.1) into (3.14) and using the integral [86]

$$\int_0^\infty \log(1+t)e^{-\mu t}t^{n-1}dt = (n-1)!e^\mu\sum_{j=1}^n\frac{\Gamma(j-n,n)}{\mu^j},\ \ n=1,2,3,\cdots\ ,\qquad\text{(A.2)}$$

we get

$$\langle C\rangle = \frac{K}{(p-1)!}\sum_{k=0}^{K-1}\sum_{i=0}^{k(p-1)}(-1)^k\binom{K-1}{k}^k a_i^k q^{p+i}e^{(k+1)q}$$

$$\cdot\,(p+i-1)!\sum_{j=1}^{p+i}\left[\frac{1}{(k+1)q}\right]^j\Gamma\left(j-p-i,(k+1)q\right)\ .\qquad\text{(A.3)}$$

Note that in (A.2) and (A.3), $\Gamma(\cdot,\cdot)$ is the incomplete gamma function, defined by

$$\Gamma(a,x) = \int_x^\infty t^{a-1}e^{-t}dt = \Gamma(a)\left[1-\widetilde{\Gamma}(a,x)\right]\ .\qquad\text{(A.4)}$$

Finally, applying the identity [82, Eq. 6.5.19]

$$\Gamma(-n,x) = \frac{(-1)^n}{n!}\left[E_1(x)-e^{-x}\sum_{j=0}^{n-1}\frac{(-1)^j j!}{x^{j+1}}\right],\ \ n=0,1,2,\cdots\ .\qquad\text{(A.5)}$$

to (A.3), we obtain the expression (3.16).

Appendix B

Proof of Proposition 4.3

Proof of (i): By applying the variable transformation (4.28) to (4.13) and using the result of Proposition 4.2, the joint PDF of $S_{k,1}, \cdots, S_{k,N}$ can be written as

$$f_{S_{k,1},\cdots,S_{k,N}}(s_1,\cdots,s_N) = Ne^{-Ns_1}\left\{\frac{1}{N\left[\prod_{i=1}^{N}\Gamma(i)\right]^2}\exp\left(-\sum_{i=2}^{N}s_i\right)\prod_{i=2}^{N}s_i^2\cdot\prod_{\substack{i>j\\i,j\in\{2,\cdots,N\}}}(s_i-s_j)^2\right\}$$

$$= f_{S_{k,1}}(s_1)f_{S_{k,2},\cdots,S_{k,N}}(s_2,\cdots,s_N) \ . \tag{B.1}$$

Thus, for any S_i $(2 \leq i \leq N)$, the joint PDF of S_i and S_1 can be derived as

$$f_{S_{k,i},S_{k,1}}(s_i,s_1) = \int_{s_i}^{\infty}\cdots\int_{s_{N-1}}^{\infty}\int_{0}^{s_i}\cdots\int_{0}^{s_3}f_{S_{k,1},\cdots,S_{k,N}}(s_1,\cdots,s_N)ds_2\cdots ds_{i-1}$$

$$ds_N\cdots ds_{i+1}$$

$$= f_{S_{k,1}}(s_1)f_{S_{k,i}}(s_i) \ . \tag{B.2}$$

Thus, $S_{k,i}$ and $\lambda_{k,1}$ are independent.

    Proof of (ii): Since the spacing $S_{k,i}$ are independent of $\lambda_{k,1}$, we have $\tilde{\lambda}_{k,i} = S_{k,i} + \tilde{\lambda}_{k,1}$ where $S_{k,i}$ and $\tilde{\lambda}_{k,1}$ are also independent. Thus, it is followed that

$$\phi_{\tilde{\lambda}_{k,i}}(\omega) = \phi_{\tilde{\lambda}_{k,1}}(\omega)\phi_{S_{k,i}}(\omega) = \phi_{\tilde{\lambda}_{k,1}}(\omega)\left[\frac{\phi_{\lambda_{k,i}}(\omega)}{\phi_{\lambda_{k,1}}(\omega)}\right] \ . \tag{B.3}$$

Note that the Laplace transform $\phi_{\lambda_{k,1}}(\omega) = N/(N+\omega)$ [82] and

$$\phi_{\tilde{\lambda}_{k,1}}(\omega) = \int_{0}^{\infty}f_{\tilde{\lambda}_{k,1}}(\lambda)e^{-\omega\lambda}d\lambda = KN\int_{0}^{\infty}(1-e^{-N\lambda})^{K-1}e^{-(N+\omega)\lambda}d\lambda = \frac{K!\,\Gamma(1+\omega/N)}{\Gamma(1+K+\omega/N)} \ , \tag{B.4}$$

where we have used the integral identity [100, eq. 3.312]

$$\int_0^\infty \left(1 - e^{-x/a}\right)^{b-1} e^{-cx} dx = \frac{a\Gamma(ac)\Gamma(b)}{\Gamma(ac+b)} \ . \tag{B.5}$$

Combining (B.4) and (B.3) yields the result of (4.29).

Proof of (iii): Since the appropriate derivative of the Laplace transform evaluated at its argument $\omega = 0$ gives rise to moments, this proof of (4.30) is completed by

$$\begin{aligned}
\mathrm{E}[\tilde{\lambda}_{k,i}] &= \left. -\frac{d\phi_{\tilde{\lambda}_{k,i}}(\omega)}{d\omega} \right|_{\omega=0} \\
&= \left. -A(0) \frac{d\phi_{\lambda_{k,i}}(\omega)}{d\omega} \right|_{\omega=0} - \left. \phi_{\lambda_{k,i}}(0) \frac{dA(\omega)}{d\omega} \right|_{\omega=0} \\
&= \mathrm{E}[\lambda_{k,i}] + \frac{1}{N}\left[\psi(K+1) + \beta - 1\right] \ .
\end{aligned} \tag{B.6}$$

Proof of (iv): We first establish the following identity

$$\sum_{i=1}^{N} \mathrm{E}\left[\lambda_{k,i}\right] = \mathrm{E}\left[\mathrm{tr}\left(\mathbf{H}_k\mathbf{H}_k^H\right)\right] = \mathrm{E}\left[\|\mathbf{H}_k\|_F^2\right] = N^2 \tag{B.7}$$

where $\|\mathbf{H}\|_F = \sqrt{\sum_i \sum_j |h_{ij}|^2}$ is the matrix Frobenius norm and $\mathrm{tr}\left(\cdot\right)$ is the trace of a matrix. Then (4.31) is achieved by using (B.7) and (4.27)

$$\sum_{i=1}^{N} \mathrm{E}[\tilde{\lambda}_{k,i}] = \sum_{i=1}^{N} \mathrm{E}[\lambda_{k,i}] + n\,\Delta_\lambda = N^2 + N\,\Delta_\lambda \ . \tag{B.8}$$

Appendix C

Derivation of Equation (4.43)

We derive the upper bound for the link capacity under the SWNSF scheduling when ρ_k is large in this Appendix. Starting from (4.41), we have

$$
\begin{aligned}
\tilde{C}_k &= \mathrm{E}\left[\log\det\left(\mathbf{I} + \frac{\rho_k}{N}\widetilde{\mathbf{H}}_k\tilde{\mathbf{H}}_k^H\right)\right] \\
&\overset{(a)}{\simeq} \mathrm{E}\left[\log\det\left(\frac{\rho_k}{N}\tilde{\mathbf{H}}_k\tilde{\mathbf{H}}_k^H\right)\right] \\
&\overset{(b)}{=} N\log\left(\frac{\rho_k}{N}\right) + \mathrm{E}\left[\log\left(\prod_{i=1}^{N}\tilde{\lambda}_{k,i}\right)\right] \\
&\overset{(c)}{\leq} N\log\left(\frac{\rho_k}{N}\right) + N\mathrm{E}\left[\log\left(\frac{\sum_{i=1}^{N}\tilde{\lambda}_{k,i}}{N}\right)\right] \\
&\overset{(d)}{\leq} N\log\left(\frac{\rho_k}{N}\right) + N\log\left[N + \frac{1}{N}(\psi(K+1) + \beta - 1)\right] \;,
\end{aligned}
\tag{C.1}
$$

where (a) follows from the large ρ_k approximation, (b) from $\det(\tilde{\mathbf{H}}_k\tilde{\mathbf{H}}_k^H) = \prod_{i=1}^{N}\tilde{\lambda}_{k,i}$, (c) from the arithmetic-geometric inequality, and (d) from (4.39) together with the Jensen's inequality.

Appendix D

Proof of Proposition 5.1

Proof of (i): Starting from (5.39), we can write

$$\sum_{n=1}^{N} \mathrm{E}[\,\tilde{\gamma}_{n:N}^{\mathrm{mi}}\,] = N\mathrm{E}[\,\tilde{\gamma}_{1:N}^{\mathrm{mi}}\,] + (N-1)\mathrm{E}[\,S_2\,] + (N-2)\mathrm{E}[\,S_3\,] + \cdots + \mathrm{E}[\,S_N\,]$$

$$= \frac{\rho}{N}\,(\,\psi(K+1)+\beta\,) + \frac{\rho}{N} + \frac{\rho}{N} + \cdots + \frac{\rho}{N} \tag{D.1}$$

$$= \frac{\rho}{N}\,(\,\psi(K+1)+\beta+N-1\,)\,, \tag{D.2}$$

where the (D.1) follows from direct calculations of (5.34) and (5.38). At the low SNR regime with $\rho \ll 1$, $\tilde{C}_{\mathrm{zf}}^{\mathrm{mi}}$ can be expressed as

$$\tilde{C}_{\mathrm{zf}}^{\mathrm{mi}} \approx \sum_{N=1}^{N} \mathrm{E}[\,\tilde{\gamma}_{n:N}^{\mathrm{mi}}\,]\,. \tag{D.3}$$

Combining (D.3) and the result (4.39) of Chapter 4, we complete the proof by

$$\lim_{K\to\infty} \frac{\tilde{C}_{\mathrm{zf}}^{\mathrm{mi}}}{\tilde{C}_{\mathrm{opt}}^{\mathrm{mi}}} = \lim_{K\to\infty} \frac{N + \psi(K+1)+\beta-1}{N^2 + \psi(K+1)+\beta-1} = 1\,. \tag{D.4}$$

Proof of (ii): To begin with, we establish the upper bound and lower bound for the $\tilde{C}_{\mathrm{zf}}^{\mathrm{mi}}$ and $\tilde{C}_{\mathrm{opt}}^{\mathrm{mi}}$ at the high SNR regime. First, the upper bound for the $\tilde{C}_{\mathrm{opt}}^{\mathrm{mi}}$ for large ρ has been given in (4.43), which is

$$\tilde{C}_{\mathrm{opt}}^{\mathrm{mi}} \le N \log\left(\frac{\rho}{N}\right) + \underbrace{N \log\left[N + \frac{1}{N}\,(\psi(K+1)+\beta-1)\right]}_{U_1}\,. \tag{D.5}$$

Second, we can obtain an upper bound for $\tilde{C}_{\mathrm{zf}}^{\mathrm{mi}}$ at the high SNR regime as follows:

$$
\begin{aligned}
\tilde{C}_{\mathrm{zf}}^{\mathrm{mi}} &= \sum_{n=1}^{N} \mathrm{E}\left[\log\left(1 + \tilde{\gamma}_{n:N}^{\mathrm{mi}}\right)\right] \\
&\overset{(a)}{<} \sum_{i=n}^{N} \log\left(\mathrm{E}[\tilde{\gamma}_{n:N}^{\mathrm{mi}}]\right) \\
&\overset{(b)}{=} \sum_{n=1}^{N} \log\left(\frac{\rho}{N}\left[\frac{\psi(K+1)+\beta}{N} + \psi(n)+\beta\right]\right) \\
&= N\log\left(\frac{\rho}{N}\right) + \underbrace{\sum_{n=1}^{N} \log\left(\left[\frac{\psi(K+1)+\beta}{N} + \psi(n)+\beta\right]\right)}_{U_2}, \quad (\mathrm{D}.6)
\end{aligned}
$$

where (a) follows from the large ρ approximation along with the Jensen's inequality and (b) from direct calculations of (5.39). Third, a lower bound for $\tilde{C}_{\mathrm{opt}}^{\mathrm{mi}}$ can be simply given by

$$
\begin{aligned}
\tilde{C}_{\mathrm{opt}}^{\mathrm{mi}} &> C_{\mathrm{opt}}^{\mathrm{mi}} \\
&\simeq N\log\left(\frac{\rho}{N}\right) + \underbrace{\left(\sum_{n=1}^{N} \psi(N-n+1) + (1-N)\beta\right)}_{L_1}, \quad (\mathrm{D}.7)
\end{aligned}
$$

where (D.7) is provided in [110, eq. 12] for large ρ. Last, a lower bound for $\tilde{C}_{\mathrm{zf}}^{\mathrm{mi}}$ can be also attained as follows:

$$
\begin{aligned}
\tilde{C}_{\mathrm{zf}}^{\mathrm{mi}} &> C_{\mathrm{zf}}^{\mathrm{mi}} \\
&\simeq N\log\left(\frac{\rho}{N}\right) + \underbrace{(-N\beta)}_{L_2}, \quad (\mathrm{D}.8)
\end{aligned}
$$

where (D.8) uses the large ρ approximation to the Taylor expansion of (5.54).

Combining (D.5), (D.6), (D.7) and (D.8), we can obtain

$$
\frac{1 + \frac{L_2}{N\log\left(\frac{\rho}{N}\right)}}{1 + \frac{U_1}{N\log\left(\frac{\rho}{N}\right)}} < \frac{\tilde{C}_{\mathrm{zf}}^{\mathrm{mi}}}{\tilde{C}_{\mathrm{opt}}^{\mathrm{mi}}} < \frac{1 + \frac{U_2}{N\log\left(\frac{\rho}{N}\right)}}{1 + \frac{L_1}{N\log\left(\frac{\rho}{N}\right)}} . \quad (\mathrm{D}.9)
$$

Since all the constants U_1, U_2, L_1 and L_2 are constants for any finite K and N, and are independent of ρ, the proof is completed by taking the limit of ρ in (D.9) to infinity.

Appendix E

Derivation of Equation (6.30)

Applying the matrix inversion lemma [90] to (6.22), we get

$$\Phi_x^{-1} = \frac{1}{P_r} \left(\Phi_k^{-1} - \frac{\Phi_k^{-1} \mathbf{a}_k \mathbf{a}_k^H \Phi_k^{-1}}{1 + \mathbf{a}_k^H \Phi_k^{-1} \mathbf{a}_k} \right) \quad . \tag{E.1}$$

Substituting (E.1) into (6.26) yields

$$
\begin{aligned}
\mathbf{w}_{mv} &= \frac{\Phi_x^{-1} \mathbf{a}_k}{\mathbf{a}_k^H \Phi_x^{-1} \mathbf{a}_k} \\
&= \frac{\Phi_k^{-1} \mathbf{a}_k - \Phi_k^{-1} \mathbf{a}_k \mathbf{a}_k^H \Phi_k^{-1} \mathbf{a}_k / (1 + \mathbf{a}_k^H \Phi_k^{-1} \mathbf{a}_k)}{\mathbf{a}_k^H \Phi_k^{-1} \mathbf{a}_k - \mathbf{a}_k^H \Phi_k^{-1} \mathbf{a}_k \mathbf{a}_k^H \Phi_k^{-1} \mathbf{a}_k / (1 + \mathbf{a}_k^H \Phi_k^{-1} \mathbf{a}_k)} \\
&= \frac{\Phi_k^{-1} \mathbf{a}_k \left[1 - \mathbf{a}_k^H \Phi_k^{-1} \mathbf{a}_k / (1 + \mathbf{a}_k^H \Phi_k^{-1} \mathbf{a}_k) \right]}{\mathbf{a}_k^H \Phi_k^{-1} \mathbf{a}_k \left[1 - \mathbf{a}_k^H \Phi_k^{-1} \mathbf{a}_k / (1 + \mathbf{a}_k^H \Phi_k^{-1} \mathbf{a}_k) \right]} \\
&= \frac{\Phi_k^{-1} \mathbf{a}_k}{\mathbf{a}_k^H \Phi_k^{-1} \mathbf{a}_k} \quad .
\end{aligned}
\tag{E.2}
$$

Note that the interference-plus-noise power in the denominator of (6.28) can be expressed as

$$(\mathbf{a}_k^H \Phi_x^{-1} \mathbf{a}_k)^{-1} - P_r = P_r \, \mathbf{w}_{mv}^H \Phi_k \mathbf{w}_{mv} \quad . \tag{E.3}$$

As a result, applying (E.2) and (E.3) to (6.28) gives the result of (6.30).

Bibliography

[1] I. Emre Telatar, "Capacity of multi-antenna Gaussian channels," *European Trans. Telecomm.*, vol. 10, no. 6, pp. 585-595, Nov.-Dec. 1999.

[2] D. Gesbert, M. Shafi, D. S. Shiu, P. J. Smith and A. Naguib, "From theory to practice: an overview of MIMO space-time coded wireless systems," *IEEE J. Select. Areas Commun.*, vol. 3, pp. 281-302, Apr. 2003.

[3] L. Zheng and D. N. C. Tse, "Diversity and multiplexing: A fundamental tradeoff in multiple antenna channels," *IEEE Trans. on Information Theory*, vol. 49, pp. 1073-1296, May 2003.

[4] TIA/EIA IS-856, "cdma2000: High rate packet data air interface specification," v.1.0.0, Dec. 2000.

[5] 3GPP TR25.950, "UTRA High Speed Downlink Packet Access," v.4.0.0, Mar. 2001.

[6] H. Holma, S. Heikkinen, O. Lehtinen and A. Toskala, "Interference considerations for the time division duplex mode of the UMTS terrestrial radio access," *IEEE J. Select. Areas Commun.*, vol. 18, no. 8, pp. 1386-1393, Aug. 2000.

[7] R. Knopp and P. Humblet, "Information capacity and power control in single cell multiuser communications," *IEEE Proc. ICC*, pp. 331-335, Jun. 1995.

[8] D. N. C. Tse and S. Hanly, "Multi-access fading channels: Part I: polymatroid structure, optimal resource allocation and throughput capacities", *IEEE Trans. on Information Theory*, vol. 44, no. 7, pp. 2796-2815, Nov. 1998.

[9] A. Jalali, R. Padovani and R. Pankaj, "Data throughput of CDMA-HDR a high efficiency high data rate personal communication wireless system," *IEEE Proc. VTC*, pp. 1854-1854, May 2000.

[10] X. Liu, E. K. P. Chong and N. B. Shroff, "Opportunistic transmission scheduling with resource-sharing constrains in wireless networks," *IEEE J. Select. Areas Commun.*, vol. 19, no. 10, pp. 2053-2064, Oct. 2001.

[11] P. Viswanath, D. N. C. Tse, and R. Laroia, "Opportunistic beamforming using dumb antennas," *IEEE Trans. on Information Theory*, vol. 48, pp. 1277-1294, Jun. 2002.

[12] G. J. Foschini and M. J. Gans, "On limits of wireless communications in a fading environment when using multiple antennas," *Wireless Personal Communications*, vol. 6, no. 3, pp. 311-335, Mar. 1998.

[13] A. Paulraj, R. Nabar and D. Gore , *Introduction to Space-Time Wireless Communications*, 1st ed. Cambridge University Press, 2003.

[14] S. Catreux, L. J. Greenstein and V. Erceg, "Some results and insights on the performance gains of MIMO systems," *IEEE J. Select. Areas Commun.*, vol. 21, pp. 839-847, Jun. 2003.

[15] G. J. Foschini, G. D. Golden, P. W. Wolniansky, and R. A. Valenzuela, "Simplified processing for wireless communication at high spectral efficiency," *IEEE J. Select. Areas Commun.*, vol. 17, pp. 1841-1852, Jun. 1999.

[16] G. J. Foschini, D. Chizhik, M. J. Gans, C. Papadias and R. A. Valenzuela, "Analysis and performance of some basic space-time architectures," *IEEE J. Select. Areas Commun.*, vol. 21, pp. 303-320, Apr. 2003.

[17] H. Haas and S. McLaughlin, "A dynamic channel assignment algorithm for a hybrid TDMA/CDMA-TDD interface using the novel TS-opposing technique," *IEEE J. Select. Areas Commun.*, vol. 19, no 10, pp. 1831-1846, Oct. 2001.

[18] W. S. Jeon and D. G. Jeong, "Comparison of time slot allocation strategies for CDMA/TDD systems," *IEEE J. Select. Areas Commun.*, vol. 18, no. 7, pp. 1271-1278, Jul. 2000.

[19] L. C. Wang, S. Y. Huang and Y. C. Tseng, "A novel interference resolving algorithm for asymmetric services in TDD mode CDMA systems with directional antenna," *IEEE Proc. VTC Spring*, pp. 327-330, 2002.

[20] W. Jeong and M. Kavehrad, "Cochannel interference reduction in dynamic-TDD fixed wireless applications using time slot allocation algorithms," *IEEE Trans. on Commun.*, vol. 50, no. 10, pp. 1627-1636, Oct. 2002.

[21] R. L.-U. Choi and R. D. Murch, "Evaluation of a pre-rake smart antenna system for TDD CDMA Systems," *IEEE Proc. VTC Fall*, pp. 1543-1547, 2001.

[22] P. V. Rooyen, M. P. Lötter and D. V. Wyk, *Space-Time Processing for CDMA Mobile Communications*, Kluwer, 2000.

[23] L. C. Godara, "Application of antenna arrays to mobile communications, Part I: performance improvements, feasibility, and system considerations," *Proceedings of IEEE*, vol. 85, no. 7, pp. 1031-1060, Jul. 1997.

[24] G. L. Stüber, *Principles of Mobile Communication,* 2nd ed. Kluwer, 2001.

[25] A. Annamalai, C. Tellambura and V. K. Bhargava, "Equal gain diversity receiver performance in wireless channels," *IEEE Trans. on Communications*, vol. 48, pp. 1732-1745, Oct. 2000.

[26] M.-S. Alouini and M. K. Simon, "An MGF-Based performance analysis of generalized selection combining over Rayleigh fading channels," *IEEE Trans. on Communications*, vol. 48, pp. 401-415, Mar. 2000.

[27] C. H. Tse, K. W. Yip and T. S. Ko, "Performance tradeoffs between maximum ratio transmission and switched-transmit diversity," *IEEE Proc. PIMRC*, vol. 2, pp. 1485-1489, Sep. 2000.

[28] S. M. Alamouti, "A simple transmit diversity technique for wireless communications," *IEEE J. Select. Areas Commun.*, vol. 16, pp. 1451-1458, Oct. 1998.

[29] V. Tarokh, H. Jafarkhani and A. R. Calderbank, "Space-time block codes from orthogonal designs," *IEEE Trans. on Information Theory*, vol. 45, pp. 1456-1467, Jul. 1999.

[30] S. Thoen, L. V. D. Perre, B. Gyselinckx and M. Engels, "Performance analysis of combined transmit-SC/receive-MRC," *IEEE Trans. on Communications*, vol. 49, pp. 5-8, Jan. 2001.

[31] C. J. Love and R. W. Heath, "Equal gain transmission in multiple-input multiple-output wireless systems," *IEEE Trans. on Communications*, vol. 51, pp. 1102-1110, Jul. 2003.

[32] T. K. Y. Lo, "Maximum ratio transmission," *IEEE Trans. on Communications*, vol. 47, pp. 1458-1461, Oct. 1999.

[33] P. A. Dighe, R. K. Mallik and S. S. Jamuar, "Analysis of transmit-receive diversity in Rayleigh fading," *IEEE Trans. on Communications*, vol. 51, pp. 694-703, Apr. 2003.

[34] M. Rupp and C. F. Mecklenbrauker, "On extended Alamouti schemes for space-time coding," *IEEE Proc. WPMC*, vol. 1, pp. 115-119, Oct. 2002.

[35] E. G. Larsson and P. Stoica, *Space-Time Block Coding for Wireless Communications,* 1st ed. Cambridge University Press, 2003.

[36] J. H. Winters, "On the capacity of radio communication systems with diversity in a Rayleigh fading environment," *IEEE J. Select. Areas Commun.*, vol. 5, pp. 871-878, Jun. 1987.

[37] A. Goldsmith, S. A. Jafar, N. Jindal and S. Vishwanath, "Capacity limits of MIMO Channels," *IEEE J. Select. Areas Commun.*, vol. 21, pp. 684-702, Jun. 2003.

[38] D. Gesbert, "Robust linear MIMO receivers: a minimum error-rate approach," *IEEE Trans. on Signal Processing*, vol. 51, pp. 2863-2871, Nov. 2003.

[39] H. E. Gamal, G. Caire and M. O. Damen, "Lattice coding and decoding achieve the optimal diversity-multiplexing tradeoff of MIMO channels," *IEEE Trans. on Information Theory*, vol. 50, pp. 968-985, Jun. 2004.

[40] B. D. Van Veen and K. M. Buckley, "Beamforming: A versatile approach to spatial filtering," *IEEE ASSP Magazine*, pp. 4-24, Apr. 1988.

[41] R. A. Monzingo and T. W. Miller, *Introduction to Adaptive Arrays,* New York: John Wiley, 1980.

[42] D. N. C. Tse and P. Viswanath, *Fundamentals of Wireless Communication,* preprint, Cambridge University Press, 2005.

[43] J. H. Winters, "Optimum combining in digital mobile radio with cochannel interference," *IEEE J. Select. Areas Commun.*, vol. 2, no. 4, pp. 528-539, Jul. 1984.

[44] L. C. Godara, "Application of antenna arrays to mobile communications, Part II: beam-forming and direction-of-arrival considerations," *Proceedings of IEEE*, vol. 85, no. 8, pp. 1195-1245, Aug. 1997.

[45] A. F. Naguib, A. Paulraj and T. Kailath, "Capacity improvement with base-station antenna arrays in cellular CDMA," *IEEE Trans. on Veh. Technol.*, vol. 43, no. 3, pp. 691-698, Aug. 1994.

[46] H. Boche and M. Schubert, "Analysis of SIR based-downlink beamforming," *IEICE*, vol. E85-B, no. 6, pp. 1160-1168, Jun. 2002.

[47] F. R. Farrokhi, K. J. R. Liu and L. Tassiulas, "Transmit beamforming and power control for cellular wireless systems," *IEEE J. Select. Areas Commun.*, vol. 16, no. 8, pp. 1437-1998, Oct. 1998.

[48] P. Bender, P. Black, M. Grob, R. Padovani, N. Sindhushyana and S. Viterbi,"CDMA/HDR: A bandwidth-efficient high-speed wireless data service for nomadic users," *IEEE Communications Magazine*, pp. 70-77, Jul. 2000.

[49] T. S. E. Ng, I. Stoica and H. Zhang, "Packet fair queueing algorithms for wireless networks with location-dependent errors," *IEEE Proc. INFOCOM*, pp. 1103-1111, Mar. 1998.

[50] S. Lu, V. Bharghavan and R. Srikant, "Fair scheduling in wireless packet networks," *IEEE/ACM Trans. on Networking*, vol. 7, pp. 473-489, Aug. 1999.

[51] A. G. Kogiantis, N. Joshi and O. Sunay, "On transmit diversity and scheduling in wireless packet data," *IEEE Proc. ICC*, vol. 8, pp. 2433-2437, Jun. 2001.

[52] F. Berggren, S. L. Kim, R. Jantti and J. Zander, "Joint power control and intracell scheduling of DS-CDMA nonreal time data," *IEEE J. Select. Areas Commun.*, vol. 19, pp. 1860-1870, Oct. 2001.

[53] J. M. Holtzman, "Asympotic analysis of proportional fair algorithm," *IEEE Proc. PIMRC* , pp. F33-F37, Oct. 2001.

[54] W. Wang, T. Ottosson, M. Sternad. A. Ahlen and A. Svensson, "Impact of multiuser diversity and channel variability on adaptive OFDM," *IEEE Proc. VTC-Fall*, Orlando, Oct. 2003.

[55] R. Gozali, R. M. Buehrer and B. D. Woerner, "The impact of multiuser diversity on space-time block coding," *IEEE Commun. Letters*, vol. 7, pp. 213-215, May 2003.

[56] V. K. N. Lau, Y. Liu and T. A. Chen, "The role of transmit diversity on wireless communications – reverse link analysis with partial feedback," *IEEE Trans. on Communications*, vol. 50, pp. 2082-2090, Dec. 2002.

[57] S. Borst and P. Whiting, "The use of diversity antennas in high-speed wireless systems: capacity gains, fairness issues, multi-user scheduling," *Bell Labs Tech. Mem.*, 2001.

[58] J. Jing, R. M. Buehrer and W. H. Tranter, "Antenna diversity in multiuser data networks," *IEEE Trans. on Communications*, vol. 52, pp. 490-497, Mar. 2004.

[59] R. W. Heath Jr., M. Airy, and A. J. Paulraj, "Multiuser diversity for MIMO wireless systems with linear receivers," *IEEE Proc. Asilomar Conf. Signals, Systems and Computers*, Pacific Grove, CA, pp. 1194-1199, Nov. 2001.

[60] J. Chung, C. S. Hwang, K. Kim and Y. K. Kim, "A random beamforming technique in MIMO systems exploiting multiuser diversity," *IEEE J. Select. Areas Commun.*, vol. 21, pp. 848-855, Jun. 2003.

[61] M. Sharif and B. Hassibi, "A comparison of time-sharing, DPC, and beamforming for MIMO broadcast channels with many users," submitted to *IEEE Trans. on Commun.*, Mar. 2004. Available at http://www.its.caltech.edu/~masoud.

[62] N. Jindal and A. Goldsmith, "Dirty paper coding vs. TDMA for MIMO broadcast channels," submitted to *IEEE Trans. on Information Theory*, Jul. 2004. Available at http://www.ece.umn.edu/users/nihar/Publications.html

[63] V. K. N. Lau and Y. K. Kwok, "Performance analysis of SIMO space-time scheduling with convex utility function: zero-forcing linear processing," *IEEE Trans. on Vehicular Technology*, vol. 53, pp. 339-350, Mar. 2004.

[64] H. Yin and H. Liu, "Performance of space-division multiple-access with scheduling ," *IEEE Trans. on Wireless Communications*, vol. 1, pp. 611-618, Oct. 2002.

[65] Z. Tu and R. S. Blum, "Multiuser diversity for a dirty paper approach," *IEEE Communications Letters*, vol. 7, pp. 370-372, Aug. 2003.

[66] G. Caire and S. Shamai, "On the achievable throughput of a multiantenna Gaussian broadcast Channel," *IEEE Trans. on Information Theory*, vol. 49, pp. 1691-1706, Jul. 2003.

[67] H. Viswanathan, S. Venkatesan and H. Huang, "Downlink capacity evaluation of cellular networks with known-interference cancellation," *IEEE J. Select. Areas Commun.*, vol. 21, pp. 802-811, Jun. 2003.

[68] R. Esmailzadeh, M. Nakagawa and E. A. Sourour, "Time-division duplex CDMA communications," *IEEE Personal Commun.*, vol. 4, pp. 51-56, Apr. 1997.

[69] M. Haardt, A. Klein, R. Koehn, S. Oestreich, M. Purat, V. Sommer and T. Ulrich, "The TD-CDMA based UTRA TDD mode," *IEEE J. Select. Areas Commun.*, vol. 18, no. 8, pp. 1375-1385, Aug. 2000.

[70] R. Esmailzadeh, M. Nakagawa and A. Wajiwara, "Power control in packet switched time division duplex direct sequence spread spectrum," *IEEE Proc. VTC*, pp. 989-992, 1992.

[71] Z. Pu, X. You, S. Cheng and H. Wang, "Transmission and reception of TDD multicarrier CDMA signals in mobile communication systems," *IEEE Proc. VTC*, pp. 2134-2138, May 1999.

[72] A. Morgado, P. Pinho, A. Gameiro and J. Fernandest, "Pre-equalization technique for interference cancellation in the UMTS-TDD downlink channel," *IEEE Proc. VTC Fall*, vol. 2, pp. 878-881, 2001.

[73] A. N. Barreto and G. Fettweis, "On the downlink capacity of TDD CDMA systems using a pre-rake," *IEEE Proc. GLOBECOM*, pp. 117-121, Dec. 1999.

[74] R. L.-U. Choi and R. D. Murch, "Transmit MMSE pre-rake pre-processing with simplified receivers for the downlink of MISO TDD-CDMA systems," *IEEE Proc. GLOBECOM*, pp. 437-441, Nov. 2002.

[75] 3GPP TS25.224, "Physical Layer Procedures (TDD)," v.6.2.0, Sep. 2004.

[76] A. J. Viterbi, A. M. Viterbi and E. Zehavi, "Other-cell interference in cellular power-controlled CDMA," *IEEE Trans. on Commun.*, vol. 42, no. 2/3/4, pp. 1501-1504, Feb./Mar./Apr. 1994.

[77] K. S. Gilhousen, I. M. Jacobs, R. Padovani, A. J. Viterbi, L. A. Weaver and C. Wheatly, "On the capacity of a cellular CDMA system," *IEEE Trans. on Veh. Technol.*, vol. 40, no. 2, pp. 303-312, May 1991.

[78] X. Wu, L. L. Yang and L. Hanzo,"Uplink capacity investigations of TDD/CDMA," *IEEE Proc. VTC Spring*, pp. 997-1001, 2002.

[79] D. G. Jeong and W. S. Jeon, "CDMA/TDD system for wireless multimedia services with traffic unbalance between uplink and downlink," *IEEE J. Select. Areas Commun.*, vol. 17, no. 5, pp. 939-946, May 1999.

[80] P. G. Hoel, S. C. Port and C. J. Stone, *Introduction to Probability Theory*, Houghton Mifflin, 1971.

[81] A. J. Goldsmith and P. P. Varaiya, "Capacity of fading channels with channel side information," *IEEE Trans. on Information Theory*, vol. 43, no. 6, pp. 1986-1992, Nov. 1997.

[82] M. Abramowitz and I. A. Stegun, *Handbook of Mathematical Functions with Formulas, Graphs, and Mathematical Tables*, 9th ed. New York: Dover, 1970.

[83] M.-S. Alouini and A. J. Goldsmith,"Capacity of Nakagami multipath fading channels," *IEEE Proc. VTC*, pp. 358-362, May 1997.

[84] C. G. Günther, "Comment on estimate of channel capacity in Rayleigh fading environment," *IEEE Trans. on Vehicular Technology*, vol. 45, pp. 401-403, May 1996.

[85] C. Y. Lee, "Estimate of channel capacity in Rayleigh fading environment," *IEEE Trans. on Vehicular Technology*, vol. 39, pp. 187-189, Aug. 1990.

[86] M.-S. Alouini and A. J. Goldsmith, "Capacity of Rayleigh fading channels under different adaptive transmission and diversity-combining techniques," *IEEE Trans. on Vehicular Technology*, vol. 48, pp. 1165-1181, Jul. 1999.

[87] H. A. David, *Order Statistics*, 2nd ed. New York: Wiley, 1981.

[88] M. K. Simon and M.-S. Alouini, *Digital Communication over Fading Channels: A Unified Approach to Performance Analysis,* 1st ed. John Wiley, 2000.

[89] F. R. Farrokhi, A. Lozano, G. J. Foschini and R. A. Valenzuela, "Spectral effeciency of FDMA/TDMA wireless systems with transmit and receive antenna arrays," *IEEE Trans. on Wireless Communications*, pp. 591-599, vol. 1, Oct. 2002.

[90] G. H. Golub and C. F. V. Loan, *Matrix Computations*, 2nd ed. Johns Hopins University Press, 1983.

[91] S. Sandhu and A. Paulraj, "Space-time block codes: a capacity perspective," *IEEE Commun. Letters*, vol. 4, pp. 384-386, Dec. 2000.

[92] J. B. Anderson, "Antenna arrays in mobile communications: gain, diversity, and channel capacity," *IEEE Propagat. Magzine*, vol. 42, pp. 12-16, Apr. 2000.

[93] S. Verdu, "Spectral effeciency in the wideband regime," *IEEE Trans. on Information Theory*, vol. 48, no. 6, pp. 1319-1343, Jun. 2002.

[94] G. Fedele "*N*-branch diversity reception of *M*-ary DPSK signals in slow and nonselective Nakagami fading," *European Trans. Commun.*, vol. 7, pp. 119-123, Mar.–Apr. 1996.

[95] V. L. Girko, *Theory of Random Determinants*, Kluwer, 1990.

[96] A. J. Viterbi, A. M. Viterbi, K. S. Gilhousen and E. Zehavi, "Soft handoff extends CDMA cell coverage and increases reverse link capacity," *IEEE J. Select. Areas Commun.*, vol. 12, pp. 1281-1288, Oct. 1994.

[97] J. S. Lee and L. E. Miller, *CDMA Systems Engineering Handbook*, Artech House, Reading, MA, 1998.

[98] A. T. James, "Distributions of matrix variates and latent roots derived from normal samples," *Ann. Math. Stat.*, vol. 35, pp. 475-501, Jun. 1964.

[99] A. Edelman, *Eigenvalues and Condition Numbers of Random Matrices*, Ph.D. thesis, M.I.T., Cambridge, MA, May 1989.

[100] I. S. Gradshteyn and I. M. Ryzhik, *Table of Integrals, Series, and Products*, 6th ed. San Diego, CA: Academic, 2000.

[101] W. H. Press, B. P. Flannery, S. A. Teukolsky and W. T. Vetterling, *Numerical Recipes*, Cambridge University Press, 1996.

[102] B. M. Hochwald, T. L. Marzetta and V. Tarokh, "Multiple-antenna channel hardening and its implications for rate feedback and scheduling," *IEEE Trans. on Information Theory*, vol. 50, pp. 1893-1909, Sep. 2004.

[103] H. Shin and J. H. Lee, "Capacity of multiple-antenna fading channels: spatial fading correlation, double scattering, and keyhole," *IEEE Trans. on Information Theory*, vol. 49, pp. 2636-2647, Oct. 2003.

[104] D. A. Gore, R. W. Heath Jr. and A. J. Paulraj, "Transmit selection in spatial multiplexing systems," *IEEE Communication Letters*, vol. 6, pp. 491-493, Nov. 2002.

[105] A. K. Gupta and D. K. Nagar, "Matrix Variate Distributions," Boca Raton, FL: Chapman & Hall/CRC, 2000.

[106] B. C. Arnold, N. Balakrishnan and H. N. Nagaraja, *A First Course in Order Statistics*. New York: Wiley, 1992.

[107] P. V. Sukhatme, "Tests of significance for samples of the χ^2 population with two degrees of freedom," *Ann. Eugenics*, vol. 8, pp. 52-56, 1937.

[108] J. H. Chang, L. Tassiulas and F. R. Farrokhi, "Joint transmitter receiver diversity for efficient space division multiaccess," *IEEE Trans. on Wireless Communications*, vol. 1, pp. 16-27, Jan. 2002.

[109] M. Z. Win and J. H. Winters, "Analysis of hybrid selection/maximal-ratio combining in Rayleigh fading," *IEEE Trans. on Communications*, vol. 47, pp. 1773-1776, Dec. 1999.

[110] O. Oyman, R. U. Nabar, H. Bolcskei and A. J. Paulraj, "Characterizing the statistical properties of mutual information in MIMO channels," *IEEE Trans. on Signal Processing*, vol. 11, pp. 2784-2795, Nov. 2003.

[111] B. Suard, A. F. Naguib, G. Xu and A. Paulraj, "Performance analysis of CDMA mobile communication systems using antenna arrays," *IEEE Proc. ICASSP*, pp. 153-156, Apr. 1993.

[112] J. Litva and T. K. Y. Lo, *Digital Beamforming in Wireless Communications,* Artech House, 1996.

[113] B. H. Khalaj, A. J. Paulraj and T. Kailath, "2D rake receivers for CDMA cellular systems," *IEEE Proc. Globecom.*, vol. 1, pp. 400-404, Nov. 1994.

[114] A. J. Paulraj and C. B. Papadias, "Space-time processing for wireless communications," *IEEE Signal Processing Magazine*, vol. 14, no. 6, pp. 49-83, Nov. 1997.

[115] A. Poon, D. N. C. Tse and R. Brodersen, "Impact of scattering on the capacity, diversity and propagation range of multiple antenna channels," submitted to *IEEE Trans. on Information Theory*, Apr. 2004. Available at http://www.eecs.berkeley.edu/∼dtse/pub.html.

[116] C. J. Chen and L. C. Wang, "A unified capacity analysis for wireless systems with joint multiuser scheduling and antenna diversity in Nakagami fading channels," submitted to *IEEE Trans. on Communications.* (See also *Proc. IEEE ICC*, vol. 6, pp. 20-24, Jun. 2004.)

[117] C. J. Chen and L. C. Wang, "Enhancing coverage and capacity for multiuser MIMO systems by utilizing scheduling," submitted to *IEEE Trans. on Wireless Communications.* (See also *Proc. IEEE Globecom*, Dec. 2004.)

[118] C. J. Chen and L. C. Wang, "On the performance of zero-forcing receivers operating in multiuser MIMO systems with reduced noise enhancement by scheduling," submitted to *IEEE JSAC* special issue on 4G wireless systems.

[119] C. J. Chen and L. C. Wang, "Suppressing opposite-direction interference in TDD/CDMA systems with asymmetric traffic by antenna beamforming," *IEEE Trans. on Vehicular Technology*, vol. 53, pp. 956-967, Jul. 2004.

Vita

Chiung-Jang Chen was born in Kaohsiung, Taiwan, R.O.C., in May 1971. He received the B.S. degree in electronics engineering from National Chiao-Tung University (NCTU), Hsinchu, Taiwan, in 1993, the M.E. degree in electrical engineering from National Taiwan University, Taipei, Taiwan, in 1995. He is currently pursuing the Ph.D. degree in communication engineering from NCTU, Taiwan.

Since 1995, he was with Telecommunication Laboratories of Chunghwa Telecom Co., Chung-Li, Taiwan. His research interests include radio network resource management, MIMO performance analysis and cross-layer optimization for high speed wireless networks.

簡　　歷

姓　名　：　陳瓊璋

性　別：　男

出生年月日　：　民國 60 年 5 月 15 日

籍　貫　：　高雄市

學　歷　：　國立交通大學電子工程系畢業 (80 年 9 月~82 年 6 月)
　　　　　　國立台灣大學電機工程研究所畢業 (82 年 9 月~84 年 6 月)
　　　　　　國立交通大學電信工程學系博士班 (90 年 9 月~)

經　歷　：　中華電信研究所副研究員 (84 年 10 月 ~)

論文題目　：　從網路觀點對天線技術於多用戶排程及分時雙工/分碼多工
　　　　　　無線系統之研究
　　　　　　A Network Perspective Investigation of MIMO Antenna
　　　　　　Techniques in Multiuser Scheduling and TDD/CDMA Systems

Publication List

Journal Papers:

1. **Chiung-Jang Chen** and Li-Chun Wang, "Suppressing opposite-direction interference in TDD/CDMA systems with asymmetric traffic by antenna beamforming," *IEEE Trans. on Vehicular Technology*, vol. 53, pp. 956-967, Jul. 2004.

2. **Chiung-Jang Chen** and Li-Chun Wang, "Enhancing coverage and capacity for multiuser MIMO systems by utilizing scheduling," submitted to *IEEE Trans. on Wireless Communications* (submitted on Apr. 2004, revised on Oct. 2004).

3. **Chiung-Jang Chen** and Li-Chun Wang, "A unified capacity analysis for wireless systems with joint multiuser scheduling and antenna diversity in Nakagami fading channels," submitted to *IEEE Trans. on Communications*, Mar. 2004.

4. **Chiung-Jang Chen** and Li-Chun Wang, "Impacts of radio channel characteristics, heterogenous traffic intensity and near-far effect on rate adaptive scheduling algorithms," submitted to *IEEE Trans. on Vehicular Technology*, Dec. 2004.

5. **Chiung-Jang Chen** and Li-Chun Wang, "On the performance of zero-forcing receivers operating in multiuser MIMO systems with reduced noise enhancement by scheduling," submitted to *IEEE JSAC*, special issue on 4G wireless systems, Jan. 2005.

Conference Papers:

1. **Chiung-Jang Chen** and Li-Chun Wang, "Coverage and capacity enhancement in multiuser MIMO systems with scheduling," *IEEE Globecom*, Dec. 2004.

2. **Chiung-Jang Chen** and Li-Chun Wang, "A unified capacity analysis for wireless systems with joint antenna and multiuser diversity in Nakagami fading channels," *IEEE ICC*, vol. 6 , pp. 20-24, Jun. 2004.

3. **Chiung-Jang Chen** and Li-Chun Wang, "An analytical framework for capacity and fairness evaluation in high speed wireless data networks," *IEEE Globecom*, vol. 2 , pp. 1-5, Dec. 2003

4. **Chiung-Jang Chen** and Li-Chun Wang, "Interference suppression in TDD/CDMA cellular systems with asymmetric traffic using MVDR beamforming," *IEEE VTC*, vol. 1 , pp. 24-28, Sep. 2002.

5. **Chiung-Jang Chen** and Li-Chun Wang, "A hierarchical TDD microcell/FDD macrocell CDMA system using antenna arrays and power ratio adjustments," *IEEE Globecom*, vol. 2, pp. 17-21, Nov. 2002.

6. **Chiung-Jang Chen** and Li-Chun Wang, "A feasibility study of beamforming techniques for suppressing interference in TDD/CDMA systems with asymmetric traffic," *IEEE ISWC*, Sep. 2002.